DOE/NASA/0289-1
NASA CR-174709
PSD FCR-5715

Advanced On-Site Power Plant Development Technology Program

1983 Annual Report

United Technologies Corporation
Power Systems Division
Fuel Cell Operations
South Windsor, Connecticut

June 1984

Prepared for
National Aeronautics and Space Administration
Lewis Research Center
Cleveland, Ohio 44135
Under Contract DEN3-289

for
U.S. DEPARTMENT OF ENERGY
OFFICE OF FOSSIL ENERGY
MORGANTOWN ENERGY TECHNOLOGY CENTER
Under Interagency Agreement DE-AI-21-80ET17088

DOE/NASA/0289-1
NASA CR-174709
PSD FCR-5715

Advanced On-Site Power Plant Development Technology Program

1983 Annual Report

United Technologies Corporation
Power Systems Division
Fuel Cell Operations

June 1984

Prepared for
National Aeronautics and Space Administration
Lewis Research Center
Under Contract DEN3-289

for
U. S. DEPARTMENT OF ENERGY
Morgantown Energy Technology Center

CONTENTS

ILLUSTRATIONS

ILLUSTRATIONS (Cont'd)

TABLES

EXECUTIVE SUMMARY

This document reports the activity of DOE/NASA Contract DEN3-289 for the first portion of the effort carried out in time period September 1982 through November 1983. The purpose of this 57-month contract is to develop phosphoric acid fuel cell component technology for on-site power plant use. All evaluation is done at atmospheric pressure using hardware consistent with a 200-kW size power plant. This effort is being conducted in parallel with a Gas Research Institute (GRI) On-Site Fuel Cell Power Plant Technology Development Program, GRI Contract 5080-344-0405, and with a field test of a number of 40-kW power plants under Contract 5080-344-0308.

In this first phase of the program, efforts were concentrated on subscale component technology development and screening, with the goal of selecting candidates for scale-up and long-term endurance testing. The next phase of the program (1984-1985) will be devoted to component development and scale-up evaluation. In the final phase, full-scale component evaluation and interaction technology will be the major activity.

In the period covered by this report, major development activity occurred in stack, inverter, reformer, and ancillary equipment technologies. In addition, an analysis of early 40-kW field test power plant data was conducted to determine if this technology development program should respond to any field test problems.

A cell stack was fabricated and is being tested over a 5000 hour period to evaluate several advanced cell and stack features. Advanced features in this stack include totally encapsulated serpentine coolers at 10 cells per cooler, electrodes containing an acid condensation zone and acid refill provisions, and dry mix type electrode processing. This stack has run 2700 hours with stable performance. An acid addition scheme will be evaluated at the end of the 5000 hour test period.

An inverter bridge electrical design was established that results in a calculated full load efficiency of 94.8%. Asymmetrical silicon controlled rectifiers (ASCR's)

were selected for use in the brassboard inverter, however, several gate turnoff (GTO) devices were selected for laboratory evaluation. Subcontracts were placed to fabricate the brassboard bridges, series reactors, and bridge control units. Evaluation of this equipment is planned in the 1984 effort of this contract. An output transformer with 99% full load efficiency was ordered and will be evaluated in the 1984 effort as part of the brassboard inverter test program.

A test program was conducted to evaluate two direct cooling approaches and one heat exchanger approach in an effort to obtain a low cost acid removal device. The spray cooling and contact saturator approaches were found to be slightly less expensive (on a $/kW basis) than the baseline 40-kW field test heat exchanger, but added significant complexity to the system. The preferred approach is a modified Teflon® covered commercial heat exchanger. This commercial unit is simpler and is one-fifth the cost per kilowatt of the bare metal heat exchanger used in the 40-kW power plant.

Reformer catalysts were screened in order to obtain a candidate with lower pressure drop and performance equivalent to that of the 40-kW field test catalyst. Several catalysts were found to have acceptable performance, with 10 to 40% of the pressure drop of the 40-kW catalyst. Alternative shift converter catalysts were evaluated, and one candidate was selected for further evaluation. Testing of a hydrodesulfurization catalyst that does not require a costly presulfide treatment was initiated during this test period. An endurance test rig was prepared for evaluation of a process train with candidate catalysts from the above screening program. This train consists of beds containing the hydrodesulfurizer, reformer, and shift catalyst candidates, and also contains the necessary heat exchangers and controls to operate the catalyst beds at design conditions. The endurance test is planned for the 1984 effort. A six to seven tube reformer configuration was selected for the development reformer, and an industrial burner was evaluated for incorporation into the design. This evaluation included water table testing to establish the burner arrangement. Also, an infrared pyrometer was purchased for evaluation as an improved temperature control approach.

Operational data from several early 40-kW power plants were reviewed to determine the need for technology development interaction with the field test efforts. The purpose of the effort was to assure that the necessary adjustments were made to the Technology Development Program to address chronic failure modes. The Technology Development Program was adjusted to expand the effort in the cooling system, inverter logic card processing, and system reliability tasks.

INTRODUCTION

INTRODUCTION

This report covers the work plan period September 1, 1982 through November 30, 1983 of the On-Site Technology Development Program (DEN3-289). The effort during this work period was divided into the following tasks:

Cell Technology (Task 1) - Evaluate fuel cell electrodes at on-site conditions in bench scale cells.

Cell Stack Development (Task 2) - Develop and evaluate electrode substrates, cell coolers, and acid replenishment techniques to improve performance and reliability and reduce costs of these components.

Power Processor Development (Task 3) - Develop inverter components and circuitry and fabricate a brassboard model for subsequent evaluation.

Heat Exchanger Development (Task 4) - Develop and evaluate alternative approaches to the condensate preheater/acid condenser heat exchanger.

Fuel Processor Development (Task 5) - Screen and select fuel processor catalyst for subsequent evaluation in a development reformer and a subscale fuel processing train.

Preprototype Power Plant Data Review (Task 6) - Assess data from verification and early field test power plants (DE-AC01-80ET-17109) to identify any additional technology development program activities.

A parallel Gas Research Institute (GRI) On-Site Technology Development Program (Contract No. 5080-344-0405) with complementary tasks was conducted in 1983. The GRI effort will be reported separately.

TASK 1 CELL TECHNOLOGY

TASK 1 - CELL TECHNOLOGY

Subtask 1.1 Electrode-Catalyst Evaluation

Objective

The objective of this task is to demonstrate that cell performance and endurance goals can be met. These goals are defined in terms of a projected cell performance, referred to as E + 20 mV, and a projected decay of 63 mV at 200 ASF in 40,000 hours, referred to as E-line decay. The goal performance is equivalent to 682 mV/cell at 200 amps per square foot at time zero. An additional objective is to determine the cell's ability to tolerate stressful operating conditions and hence to define an acceptable operating envelope consistent with the decay goal.

Summary

Nine subscale cells with three different cathode catalysts on three different supports were evaluated under on-site conditions to select the best cathode catalyst/support combination for further testing. These cells are referred to as Series I cells in the discussion. This test series was initiated in the GRI On-Site Technology Development Program, as discussed in FCR-4991A. The GSB-18 cathode, modified to increase its hydrophobicity, was determined the best candidate.

Four subscale cells with different versions of the GSB-18 cathode were next run for 3000 hours under on-site conditions. Cells from these tests are referred to as Series II cells in this discussion. The two cells that showed the greatest stability were subjected to further tests to determine their tolerance to electrolyte volume swings and to shutdowns. After 8000 hours of operation one cell remains, running at 0.625 V, 200 ASF, 400°F, 80%:50% fuel:air utilization, and 29 mV below the program goal performance. Three cells containing GSB-18 cathodes representative of those in the 30-cell stack are also being tested to provide a subscale versus full-scale performance comparison.

Highlights

- The HYCAN anode, manufactured by production methods, has shown excellent performance and stability in all of the subscale cell tests.
- Two cells with laboratory-made GSB-18 cathodes were within 7 mV of the on-site performance goal of E + 20 mV after 2000 hours of operation. Subsequent losses in performance occurred following diagnostic test procedures.
- The better of the above cells is 29 mV below the on-site goal after 8000 hours of operation, during which time it has been subjected to three electrolyte dilution cycles and eighteen shutdowns.
- Further development is required to meet performance goals over long operating periods.
- Catalyst scaleup work is required to match the performance level of the production catalysts/electrodes to that of the laboratory version.

Discussion

Series I Cells

Nine subscale cells were started under the GRI Technology Development Program to compare the performances of three different cathode catalysts on three different supports. The purpose of this test was to select the best cathode catalyst/support combination for the on-site power plant. The supports were designated GSA, GSB, and GSC. Tests in the laboratory conducted in an earlier UTC-funded program showed that the GSB and GSC supports are more resistant to oxidation than GSA at high cathode potentials. This statement is based on direct measurements of the corrosion currents obtained from different support materials. The catalysts were

platinum and two alloys of platinum. The alloys are proprietary UTC electrocatalysts identified by the numbers "6" and "18".

The supported catalysts were fabricated into electrodes on porous, ribbed, carbon substrates. The platinum loading was 0.5 mg/cm^2 of electrode. Portions of these laboratory-made electrodes, having an active area of 2 inches by 2 inches, were paired with HYCAN anodes prepared in the electrode production shop.

The HYCAN anode used in all of the tests is a UTC-developed electrode that has been adopted for general use. The platinum loading on the HYCAN anodes was 0.25 mg/cm^2. The electrode pairs were built into subscale phosphoric acid fuel cells with silicon carbide matrices. Figure 1-1 shows the components of a typical subscale cell excluding the gaskets and seals. Figure 1-2 is a photograph of the test stand in which the cells were run.

The cells were operated at the following conditions:

- 200 ASF
- 400°F
- Dry air at 50% utilization
- Fuel (70% H_2, 1% CO, 29% CO_2) at a dew point of 140°F and 80% utilization
- 40% electrolyte fill of the substrates

Diagnostic tests were run on the cells when they attained their maximum performances (at approximately 200 hours) and after each 1000 hours of load time.

In September 1982 the five cells with alloy cathode catalysts that were still on test and had accumulated 1600 hours on load under the GRI effort were transferred to this program. Figures 1-3, 1-4, and 1-5 are voltage versus time plots showing the entire performance histories of the nine original cells, including the period prior to the change of sponsorship. The solid line indicates the performance/endurance goal for the program. Results and conclusions from the Series I tests are summarized in the following sections.

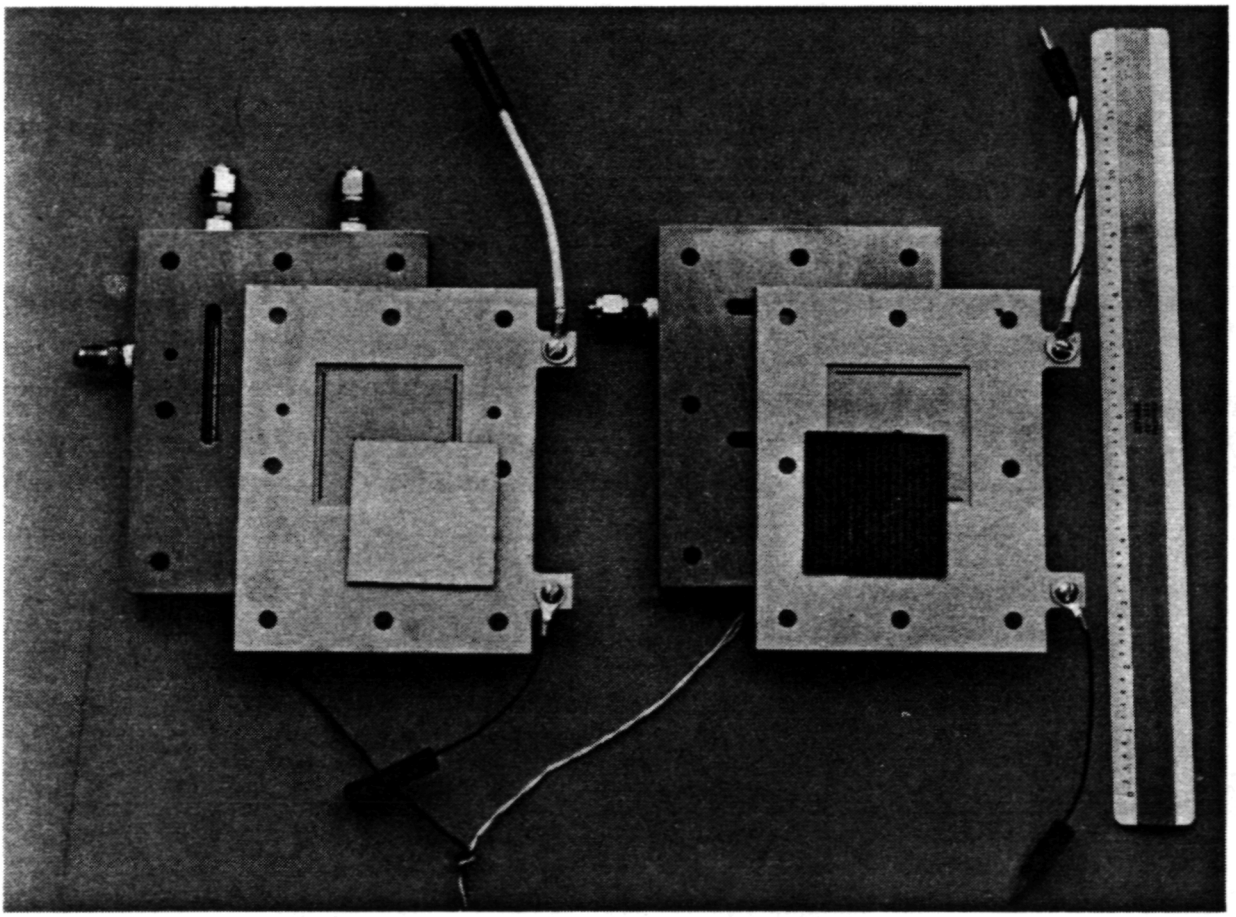

WCN-6515

Figure 1-1. Components of a Subscale Cell Excluding Gaskets and Seals

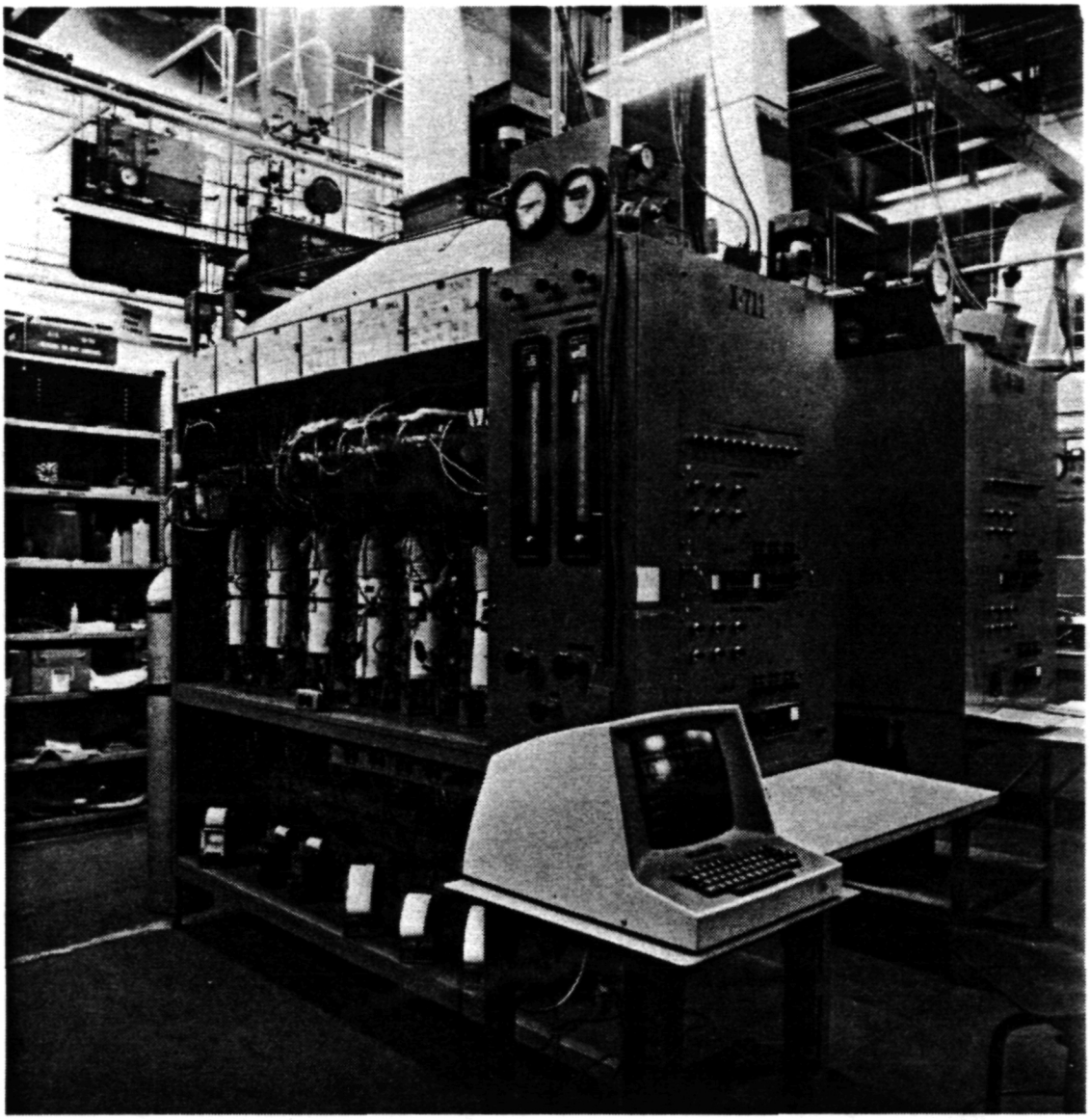

WCN-7028

Figure 1-2. View of Stand Used to Test Subscale Cells

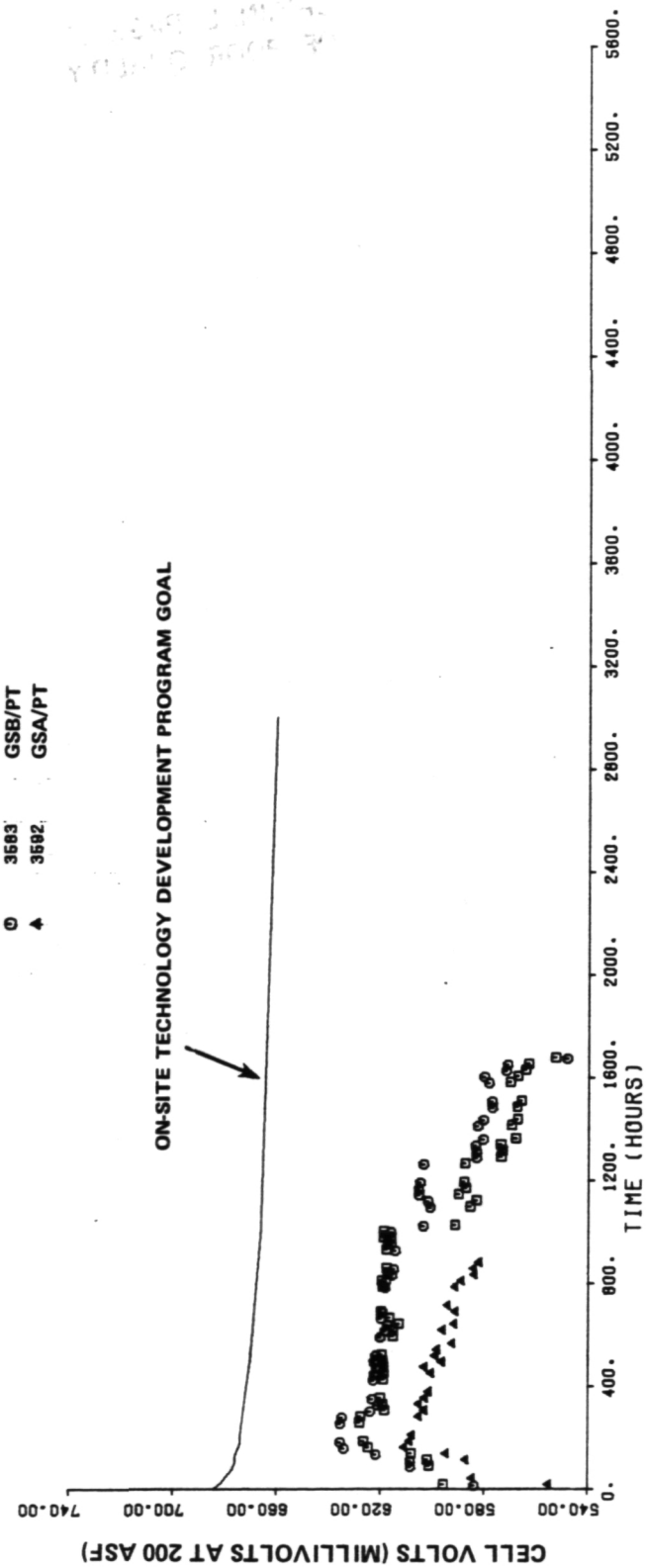

Figure 1-3. Performance History of Series I Platinum Catalyst Cells

ORIGINAL PAGE IS
OF POOR QUALITY

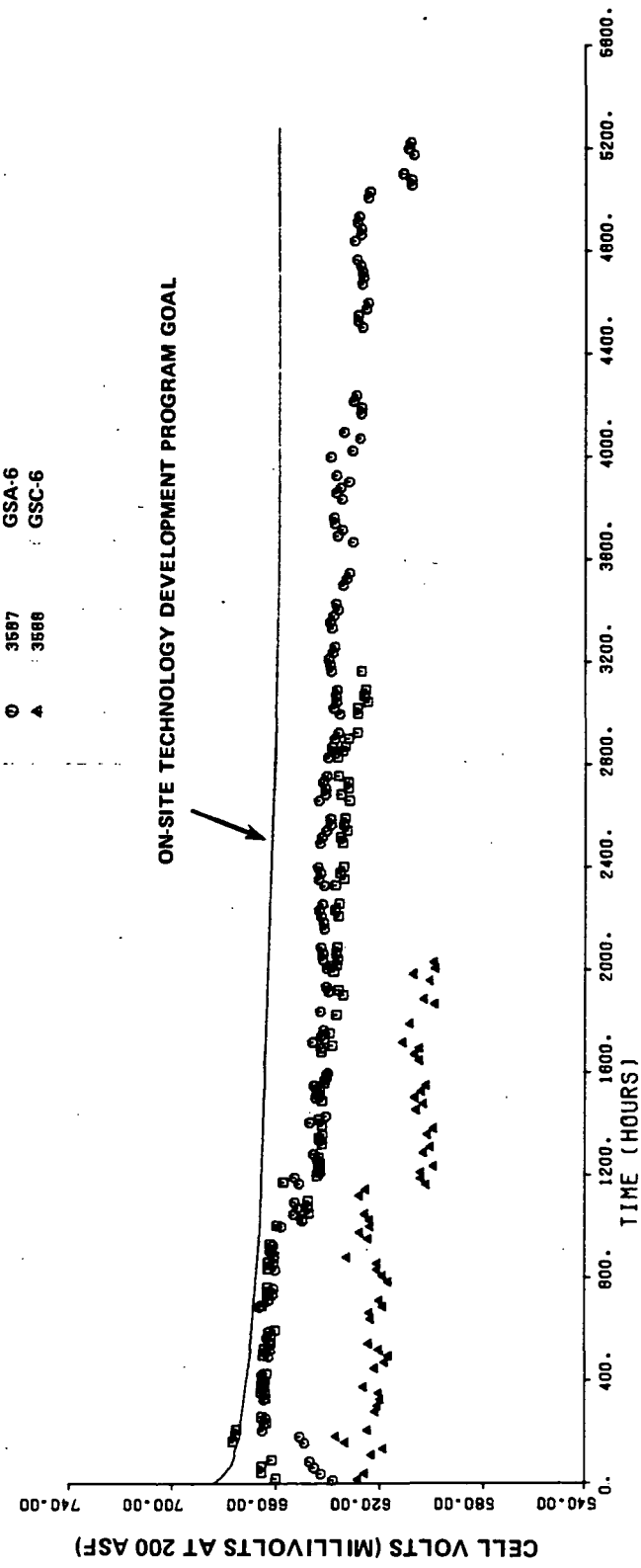

Figure 1-4. Performance History of Series I "6" Alloy Catalyst Cells

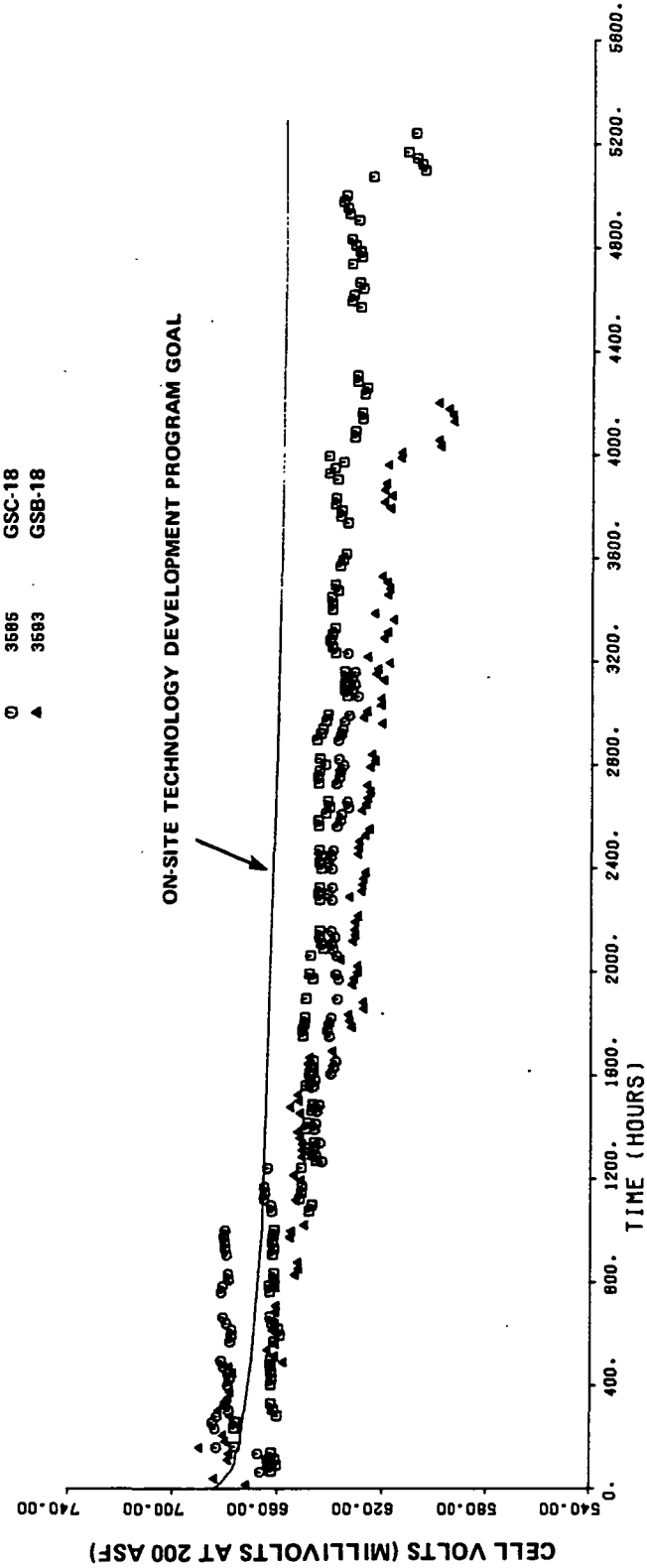

Figure 1-5. Performance History of Series I "18" Alloy Catalyst Cells

Anodes - Hydrogen gain is the principal diagnostic used to measure the performance and endurance of an anode. It is the increase in cell voltage that occurs when pure hydrogen is substituted for the normal fuel mixture, all other conditions being held constant.

The HYCAN anodes in the Series I tests performed very well. With the exception of Cell 3588 (GSC-6 cathode), the hydrogen gains were all within the range of 21 ±3 mV at 200 ASF and remained constant throughout the test program. The hydrogen gain for Cell 3588 was 35 mV, which is atypical for this type of anode. It is concluded that the HYCAN anode can meet the performance and stability requirements of the On-Site Program.

Matrix - The internal resistance of all the cells was 22 ±2 mV at 200 ASF, and remained constant throughout the test. At no time were there any signs of shorting or crossover. It is concluded that the silicon carbide matrix has the requisite integrity and stability for use in the on-site power plant.

Cathodes - The invariance of the anodes and of the cell internal resistance leads to the conclusion that the differences in cell performance levels and decay characteristics (shown in Figures 1-3, 1-4, and 1-5) reflect differences in the cathodes. Oxygen gain, as discussed below, is the increase in voltage of a cell when oxygen is substituted for air on the cathode and all other conditions are held constant.

(a) GS/Pt Cathodes: The cells with unalloyed, supported platinum as their cathode catalyst performed poorly and decayed rapidly (Figure 1-3). All three GS/Pt cells had large oxygen gains (~110 mV at 200 ASF) at the beginning of the test, and three increased to ~155 mV at 200 ASF by the time the tests were concluded. The desired value for this parameter is 80 mV at 200 ASF.

(b) Alloy Cathodes - Performance: The cathodes with the "6" and "18" platinum alloys as electrocatalysts also had increased oxygen gains with time. Not only were the oxygen gains high initially, but they also increased appreciably at around 1000 hours following diagnostic tests. This caused a sharp drop in cell performance in the 1000-1200 hour time period (Figures 1-4 and 1-5).

Peak performance data taken early in life are given in Table 1-1. The data show that the "18" alloy is more active initially than the "6" alloy.

TABLE 1-1. SERIES I CELLS - PEAK PERFORMANCE DATA

Cell #	Cathode	Peak Performance on H_2/O_2 (iR-free volts at 200 ASF)	
3592	GSA/Pt	0.775	Average
3583	GSB/Pt	0.777	0.776
3582	GSC/Pt	0.775	
3587	GSA-6	0.795	Average
3586	GSB-6	0.802	0.796
3588	GSC-6	0.791	
3584	GSA-18	0.803	Average
3593	GSB-18	0.808	0.807
3585	GSC-18	0.809	

(c) Alloy Cathodes - Decay: Some of the cells were run for extended periods to obtain data regarding electrode stability. Data from diagnostic tests at 3000, 4000, and 5000 hours are shown in Table 1-2. At these times the oxygen gains of all the cathodes were in excess of 100 mV.

TABLE 1-2. SERIES I CELLS - H_2/O_2 PERFORMANCE WITH TIME

Cell #	Cathode	Performance on H_2/O_2 (iR-free volts at 200 ASF) 3000 Hr.	4000 Hr.	5000 Hr.
3587	GSA-6	0.775	0.779	0.773
3586	GSB-6	0.772	-	-
3584	GSA-18	0.780	0.777	0.775
3593	GSB-18	0.776	0.780	-
3585	GSC-18	0.784	-	-

Conclusions

- The on-site performance goal can be met, at least initially, with cells containing the "18" alloy as cathode catalyst.
- GSB is the preferred support for the cathode catalyst because of its high resistance to oxidation.
- The Series I cathodes were inadequately wet-proofed, as indicated by the rapidly decaying cell performance and associated increases in oxygen gain.

Series II Cells -

The Series II cells all contained HYCAN anodes paired with GSB-18 cathodes (Table 1-3).

TABLE 1-3. IDENTIFICATION OF SERIES II CELLS

Cell #	Cathode	% Fill
3639	GSB-18A	30
3638	GSB-18B	30
3637	GSB-18B (S)	40
3636	GSB-18A (S)	30

Operating Conditions: 200 ASF/400°F. Dry air at 50% utilization. Fuel (70% H_2, 1% CO, 29% CO_2) at a dew point of 140°F and 80% utilization.

These cathodes were all more hydrophobic than those in the Series I cells, the 18B cathodes being the most hydrophobic. In two of the Series II cells (indicated by "S"), the cathode catalyst layers were structurally modified to improve the transfer of electrolyte across the cell.

The performance histories of the cells out to 3000 hours are shown in Figure 1-6. The cells did not attain their maximum voltages until 200-600 hours into the test. Only one cell attained the performance goal, and then only for a brief period. By 3000 hours, differences in performance had disappeared, and all four cells were clustered around E-line. Diagnostic tests showed that the oxygen gains for Series II cells were appreciably lower than for Series I cells (~85 mV at 200 ASF, as compared to 120 mV at 200 ASF for Series I cathodes), confirming that the tendency of the catalyst layers to flood was greatly reduced.

Following the diagnostic tests, at 3000 hours the two cells containing cathodes of the "S" variety (builds 3636 and 3637) showed unacceptably large losses in performance accompanied by erratic behavior, and were terminated. It was concluded that the modification made to improve electrolyte transfer through the cathode catalyst layer caused other electrolyte management problems.

The two remaining cells (builds 3638 and 3639) were then subjected to the stress tests of electrolyte dilution and shutdowns.

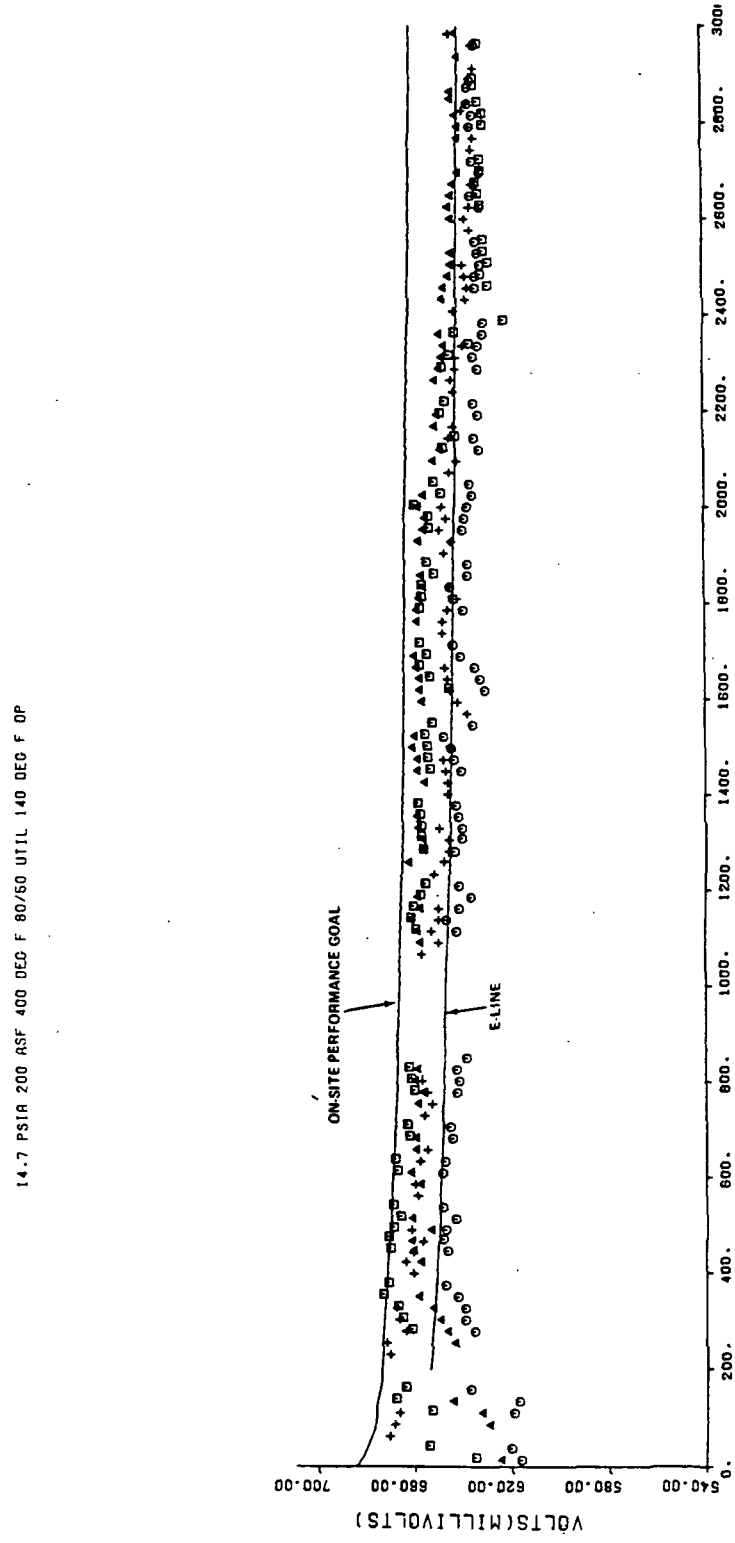

Figure 1-6. Performance History of Series II Cells

Electrolyte Dilution Tests - Electrolyte dilution of cells 3638 and 3639 was established by lowering the cells' temperatures to 156°F while maintaining the dew point of the fuel. In this way, the electrolyte in the cells became diluted (from 99% to 50% H_3PO_4), and its volume expanded to fill 80% of the available capacity of the substrates. The electrolyte dilution cycle (i.e., wet-up followed by dry-out) was run three times on each cell. Cell 3638 with the GSB-18B cathode showed a small loss in performance, whereas Cell 3639 with the GSB-18A catalyst layer showed a substantial loss (Figure 1-7).

Tolerance to Shutdown/Restart - Following the completion of the electrolyte dilution tests, the two remaining Series II cells with GSB-18 cathodes and HYCAN anodes were subjected to shutdown trials. In the period from 4885 hours to 5794 hours Cell 3638 was subjected to a series of 11 three-day shutdowns to room temperature. The cell was removed from load and a semiconducting diode was placed across it to keep cathode potential at around .5V. It was allowed to cool to room temperature (about one hour) on a trickle flow of dry H_2 and stagnant air. At room temperature the cell was capped. There was no protection from solidification of electrolyte. The cell was restarted on the third day. Measurements of conductivity show that the electrolyte does not solidify in that time. This resulted in a net loss in performance of about 5 mV at 200 ASF. Between 4860 hours and 5340 hours, Cell 3639 was shutdown six times and suffered a net loss of 18 mV. Cell 3639 was terminated. The catalyst layer in Cell 3638 is more hydrophobic than that in Cell 3639.

The only surviving Series II cell (Build 3638) has now been on test for over 8000 hours (Figure 1-8) and has experienced a total of eighteen shutdowns. Its present performance is 0.629V/200 ASF -- 5 mV below E-line -- and it will continue running at on-site conditions to 10,000 hours.

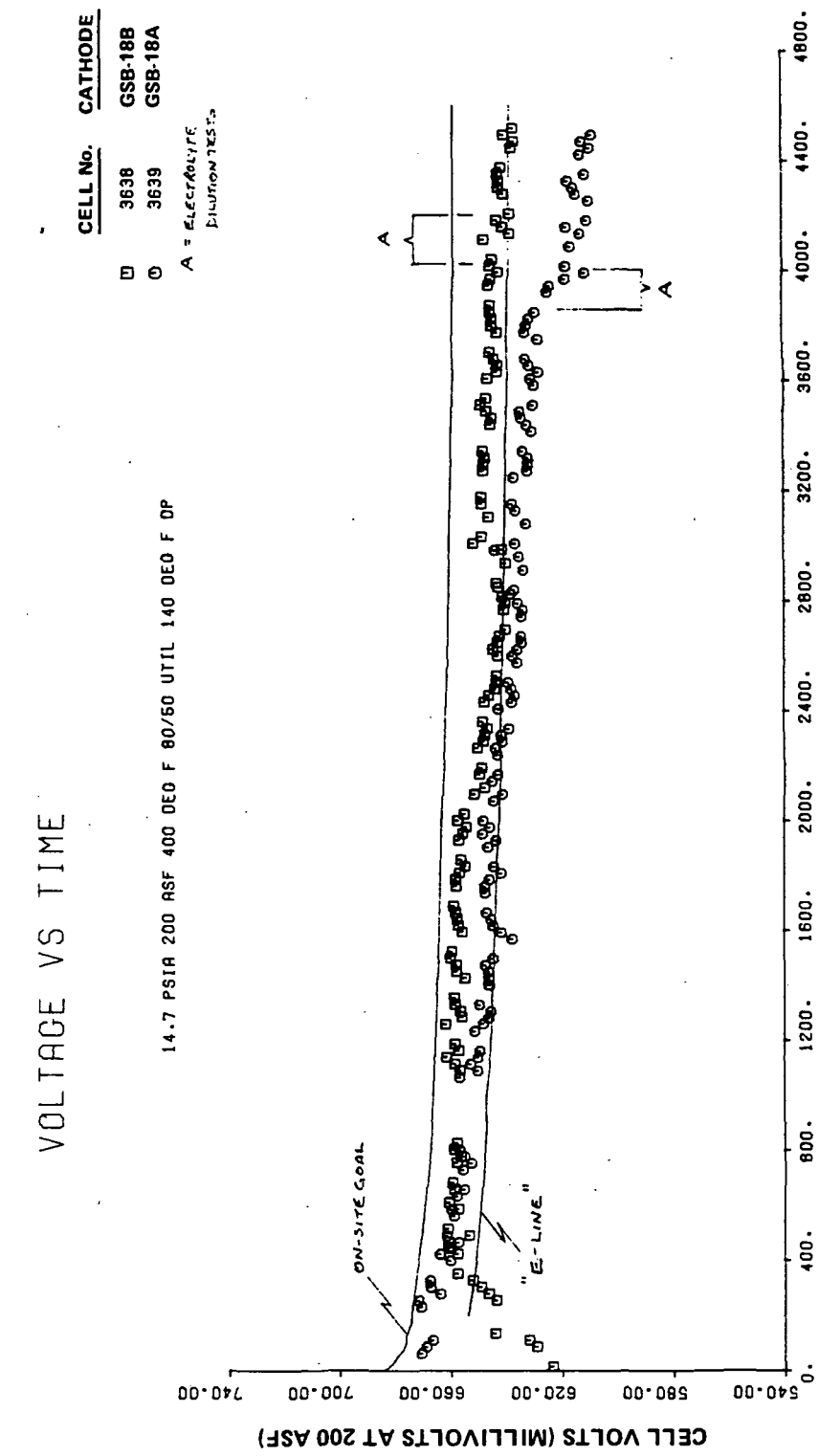

Figure 1-7. Performance History of Series II Cells

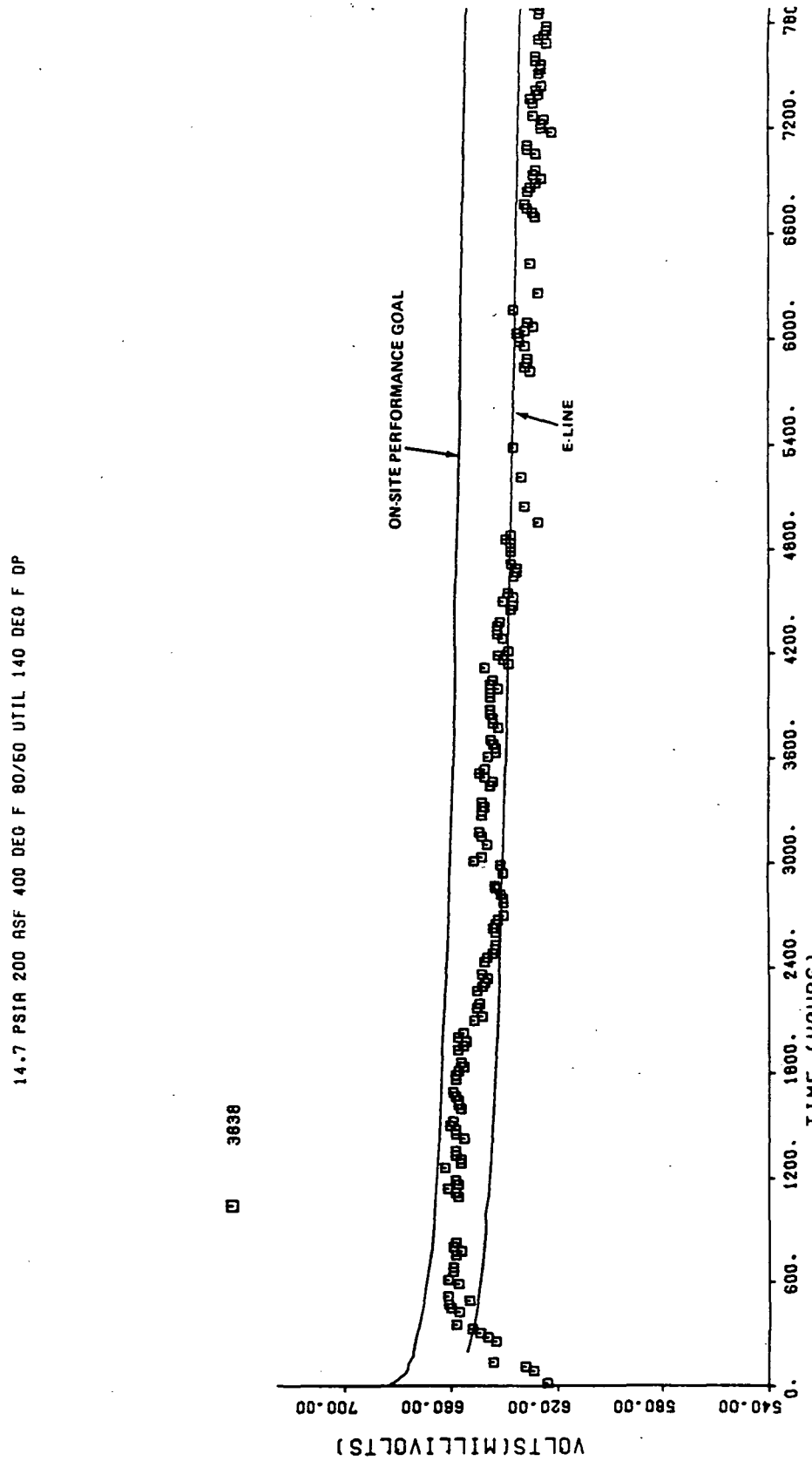

Figure 1-8. Performance History of Cell 3638

Evaluation of Production Catalysts and Electrodes

Catalysts and electrodes prepared in the laboratory that have shown acceptable performance and stability in subscale cell tests are subsequently evaluated in full size stacks. This involves increasing the catalyst batch sizes from grams to kilograms in order to provide sufficient catalyst for the larger electrodes. To evaluate the scaleup trials, sections cut from experimental fabrication runs of full size electrodes are tested in subscale cells. Electrodes that are finally selected for stack testing are also pre-tested in subscale cells to obtain a preview of their behavior and operating characteristics.

Subscale Tests of 30-Cell Stack Electrodes - Both wet mix and dry mix procedures were used to make catalyst layers for the 3.2-ft^2 electrodes in the 30-cell stack, as described in Subtask 2.4. The dry mix electrode procedures were developed in the associated GRI On-Site Technology Development Program.

To obtain a preview of the stack performance, pieces cut from 3.2-ft^2 electrodes were built into 2-inch by 2-inch cells. Descriptions of these cells and their short-term performance are given in Table 1-4.

TABLE 1-4. SUBSCALE CELL TESTS OF ELECTRODES OF THE TYPES USED IN THE 30-CELL STACK

Cell #	Cathode	Anode	Load Time (Hours)	Cell Voltage (Volts at 200 ASF)
3700	GSB-18 Wet Mix	HYCAN Dry Mix	953	0.642
3701	GSB-18 Wet Mix	HYCAN Wet Mix	831	0.627
3707	GSB-18 Dry Mix	HYCAN Dry Mix	593	0.624

Operating Conditions: 200 ASF; 400°F. Dry air at 50% utilization. Fuel (70% H_2, 1% CO, 29% CO_2) at a dew point of 140°F and 80% utilization.

Performance levels of subscale cells containing stack electrodes are lower than the Series II cells, whose average performance was 0.650V at 200 ASF at the same load time.

Cell 3707 was damaged due to a test stand malfunction, the other two cells have now run for over 4000 hours and their performance histories are shown in Figure 1-9. This figure also shows the average performance of cells in the 30-cell stack and confirms the usefulness of subscale cell tests in predicting the performance of full size components. Development work designed to raise the performance level of the production electrode is in progress under the GRI On-Site Technology Development Program.

Evaluation of Production Electrodes

Two subscale cells with shop-made GSB-18 cathodes (Builds 3739 and 3771) and two cells with shop-made GSB-26 cathodes (Builds 3751 and 3772) have been started recently to obtain long-term endurance data on scaled-up catalysts and electrodes. The GSB-26 is a derivative of the GSB-18 and, in laboratory versions, has shown improved performance when tested under the GRI On-Site Program. These tests will be continued through 1984.

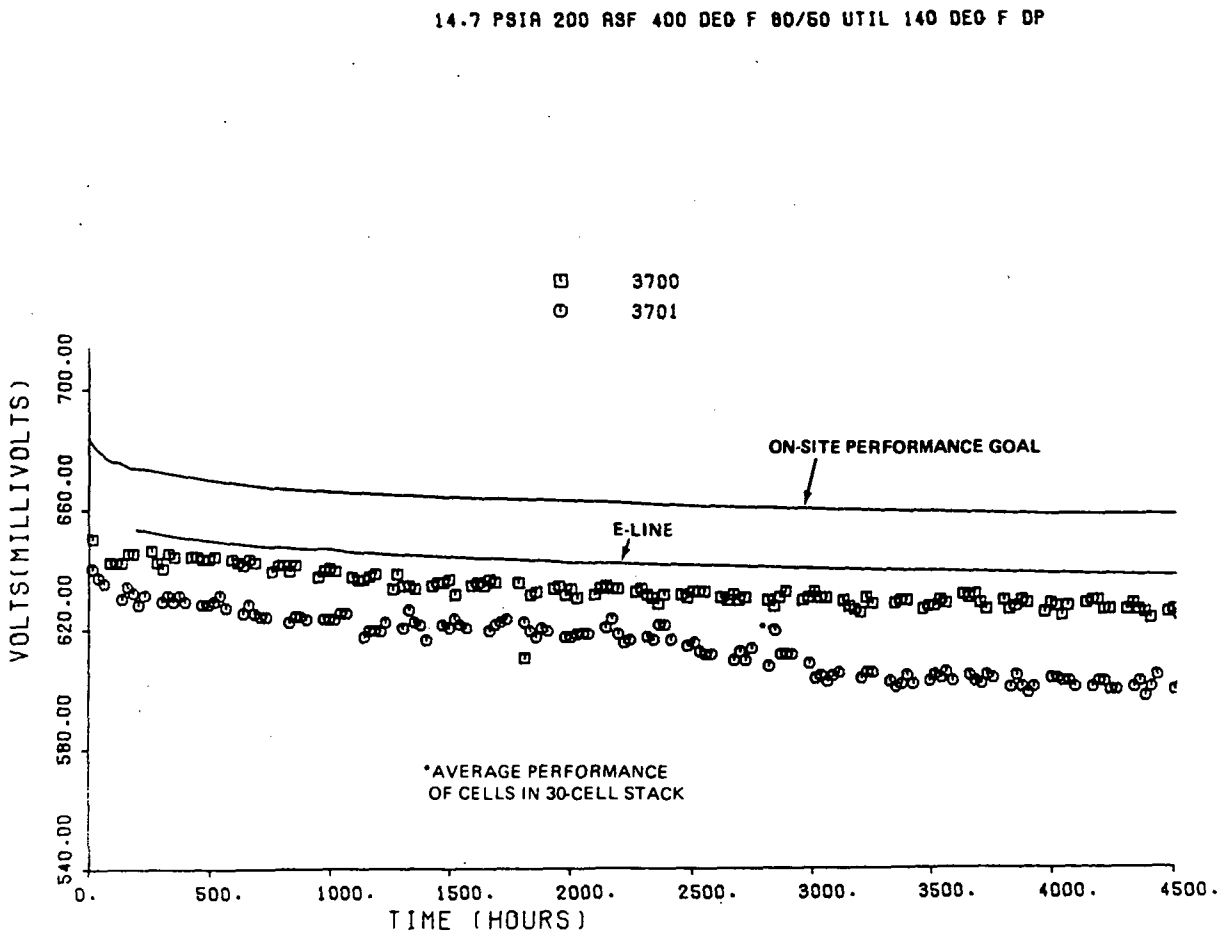

Figure 1-9. Stack Cell Performance Compared to Subscale Cell Performance

TASK 2 STACK DEVELOPMENT

TASK 2 - STACK DEVELOPMENT

Subtask 2.1 - Electrode Substrate Technology

Objectives

The objectives of this subtask are to increase the acid storage capacity of the cell by approximately 50% without compromising performance or cost, and to develop lower cost substrate materials. To increase acid storage, a dual porosity substrate will be formed having finer pores in the rib than in the web, thereby providing the capacity for storing additional acid in the rib. To reduce costs, mass produced precursors are being heat treated to produce fuel cell substrates.

Summary

Dual porosity substrates were formed on the dual belt substrate machine, developed in the Electric Utility Technical Development Program (DEN3-191), by forming web and substrate layers in separate operations. The effective diffusion coefficient of the dual porosity substrates indicates a lower diffusional resistance than that of a conventional substrate with an equivalent electrolyte fill. Two-inch by two-inch cells containing dual porosity substrates were started at the end of the period and are being performance tested. Performance is good, and will ultimately be determined as a function of electrolyte fill and compared to that of a standard substrate.

The influence of fiber diameter on the substrate's pore spectra was determined through tests using combinations of two and three distinct fiber diameters. It was found that median pore size and the breadth of pore distribution are a function of weighted fiber diameter.

Scaleup of low cost substrates, demonstrated previously at the subscale level, was initiated. Vendors having the potential to produce the requisite precursors were identified. Two production runs of material were made. Parts from both runs were unacceptable after carbonization, due to delamination in one case and cracking in

another. Minor changes in materials and processing are being made to overcome these problems.

Highlights

- Dual porosity substrates achieved performance equivalent to conventional substrates.
- Dual porosity substrates have lower diffusional resistance than conventional ribbed substrates with an equivalent electrolyte fill.
- The pore spectra of a substrate can be broadened by using combinations of fibers with larger diameters.
- Median pore size increases as fiber diameter increases.

Discussion

Dual Porosity (Electrolyte Management) - Initial development of dual porosity substrates under GRI Contract 5080-344-0405 showed that the desired acid distribution could be obtained, but electrode performance was deficient. "Second generation" dual porosity handsheets, with the rib layer containing a combination of standard and short, or "whisker", fibers increased electrolyte storage by shifting the pore spectra between the rib and web components. Typical pore spectra are shown in Figure 2.1-1.

Two-inch by two-inch cells built from handsheet bilayers had marginal performance due to higher-than-normal diffusion losses. The cause of the high diffusion losses was not understood and pointed to the need for a more analytical technique to characterize substrate diffusion resistance.

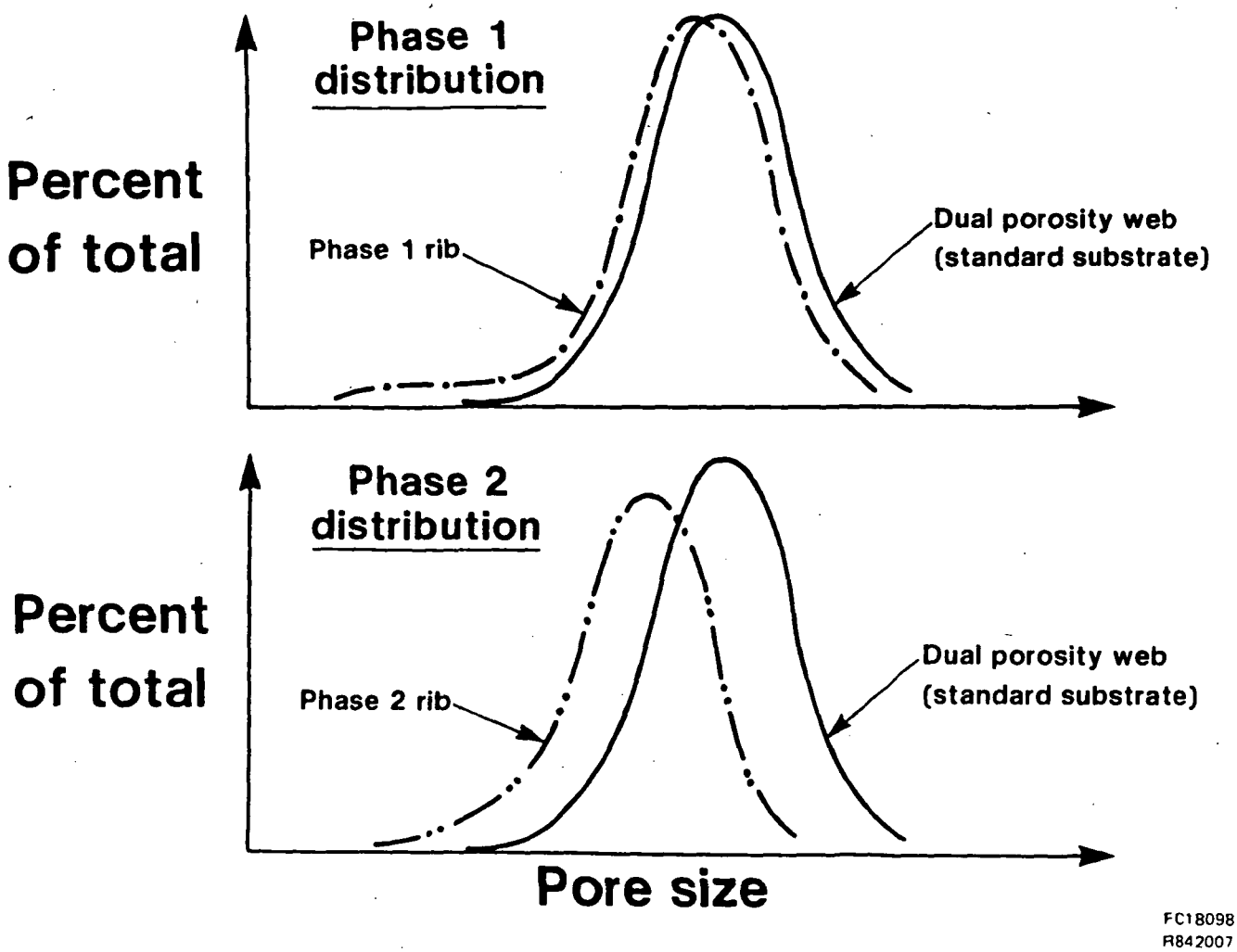

Figure 2.1-1. Pore Distribution of Dual Porosity Substrates

An apparatus and measurement technique was developed to measure the effective diffusion coefficient of a substrate. A schematic of the apparatus is shown in Figure 2.1-2. Substrate samples 1-1/8 inches by 1-1/8 inches are mounted on Teflon® gaskets with an open area of 7/8-inch by 7/8-inch. Three substrate samples are stacked one on top of the other, with rubber-type spacers between the Teflon gaskets to facilitate good sealing. SF_6 is used as the diffusing gas and N_2 as the purge gas. A pressure transducer that measures 1/10,000" H_2O is used to monitor ΔP across the sample. The apparatus and technique have been used to measure the effective diffusion coefficient of flat electrode samples, conventional ribbed substrate samples, and dual porosity ribbed substrate samples. Figure 2.1-3 shows how ribbed, dual porosity samples compared with a conventional ribbed sample. It should be noted that the dual porosity samples have a somewhat higher diffusion coefficient at equivalent electrolyte fills. The dual porosity diffusion data is an average of the data obtained on first and second generation components. The dual porosity substrates that exhibited high diffusional losses were made as handsheets. The dual porosity substrates tested this year were made on the double belt substrate machine and did not have a diffusion problem. The difference in behavior between the two groups is attributed to differences in fabrication procedure.

The feasibility of manufacturing dual porosity substrates was investigated by forming full size dual porosity substrates on the double belt substrate machine. Standard length fibers were used to form a low density web 25-30 mils thick. The desired rib density was achieved with both first generation and second generation handsheet approaches. The first generation approach used an alternate fiber 30% shorter than the standard fiber. The second generation approach uses a 50/50 combination of regular standard fibers and standard fibers that were chopped to 1/10 of their original length. The rib layer was deposited on the previously cured web layer, and the two layers were joined by hot compaction.

Seventy full size dual porosity substrates were formed, carbonized, and graphitized. Four typical full size parts were used for electrode processing. One anode and one cathode were made for both first and second generation dual porosity substrates.

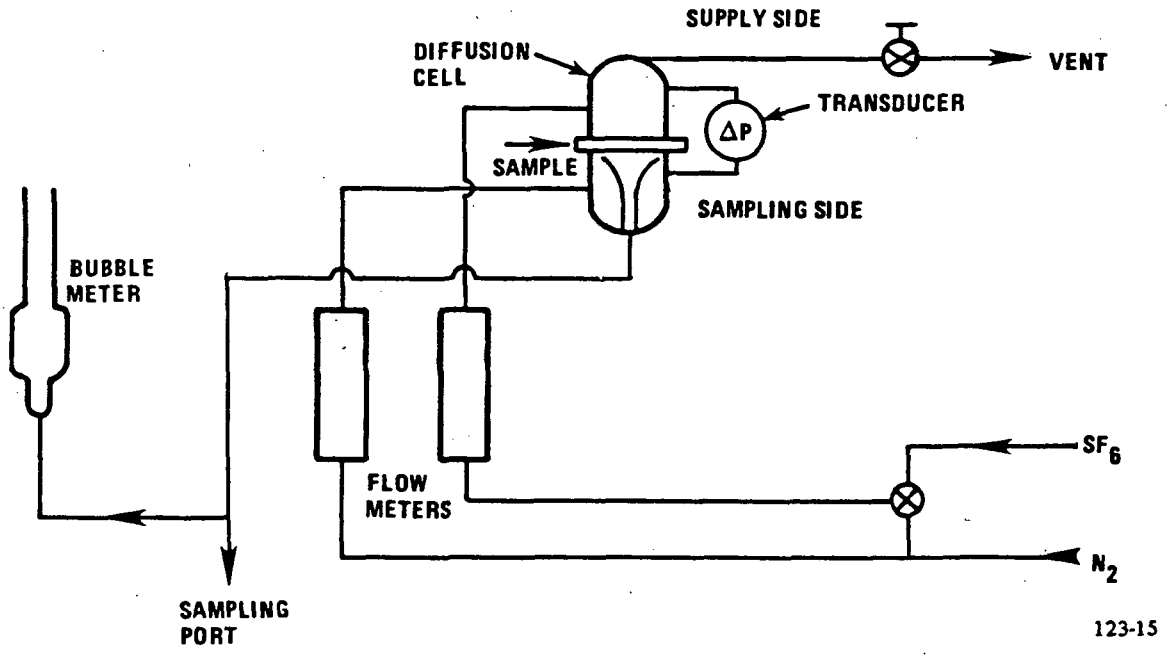

Figure 2.1-2 Schematic of Diffusion Apparatus

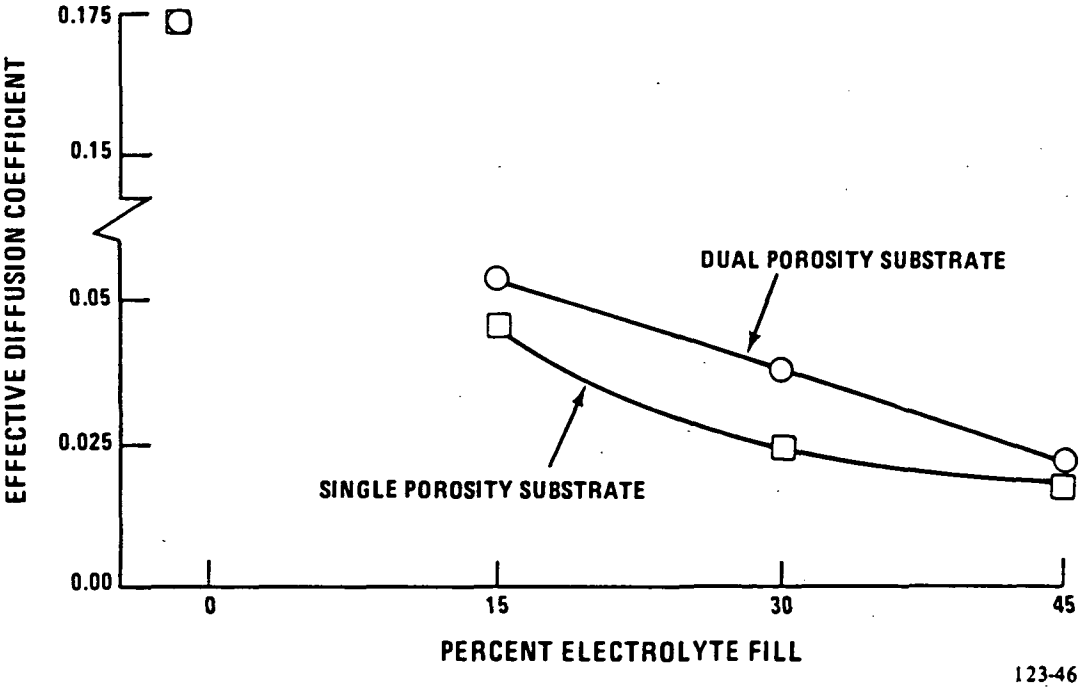

Figure 2.1-3 Effective Diffusion Coefficient vs. Percent Electrolyte Fill for Dual Porosity and Single Porosity Substrates

Diffusion samples were formed from both types of dual porosity substrates also. Two-inch by two-inch cell performance and diffusion results are reported herein.

Subscale cells containing dual porosity substrates made on the dual belt substrate machine were started near the end of the reporting period. Initial performance of the cells is very good. The initial electrolyte fill is equal to 30% of the substrate void volume. Additional electrolyte fill will be added in increments and the performance as a function of percent fill will be compared to a conventional ribbed substrate.

Build	Configuration	Time	Volts/200 ASF	E-Line
3762	Control (single pore substrate)	282	0.679	.654
3784	1st Generation (dual pore substrate)	278	0.664	.654
3783	2nd Generation (dual pore substrate	278	0.674	.654

Another approach to forming a dual porosity substrate is to vary the pore spectra of the substrate by varying fiber diameter and fiber length. The approach used in the first and second generation handsheets was to vary density by varying fiber length. Experimental fibers comprised of three fiber diameters and three nominal lengths were obtained for use in evaluating the influence of fiber diameter and of fiber length. A test matrix with 28 elements was developed and subscale substrates were formed. The test matrix is summarized in Table 2.1-1.

The substrates include nine made from the basic fiber diameter with variable length, nine made from combinations of two different diameters holding length constant, and ten made from combinations of three diameters holding length constant. The subscale substrates were heat treated and samples submitted for porosimetry.

TABLE 2.1-1. FIBER LENGTH-DIAMETER TEST MATRIX

Sample No.		Nominal Fiber Diameter			1.5 x Nominal Fiber Diameter			2 x Nominal Fiber Diameter			Weighted Fiber Diameter	Mean Pore Size μ	80% Pore Breadth
		0.5 Nominal Length	Nominal Length	1.5 Nominal Length	0.5 Nominal Length	Nominal Length	1.5 Nominal Length	0.5 Nominal Length	Nominal Length	1.5 Nominal Length			
	1	1									1 ND	36.3	31.4-41.3
	2		1								1 ND	34.4	29.7-39
	3			1							1 ND	32.5	28-37.6
	4				1						1.5 ND	43.0	35-49
Nine	5					1					1.5 ND	39.3	33.3-46.3
Basic	6						1				1.5 ND	39.0	32.3-45.7
Batches	7							1			2.0 ND	33.8	28-36.5
	8								1		2.0 ND	60.2	46-68
	9									1	2.0 ND	52.0	39.5-69.3
	10		1/2			1/2					1.25 ND	41.0	33.2-45.7
	11		1/4			3/4					1.37 ND	43.1	35.0-49.8
	12		3/4			1/4					1.13 ND	39.5	32.2-44.9
	13		1/2						1/2		1.5 ND	41.0	34.7-47.1
Nine	14		1/4						3/4		1.75 ND	53.9	43.8-58.7
Binary	15		3/4						1/4		1.25 ND	39.2	31.7-42.5
Combinations	16					1/2			1/2		1.75 ND	69.4	51.3-81.5
	17					1/4			3/4		1.87 ND	52.6	41.8-63.4
	18					3/4			1/4		1.62 ND	50.9	42.5-57
	19		1/3			1/3			1/3		1.5 ND	38.0	29.8-45.7
	20		1/6			1/3			1/2		1.67 ND	50.5	39.8-57.3
	21		1/6			1/2			1/3		1.58 ND	47.8	40.5-55.7
Ten	22		1/6			1/6			2/3		1.75 ND	49.5	41.2-58.3
Three	23		1/2			1/6			1/3		1.42 ND	43.3	36.7-48.2
Component	24		2/3			1/6			1/6		1.25 ND	35.5	30.5-43.2
Combinations	25		1/3			1/6			1/2		1.58 ND	43.2	36.3-49.5
	26		1/3			1/2			1/6		1.42 ND	38.0	32.5-46.3
	27		1/2			1/3			1/6		1.33 ND	40.0	34.3-47.7
	28		1/6			2/3			1/6		1.5 ND	43.5	36.8-53.3

ND = Nominal Diameter

The results of the porosimetry are presented in Figures 2.1-4 and 2.1-5. In these figures pore size is shown as a function of weighted fiber diameter. The attempt to broaden the pore distribution by using combinations of fibers was a qualified success. Figure 2.1-5 shows that the breadth of the pore distribution increases with the weighted fiber diameter.

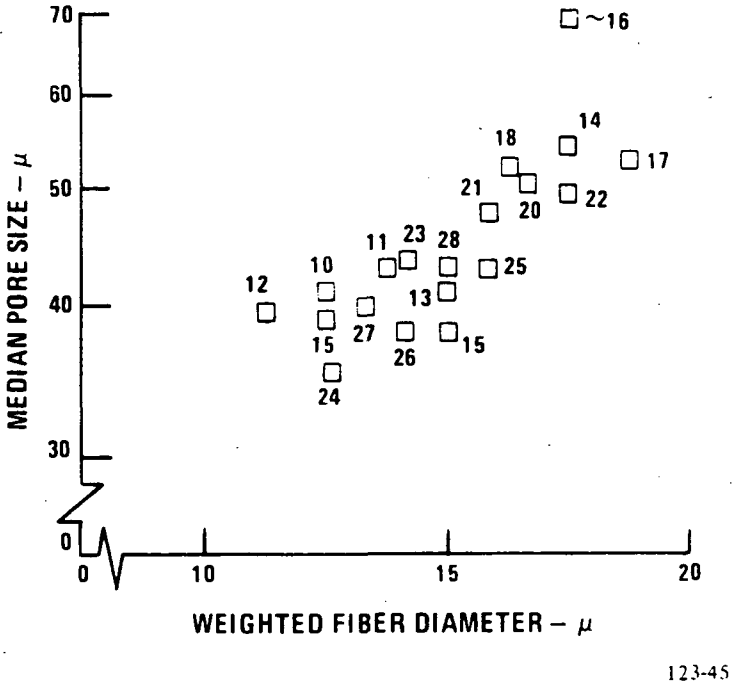

Figure 2.1-4 Median Pore Size vs. Weighted Fiber Diameter

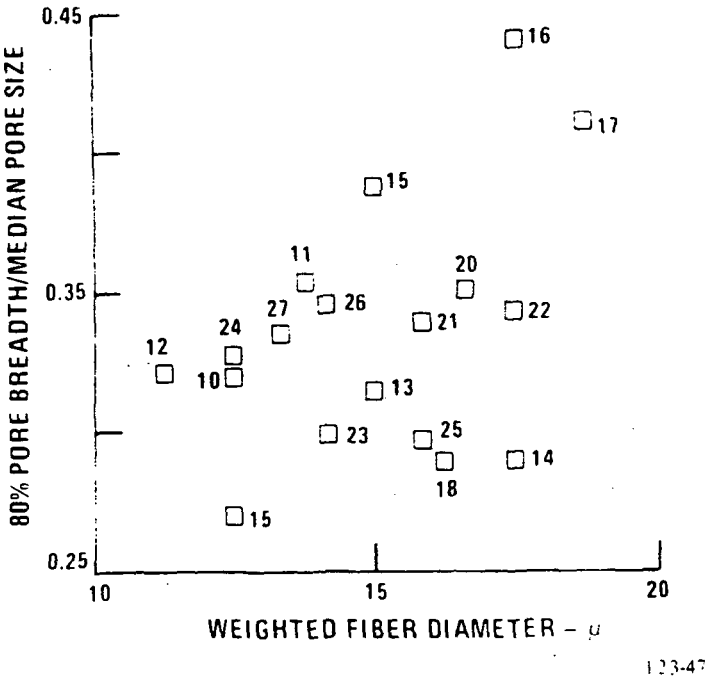

Figure 2.1-5 Breadth of Pore Distribution vs. Weighted Fiber Diameter

Low Cost Substrate Development

The purpose of this effort is to develop a low cost replacement for the conventional graphite fiber-based material presently used in all acid power plants. In order to achieve the lowest possible cost, the approach taken was to identify vendors who could supply appropriate resin-impregnated fiber sheets on a mass produced basis.

These precursor sheets are then converted to useful fuel cell substrates through a series of processing steps.

Several candidate materials have been identified through efforts conducted in this and parallel programs to develop lower cost substrates. An analytical study was done to assess the effect of variations in substrate properties on power section cost. Table 2.1-2 shows the effect of thermal conductivity on power section cost.

The baseline is a substrate made from the standard pitch based carbon fiber with a nominal thermal conductivity of 4 Btu/hr ft °F.

TABLE 2.1-2. EFFECT OF THERMAL CONDUCTIVITY ON POWER SECTION COST

Relative Thermal Conductivity	Change in Power Section Cost
0.25	+6.5%
0.50	+2.4
1.00 (Baseline)	0.0
2.00	-1.6
4.00	-2.7

Table 2.1-3 shows the variation of cell stack cost with substrate electrical conductivity performance differences. The baseline is a substrate made from the standard pitch based carbon fiber with a nominal resistance of 0.5×10^{-2} mv/mil at 100 ASF. These analyses will be used in evaluating the candidate materials.

TABLE 2.1-3. VARIATION OF STACK COST WITH ELECTRICAL CONDUCTIVITY

Change in Performance at 300 ASF	Required Cell Area - Ft^2	Change in Power Section Cost
-30 mV	4.6	+23%
-20	4.4	+19
-10	4.0	+ 7
0(Baseline)	3.7	0
+10	3.3	-10
+20	3.0	-19
+30	2.7	-27

Three vendors having the potential to make the requisite precursor sheets have been identified. Test samples have been received from each of them. Samples from two of them have included variations in resin content and density. These have been processed into substrates, evaluated in out-of-cell tests and, in the case of the best materials, run in subscale cell tests.

In the course of this work it became apparent that the basic carbon structure generated from these precursor materials was less dense than the fiber employed in conventional substrates. This leads to lower thermal and electrical properties at comparable densities. On the other hand, the low cost materials are stronger. This has led to a series of compromises in order to achieve the most cost effective

substrate. Figure 2.1-6 compares the properties of one of the best sample substrates to properties of substrates currently used in power plants.

It can be seen from these data that these new materials are stronger, but as yet do not meet the thermal, electrical, and corrosion properties of the conventional structures.

It was considered appropriate to address the next issue, scaleup to full size sheets, at this point in the program. This decision reflects both the expectation that further development will continue to improve the properties of the new materials, and the concern that the high shrinkage experienced by these precursor materials during heat treatment may lead to cracking or other types of distortion.

An experimental fabrication run of 50-inch by 50-inch sheets was ordered from the vendor. This is the maximum size that present heat treat tooling will allow. Initial heat treat trials with this material revealed a significant delamination problem. Delamination has not been seen in the test samples used in the earlier phase of the treatment. A modified process was developed that was evaluated with handsheets and found to give results similar to those found for the earlier process. An order was then placed for a second production run, this time employing the new process.

The order of approximately 150 sheets of the 50-inch by 50-inch size was recently received from the vendor. Thickness was not as uniform for this run. The edges of the sheets tended to be thicker than the centers. Half of the sheets were stacked in the heat treat furnace, taking care to minimize accumulations of high spots. No delaminations were observed, but only ten of the sheets survived without cracks.

The absence of any delaminations was encouraging. The cracking was believed to have occurred due to hang up of the high spots on the graphite fixtures. The remaining sheets will be microground to a uniform thickness prior to heat treatment.

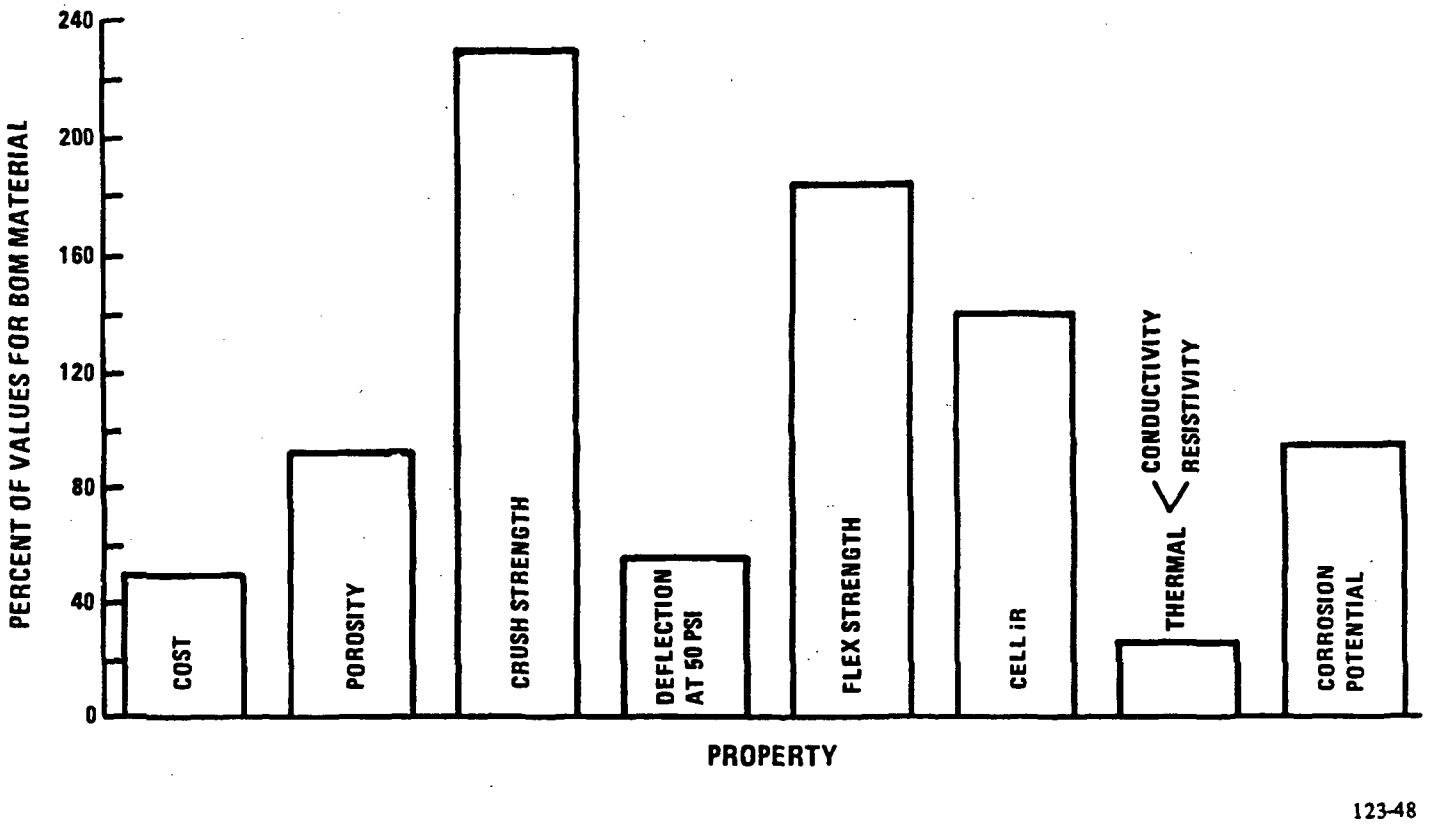

Figure 2.1-6 Low Cost Substrate Properties Compared to Properties of Substrates Used in Power Plants

A third order has also been placed in order to demonstrate improved thickness uniformity and other minor changes. This material will be evaluated in the next report period.

Subtask 2.2 - Cooler Technology

Objectives

The objectives of this subtask are to reduce cooler cost while improving cooler reliability, and to minimize evaporative loss of electrolyte from the cell. Lower cooler cost will be addressed by increasing the number of cells per cooler, through enhanced heat transfer and advanced cooler design. Evaporative losses of acid will be minimized by designing the cell to have a lower exit temperature.

Summary

A totally encapsulated, single-element serpentine cooler has been successfully developed and is being tested in a 30-cell stack. By increasing the cells per cooler from five to ten, and by lowering cooler array costs by a factor of three, cooler costs were reduced by more than 80 percent. Cooler reliability was improved by encapsulating the cooler array in an acid-proofed enclosure and by eliminating the need for small diameter flow control orifices that would prevent cooler-to-cooler flow maldistribution. The acid getter concept significantly reduced corrosion by H_3PO_4 in the cooler tube. Tests are being conducted to define the long-term burst pressure characteristics of the dielectric connector hoses.

Analytical predictions show that the acid condensation zone concept for reducing the acid evaporation rate from a cell has the potential to double the mean time between refills. This concept is being evaluated in a 30-cell stack.

Highlights

- An encapsulated serpentine cooler was developed.
- The encapsulated cooler increased reliability by eliminating flow control orifices.
- The design reduces cooler costs by more than 80 percent.

Discussion

Cooler development activities consisted of analytical studies to define the heat transfer and hydrodynamic characteristics of the serpentine cooler, testing of experimental cooler assemblies in the heat transfer rig to verify their thermal performance, fabrication of cooler assemblies for a 30-cell stack, materials testing to support advanced cooler concepts, and analysis of the acid condensation zone concept to reducing acid evaporation.

Cooler Design - The heat transfer characteristics of the 3/8-inch bare metal serpentine cooler were analyzed. Design conditions were 400°F average cell temperature, 425°F hot spot temperature, 350°F water-steam coolant temperature, and performance corresponding to E-line +20mV at 200 ASF. These conditions can be satisfied by a cooler spacing of 10 cells/cooler for substrates and cooler holders made from the standard pitch based carbon fiber.

The fluid dynamic analysis of the 3/8-inch tube diameter cooler was completed. The pressure drop across the cooler is about 7 psi, and the exit velocity is about 45 ft/sec at rated power with 10 cells/cooler with a nominal exit quality of 10%. The flow characteristics of this cooler configuration are such that flow control orifices are not required to prevent cooler-to-cooler flow maldistribution. A test program was initiated to define the influence of oxygen content and velocity on erosion-corrosion inside 3/8-inch horizontal tubes.

The simplicity of the serpentine cooler results in a cost which is one-third of that of the conventional cooler. The 3/8-inch bare metal serpentine cooler allows the cells per cooler to be increased from five to ten. The combination of these results in a cost reduction of more than 80 percent when compared to the cooler configuration used in the 40-kW power plant.

Heat Transfer Rig - The thermal resistance of an experimental cooler is determined by testing in a heat transfer rig. The rig contains electric heaters which provide a precisely measured heat flux to the cooler. A two-phase water-steam coolant is

circulated through the cooler array at a flow rate of 40 lbs/hr. The cooler assembly is instrumented with thermocouples to define the temperature at the outside surface of the cooler assembly and the coolant inlet and exit temperature. The thermal resistance is calculated from the measured heat flux and temperatures using a UTC-developed analytical model. The 3/8-inch O.D. bare metal serpentine cooler was assembled in a cooler holder and tested in the heat transfer rig. The measured (0.012 hr ft^2 °F/Btu at 1.3 inch tube pitch) for this cooler was determined to agree with the predicted value used to establish the 10 cells per cooler spacing for the 30-cell rig.

Fabrication of Cooler Assemblies for 30-Cell Stack - Cooler assemblies were fabricated for the 30-cell stack tested in Subtask 2.4. The assemblies contain a 3/8-inch single-element bare copper serpentine cooler array and a totally encapsulated cooler holder configuration. The design was developed under the GRI On-Site Technology Development Program. The design requires a 0.05-inch thickness of graphite over gaps associated with the tube bends. Two 0.032-inch thickness were used for this trial because of hardware availability.

The completely encapsulated cooler assemblies for the 30-cell stack were characterized. The measured iR across the cooler assemblies averaged 13 mV at 100 ASF, which amortizes to 1.3 mV/cell at 10 cells per cooler. A gas leak check was made on each cooler assembly to check for leaks at the cooler tube penetrations between the bonded halves of the cooler holder. No leaks were observed. Application of an aggravated 100 psi axial load did not initiate cracks in the sections of the plate associated with the tube bend gaps. Radiographs were obtained of each cooler assembly, which will serve as the basis for comparison at the planned 5000 hour inspection point.

Materials Testing - Support testing on advanced cooler concepts consisted of determination of burst pressure characteristics of Teflon® hoses, verification of effectiveness of acid proofing of encapsulated cooler, proof of concept test of acid getter approach, and initiation of a water-steam erosion-corrosion test.

Dielectric Hoses - The coolers are connected to a coolant manifold with a dielectric hose to prevent electrical shorting. The 3/8-inch O.D. serpentine cooler and coolant operating conditions require a Teflon hose with a 3/8-inch O.D. and a 0.150-inch wall thickness. Tests were run to establish short-term and and long-term burst characteristics of this hose. Initial trials to clamp this hose to the cooler nipples were successful and showed no leakage at 600 psi and room temperature. No leakage was measured after 15 thermal cycles from 70°F to 425°F. Room temperature burst pressure is 1100-1200 psi, which translates to a 400-450 psi burst pressure at 400°F.

Short-term burst pressure data was generated as a function of temperature. The results are:

No. of Samples	Temperature, °F	Burst Pressure, psi
1	375	500
1	375	490
2	400	460
1	425	420

This burst pressure is adequate since maximum operating coolant pressure is 230 psi at 400°F. Tests to define the long-term burst pressure characteristics of this hose are being conducted using procedures outlined in ASTM-D-2837 for evaluating thermoplastic hose materials. A subcontract was issued to a testing laboratory familiar with the ASTM-D-2837 procedure for distinguishing burst pressure characteristics of thermoplastic hose materials. Characterization of the long-term burst strength of the advanced 3/8-inch dielectric hoses continues. Burst strength is being determined as a function of time at temperatures of 350°F and 400°F. Some of the samples have reached 3600 hours of a planned 10,000 hour test. Statistically significant data will be reported.

Verification of Encapsulated Cooler Concept - Mockups of encapsulated coolers were fabricated to evaluate the design's acid-proofing effectiveness. Three 12-inch by

12-inch mockups of the uncoated encapsulated cooler completed 2000 hours of testing at 375°F in a simulated stack acid environment. Acid take-up of the assemblies was low, approximately 20% of the void volume of the separator plates. Comparison of radiographs taken at 2000 hours with pre-test radiographs showed no signs of corrosion. One assembly was dismantled and visually examined and there were no signs of corrosion.

Acid Getter - An acid getter was incorporated into the cooler assembly to protect the metal cooler tubes from corrosion in the event of an encapsulation failure. Corrosion tests were run to establish the effectiveness of this concept. This test simulates a failure of the cooler holder encapsulation. Samples were examined after 1000 and 3000 hours exposure to acid. In both cases the copper tube tested in the presence of the getter exhibited significantly less corrosion than a copper tube tested as a control.

Erosion-Corrosion - Coolant side corrosion of the cooler array is a concern due to the high velocities intrinsic in a single-element serpentine cooler. The heat transfer rig was redesigned to evaluate cooler erosion under controlled conditions. Major changes consist of increasing the power density of the heaters to increase the heat flux to the coolers, increasing the coolant flow from 40 to 200 lb/hr, addition of a feedwater system that will allow the dissolved O_2 level to be controlled, and the addition of ion-exchange beds that will allow pH to be controlled. A schematic of the test stand is shown in Figure 2.2-1. Construction and testing of the erosion-corrosion rig was completed. A stainless steel cooler array was obtained for evaluation in this rig and the rig was assembled. Testing will begin in December 1983.

Acid Condensation Zone - Success in increasing cell performance in Task 1 will result in higher operation current densities and increased acid evaporation rates. The objective of the acid condensation zone is to lower the rate of acid evaporation from the stack. This is accomplished by lowering the air temperature at the cell exit. This approach was incorporated into the 30-cell stack that is currently being tested. Analytical predictions indicate the reduced acid loss will increase time between acid replenishment by 85 percent, compared to conventional cell stack

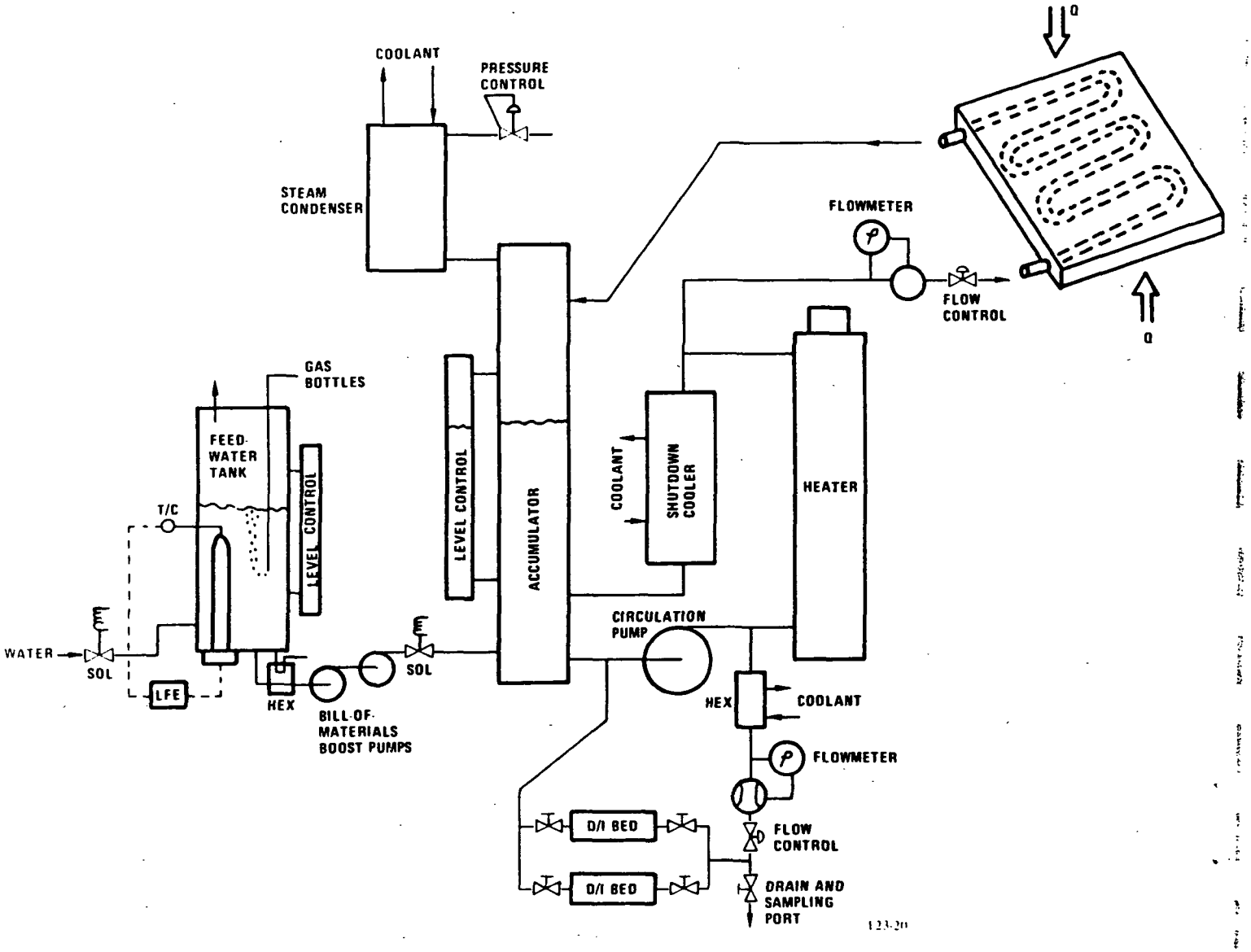

Figure 2.2-1 Test Stand Schematic

designs where no special edge cooling is used. Plans are to test this stack 5000 hours and then dismantle it and obtain acid inventory data. The data obtained will be the basis for verifying this particular design.

Subtask 2.3 - Non-Repeat Component Technology

Objective

The objective of this subtask is to extend stack overhaul period by developing a method of periodically adding electrolyte to the cells in the field. Subscale component tests will assess previously identified methods of electrolyte addition. The most promising approach compatible with the current cell and stack configuration will be evaluated in a non-operating stack of approximately 270 cells and in an operational short stack if appropriate.

Summary

An approach to replenish acid in a stack was developed. Three refill concepts were previously identified under GRI contract 5080-344-0405: drip-wicking, acid injection, and spray. Ten-cell, quarter-scale mockups of the three concepts were evaluated. The spray approach was selected for trials on a 40-kW stack after it was judged to be the fastest, most reliable, least sensitive to stack tilt, and having a moderate cost. The feasibility of the spray approach as a means to add acid was evaluated with a 270-cell 40-kW size stack. The process was completed in one hour. This concept will be evaluated on the 30-cell stack when it is rebuilt at 5000 hours to determine whether refill affects cell performance.

Highlights

- Evaluated drip-wick, acid injection, and spray approaches to acid addition in laboratory tests.
- Selected spray approach for trials on a 40-kW stack.
- Evaluated feasibility of acid refilling via the spray approach on a 270-cell 40-kW stack.

Discussion

The three fill concepts have several common features: acid is added to a non-operating stack, one electrode of each cell is saturated with dilute acid, and acid slowly redistributes within the cell as the acid is concentrated to operating concentration during a modified stack start-up cycle. The fill apparatus is the means to supply acid to each cell.

Drip-Wick Approach - The drip-wick approach to acid addition is a subject of a patent disclosure, therefore, discussion of this approach must be limited at this time. Testing of a quarter-scale, 10-cell mockup of this approach resulted in fill within 30 minutes. Teardown confirmed the electrode substrates were saturated with acid.

Acid-Injection Approach - The acid injection approach adds acid to each cell by a small diameter Teflon® tube. This tube is inserted into a reactant flow channel at each cell. The individual tubes are gathered into a bundle, and the bundle is sealed to form an acid distribution reservoir.

A quarter-scale, 12-cell mockup of this approach was evaluated. The test was run on a subscale stack consisting of three groups of cells separated by one foot spacers, giving a total height of two feet. The separator plates contained tabs. This was done to evaluate the effect of tube length on acid flow distribution. Acid flow through the tubes, which had lengths of 11, 22, and 33 inches, was found to be within 10% uniformity, with a 12-inch acid head in the reservoir.

During acid addition, the flow channel containing the Teflon tube is the first to fill with acid. The acid flows out of this channel and is laterally transported across the face of the stack by the tabs on the separator plates. The acid is wicked into the cell by the reactant flow channels. The excess acid cascades down the face of the stack and is collected from the bottom of the reactant manifold. Again the cells were visually saturated with acid in about 30 minutes. The mockup was disassembled and gravimetrically verified that the substrates were saturated with acid.

Spray Approach - The spray approach adds acid to the cell by spraying the face of the stack with acid.

A plexiglass manifold was built to fit the quarter-scale, 10-cell mockup. Candidate spray nozzles were mounted into this manifold. Acid was applied to the face of the stack and wicked down the flow channels. Within 15 minutes the flow channels were visually saturated. Teardown analysis confirmed that the substrates were filled. No obvious acid distribution or acid containment problems were observed.

Teflon is the preferred nozzle material because of its corrosion resistance. A test was run to evaluate the stability of the Teflon spray nozzles. The nozzles were aged in air at 400°F. Determination of the spray pattern after 1000 and 1700 hours aging showed no deterioration of the spray pattern when compared to a new nozzle.

Selection of Approach for Full-Scale Mockup Test - The basic conclusion from the subscale work is that the drip-wick, spray, and acid injection concepts are all feasible. The rationale for selecting one approach over another comes down to cost and reliability. A qualitative comparison of three approaches is presented in Table 2.3-1.

TABLE 2.3-1. COMPARISON OF ELECTROLYTE ADDITION APPROACHES

Refill Approach	Hardware Complexity & Cost	Rate of Refill	Sensitivity to Stack Tilt	Estimated Reliability
Drip-Wick	Lowest	Slowest	Highest	Lowest
Spray	Intermediate	Fastest	Lowest	Highest
Injection	Highest	Intermediate	Intermediate	Intermediate

The spray approach is the fastest, most reliable, least sensitive to stack tilt, and has a moderate cost. This approach was selected for evaluation in a 270-cell mockup.

Acid Addition to 40-kW Stack

Acid refill trials were conducted on a used 270-cell 40-kW stack to evaluate the feasibility of the overall refill approach. Approximately 100 cells were replaced with new cells. The new cells were filled with varying amounts of acid; some cells were empty, while others were 10, 20, and 30% full. These cells were assembled into six-cell substacks, and the substacks were located throughout the entire stack. A reactant manifold was modified to contain four spray nozzles, and plexiglass sections were installed on two manifolds to permit visibility during the spray refill process. The suitability of the spray nozzles and support equipment was verified using 50% H_3PO_4. A teardown inspection will then be conducted to determine the acid inventory of each specially filled cell.

An acid addition trial was completed on this stack. A photograph of the acid spray rig is shown in Figure 2.3-1. A total of 19.6 gallons of 50% H_3PO_4 was added to the stack in approximately 63 minutes, and the acid was sprayed at a rate of approximately 0.5 gpm. The reactant flow channels on the electrode exposed to the acid spray were all visually filled with acid at the end of this period. Excess acid present on the separator plate tabs when the flow was stopped was absorbed by the cells in a period of 60 minutes. The acid was contained in the reactant manifolds. There was no external leakage of electrolyte and no operational problems were noted. No shunt currents were observed after the refill cycle had been completed.

The acid in the stack will be concentrated from 50% to 80% H_3PO_4 by flowing inert gas across the stack. The stack will then be disassembled and the acid gained by each cell determined gravimetrically.

Subtask 2.4 - Cell Stack Testing

Objective

The objective of this task is to evaluate previously developed stack components in a 30-cell stack. This stack will be used to evaluate the performance and decay characteristics of electrodes containing advanced catalysts at on-site power plant

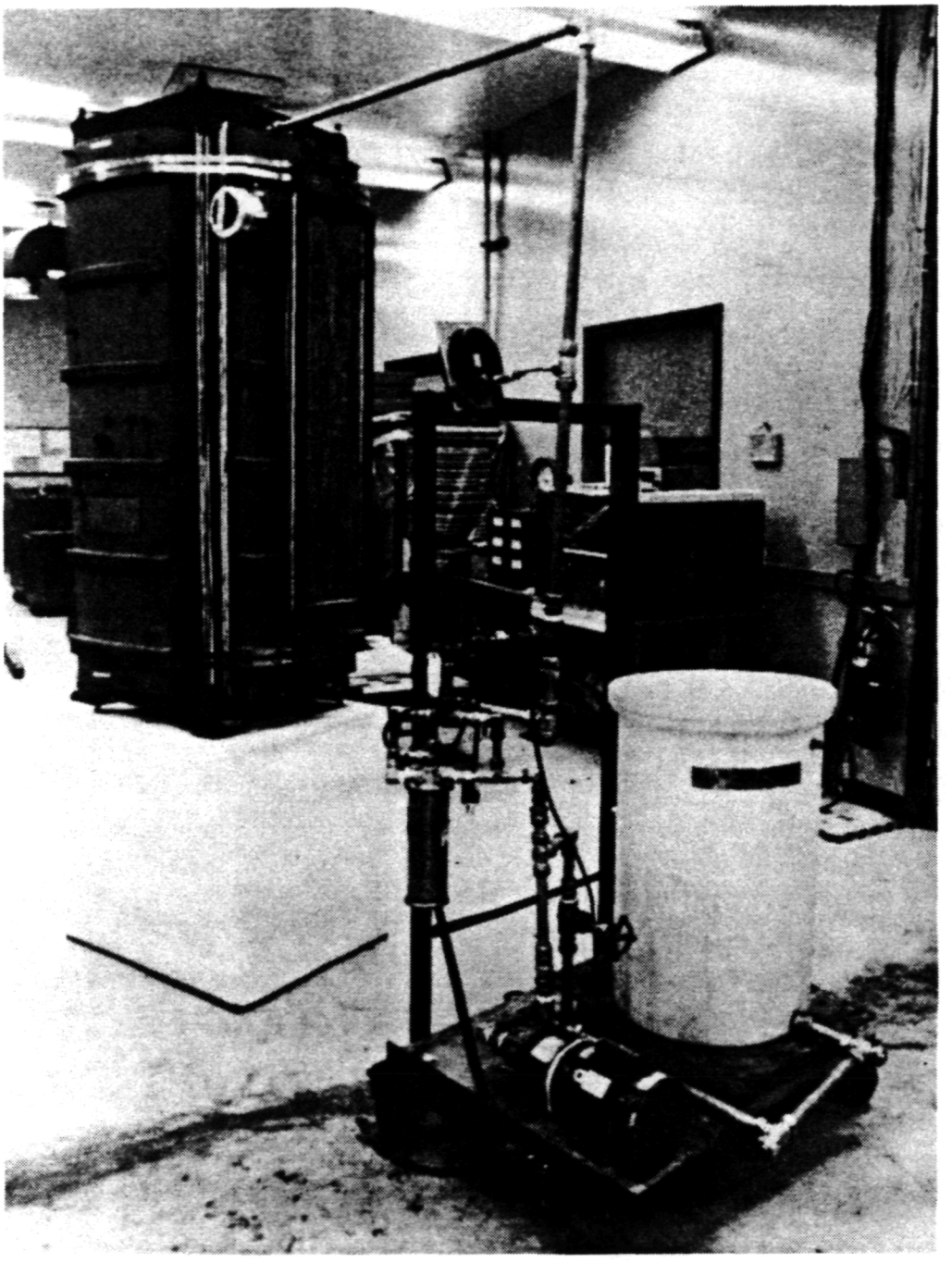

WCN-10844

Figure 2.3-1 Acid Replenishment Test Rig

operating conditions. The components in this stack contain advanced features developed in this program and in parallel programs. The test program will be conducted for 5000 hours, after which the stack will be disassembled and a non-destructive post-test analysis will be performed on the components. The stack will be reassembled for additional testing if judged useful and if the components are acceptable.

Summary

An advanced technology 30-cell stack with a 3.2-ft^2 active area was fabricated, assembled, and tested. Component features being evaluated are a totally encapsulated, single-element serpentine cooler at 10 cells/cooler; electrodes containing an acid condensation zone and acid refill provisions; a GSB-18 cathode catalyst with wet mix and dry mix formulations; substrates made with two-stage resin; lower cost silicon carbide in matrix; and a new end plate configuration. The stack was tested at 14.7 psia, 400°F average cell temperature, and at 200 ASF. Test time was 2900 hours at the end of November, and the test is continuing. Performance of the encapsulated cooler met design requirements at 10 cells/cooler. Performance was 5-10 mV below E-line and tracked E-line for 2900 hours. Performance and stability of the dry mix electrodes was equal to the wet mix electrodes. Two PPS-coated steel manifolds were installed on the stack at 2700 hours. The test program will continue to 5000 hours, after which the stack will be disassembled and a non-destructive post-test analysis will be performed on the components. The stack will be reassembled for additional testing if judged useful and if the components are acceptable.

Highlights

- Tested an advanced technology 30-cell stack for 2900 hours at 14.7 psia, 400°F, and 200 ASF.

- Totally encapsulated, single-element serpentine cooler performance met design requirements at 10 cells/cooler.

- Electrodes contained an acid condensation zone to minimize acid evaporation and also contained acid refill provisions.

- Performance was 5-10 mV below E-line and tracked E-line for 2900 hours.

- Performance and stability of the dry mix electrodes was equal to the wet mix electrode.

Discussion

An advanced technology 30-cell stack was fabricated, assembled, and endurance tested for 2900 hours. This 30-cell stack contains the following special features:

- Thirty cells with GSB-18 cathode catalyst and HYCAN anode catalyst. Both dry mix and wet mix anode and cathode catalyst formulations are being evaluated.

- Totally encapsulated, single-element uncoated serpentine coolers with 10 cells per cooler.

- Acid condensation zone to reduce acid loss.

- Acid refillable cell configuration.

- End plate cell contact surface formed by bonding half cooler holder to porous carbon end plate.

- Carbon fiber material used to achieve low resistance contact between end plate and current collectors.

- Lower cost matrix material.

A photograph of this stack is presented in Figure 2.4-1, which shows the completed stack assembly prior to installing the thermal insulation and connecting to the test facility.

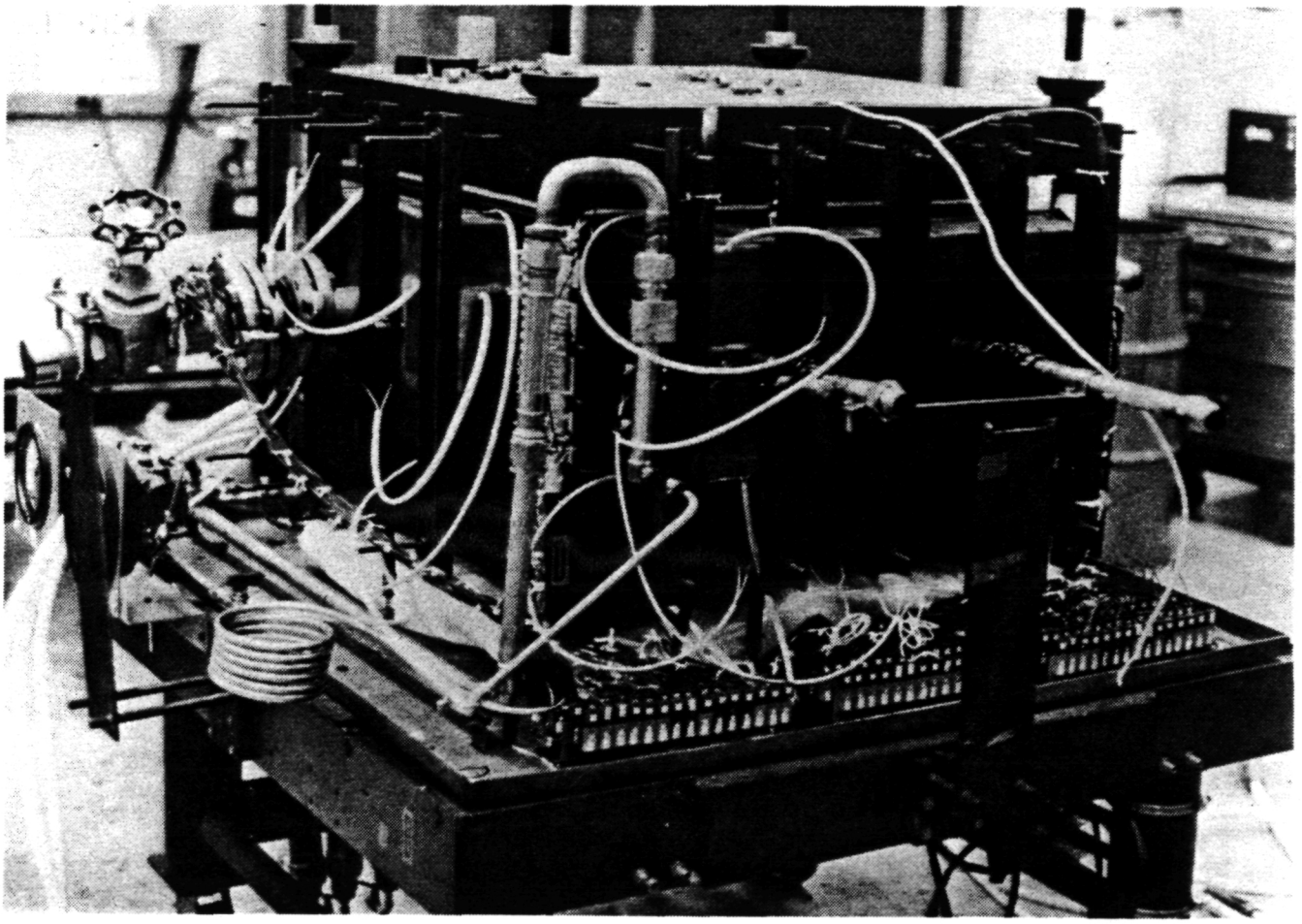

WCN-10438-5

Figure 2.4-1 Stack Assembly, Prior to Thermal Insulation

The endurance test is being conducted at 14.7 psia reactant pressure and at 400°F average cell temperature. The cell operating conditions are 200 ASF, 80% fuel utilization, 60% air utilization, and 148°F fuel dew point.

The performance characteristics of this stack have been documented by a series of diagnostic tests that were run at 300, 1200, and 2800 hours of operation. These diagnostic tests include a cell performance calibration, cell performance change with test time, reactant gas utilization sensitivity to cell performance, anode and cathode performance gains for pure reactant gases, reactant gas crossover and leakage, cell package electrical resistance, cell and stack thermal profile, and axial load reduction with test time. (Cathode oxygen gain measurement is run only at 3000 and 5000 hours because of the difficulty of the test.)

The cell performance calibration data compared to E-line performance is presented in Figure 2.4-2. The cell performance history is presented in Figure 2.4-3. This data is also compared to the E-line performance goal decay rate and it indicates that the performance is stable and 5 to 10 mV below the goal through 2900 hours of operation. The cell to cell performance variation is presented in Figure 2.4-4. This indicates that the performance level of the different types of catalyst formulations is essentially the same. The performance difference that is indicated in this data is due to the differences in the cooler assembly electrical resistance.

The reactant gas utilization effect on cell performance is presented in Figure 2.4-5. This indicates that the change in cell voltage is at the predicted or theoretical level.

The anode and cathode performance gain for pure reactant gases is presented in Figure 2.4-6. The cathode performance gain was documented at 300 hours. The anode performance gain was documented at both 300 and 2800 hours. This indicates that there is no change in the anode performance. The anode and cathode performance gains are also at the expected levels for these types of anode and cathode catalysts.

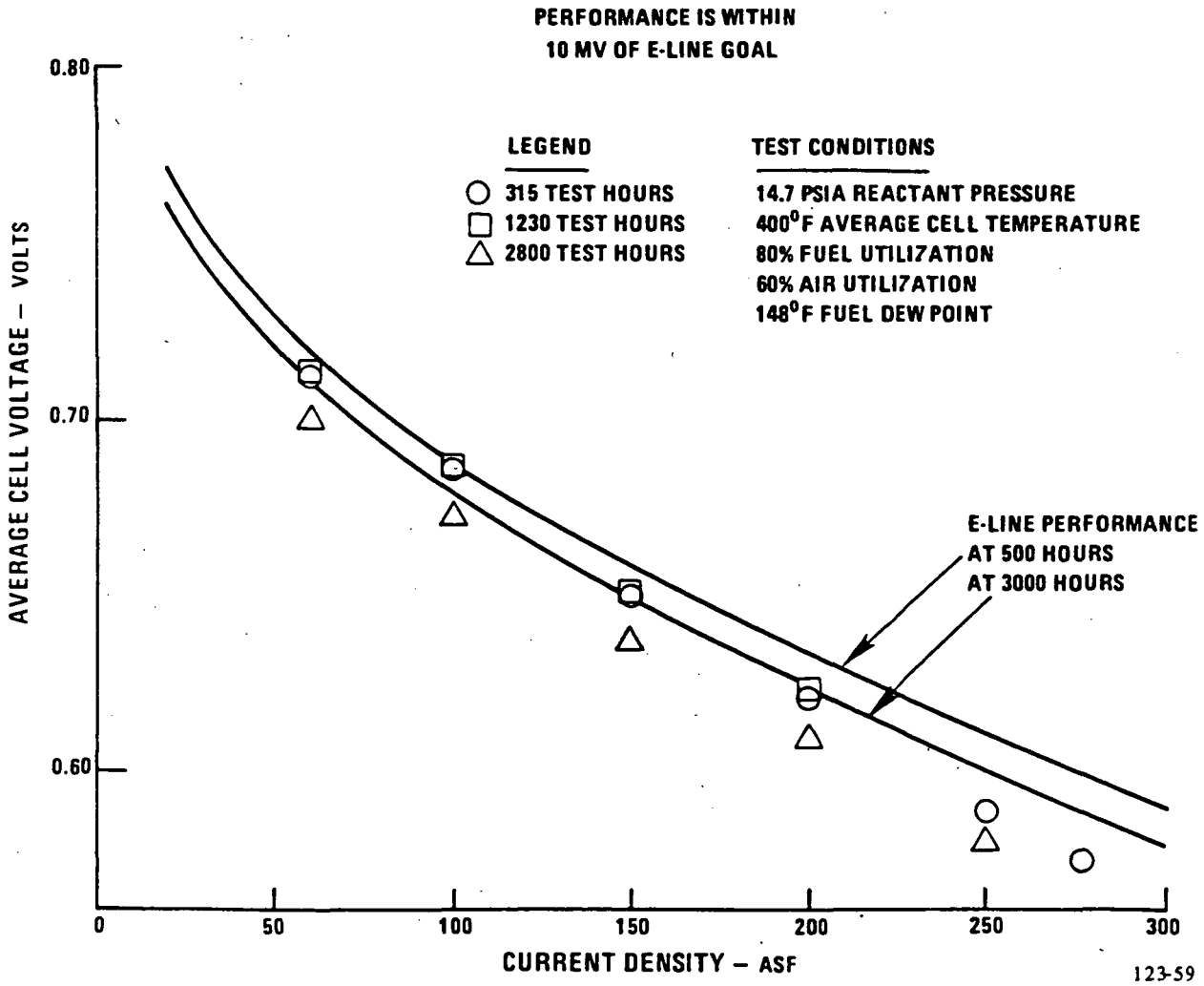

Figure 2.4-2 Average Cell Voltage vs. Current Density

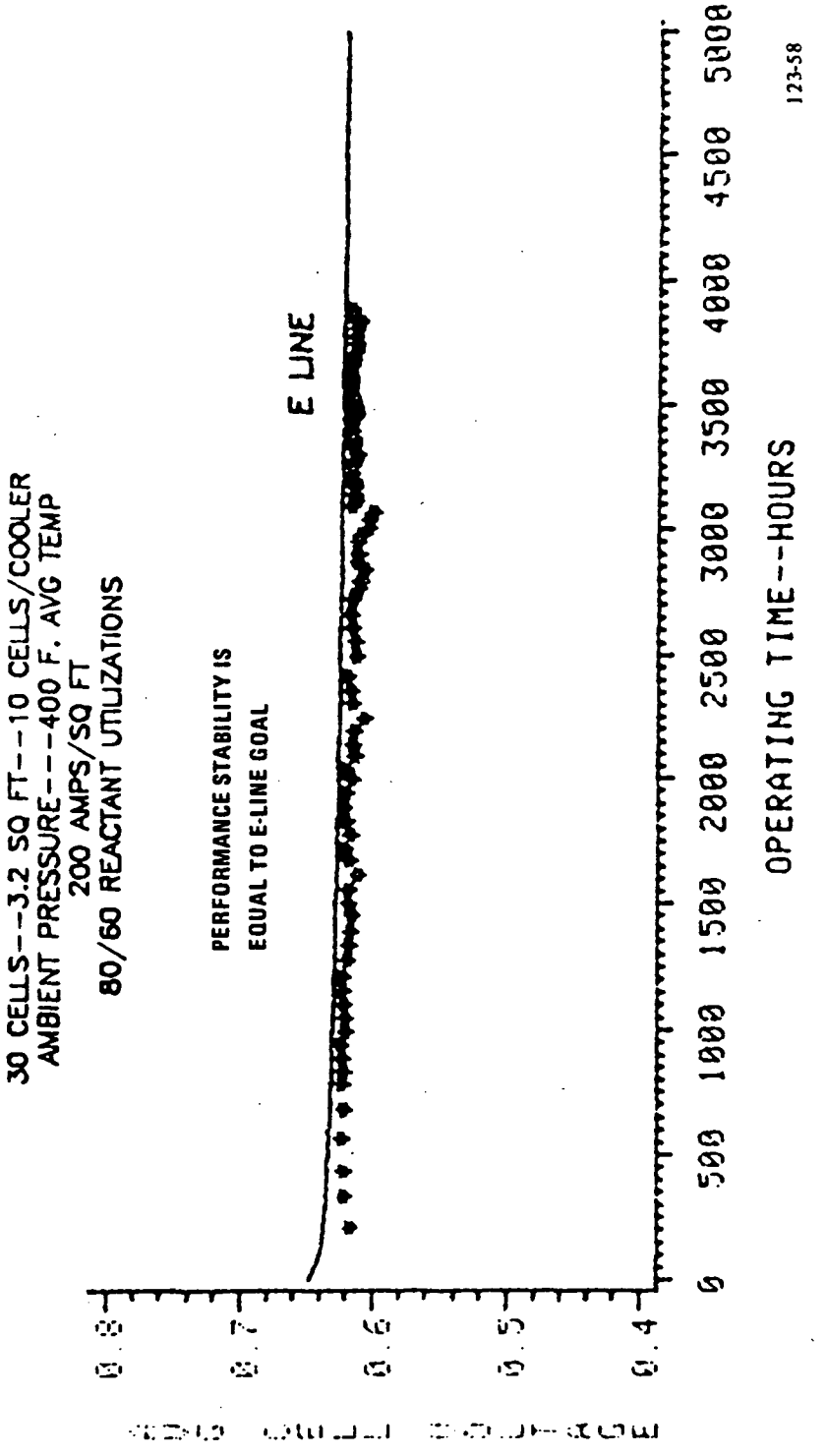

Figure 2.4-3 Cell Stack Performance History

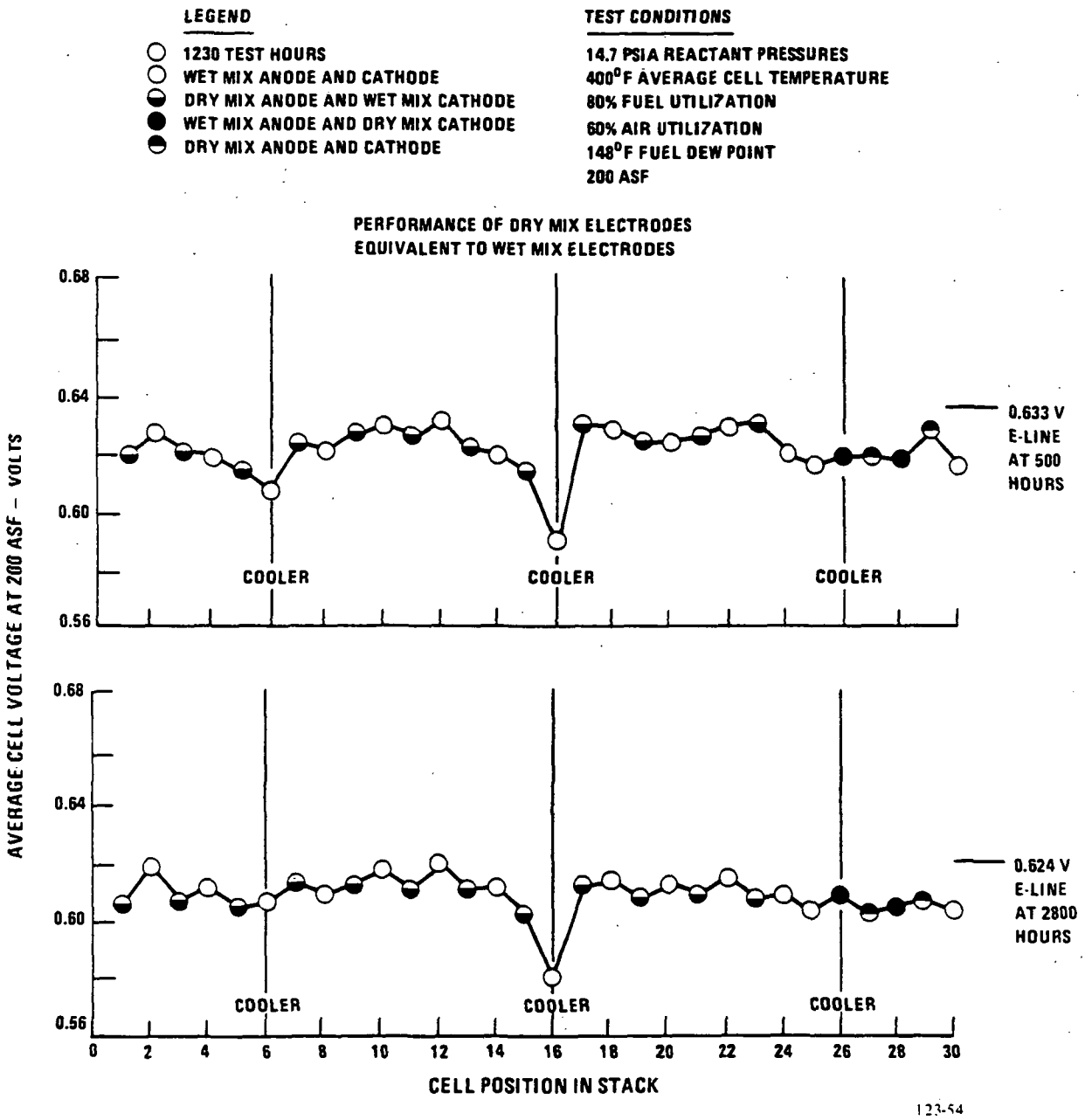

Figure 2.4-4 Cell Performance vs. Cell Position

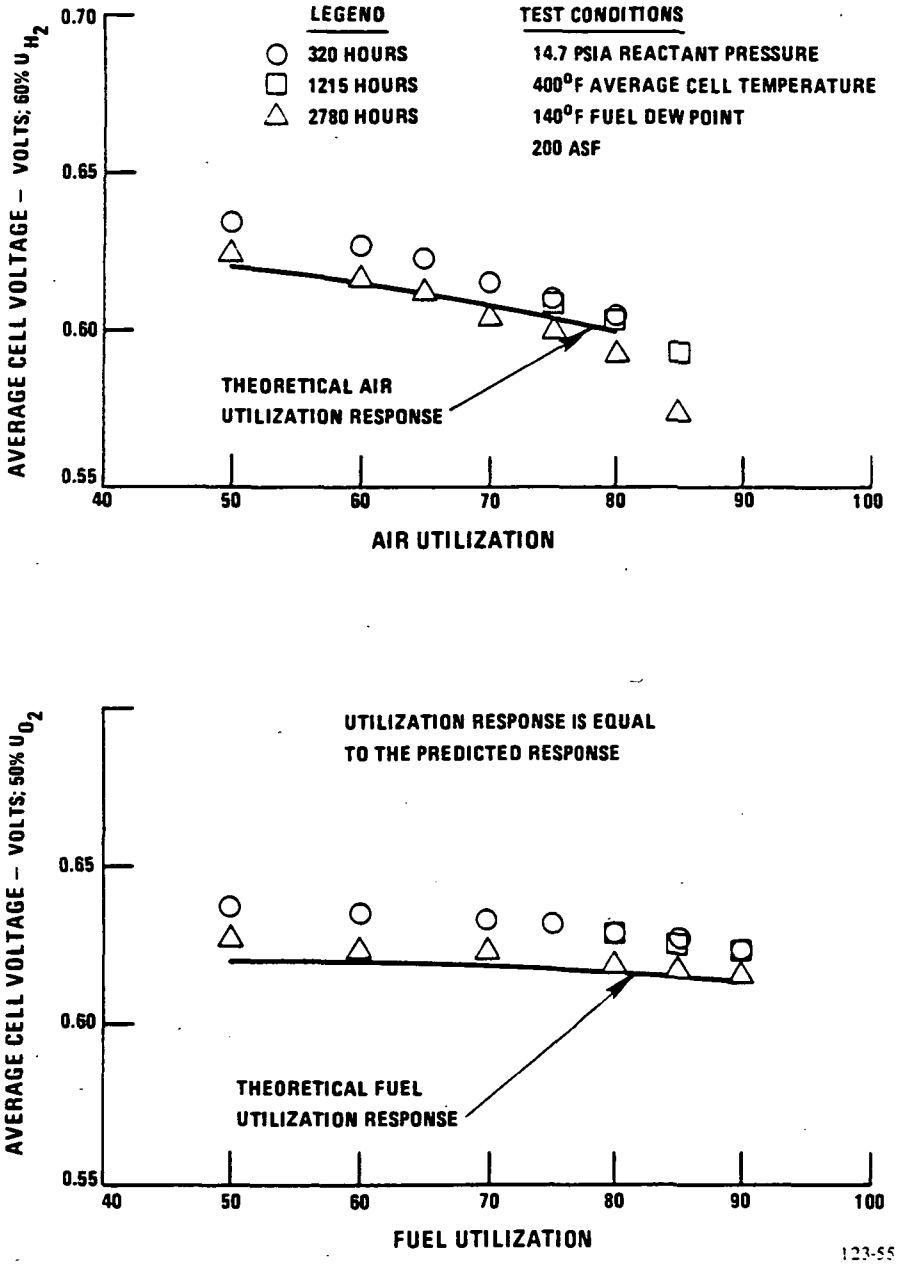

Figure 2.4-5 Reactant Gas Utilization vs. Average Cell Voltage

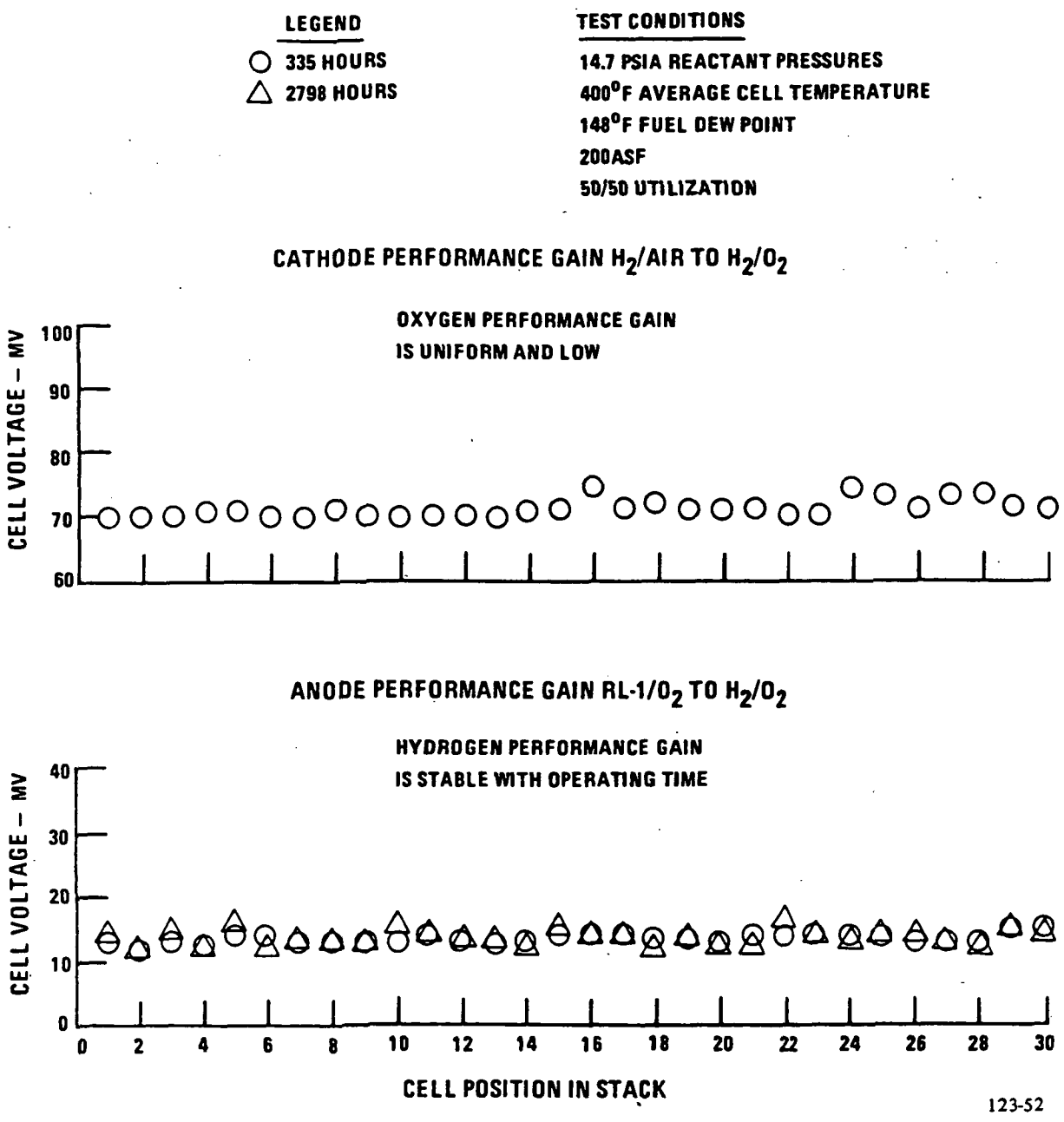

Figure 2.4-6 Anode and Cathode Performance Gain for Pure Reactants

The reactant gas crossover leakage is presented in Figure 2.4-7. This figure presents the cross-leakage measured as a change in the open circuit voltage for a change in reactant gas cross-pressures. This indicates that the cross-leakage is very low and at an acceptable level in each cell. The total reactant leakage for the stack is 0.01% of fuel flow at rated power for a one inch of water cross-pressure, which is unchanged through 2900 hours of operation.

The cell package electrical resistance data is presented in Figure 2.4-8. The average iR for both the cells with separator plates and the cells with cooler assemblies is at the predicted levels. The cell iR has not changed through 2800 hours of operation.

The cell and stack thermal profile data are presented in Figure 2.4-9. The data indicated that the thermal data within a cell and within the stack are at the design level. This indicates that the thermal performance of the encapsulated cooler meets the design requirements and that this thermal performance has remained constant through 2900 hours of operation. These data also show that acid condensation zone temperatures are being achieved.

The stack axial load reduction with operating time is presented in Figure 2.4-10. The reduction in axial load is at the expected level.

The endurance test for this stack was interrupted after 2700 hours of operation. At this time the air exit and fuel in/out manifolds were removed, and manifolds fabricated of carbon steel with a PPS protective coating were installed. An acid scrubber was also installed in the air exhaust for measurement of the acid loss rate from the stack.

The endurance test program is continuing. Over 2900 hours of operation have been accumulated, including 10 thermal cycles. This endurance program will continue until 5000 hours have been accumulated, after which time the stack will be disassembled and a non-destructive post-test analysis will be performed on the components. The acid loss rate will be determined and compared to predictions to establish the effectiveness of the acid condensation zone. The effectiveness of the

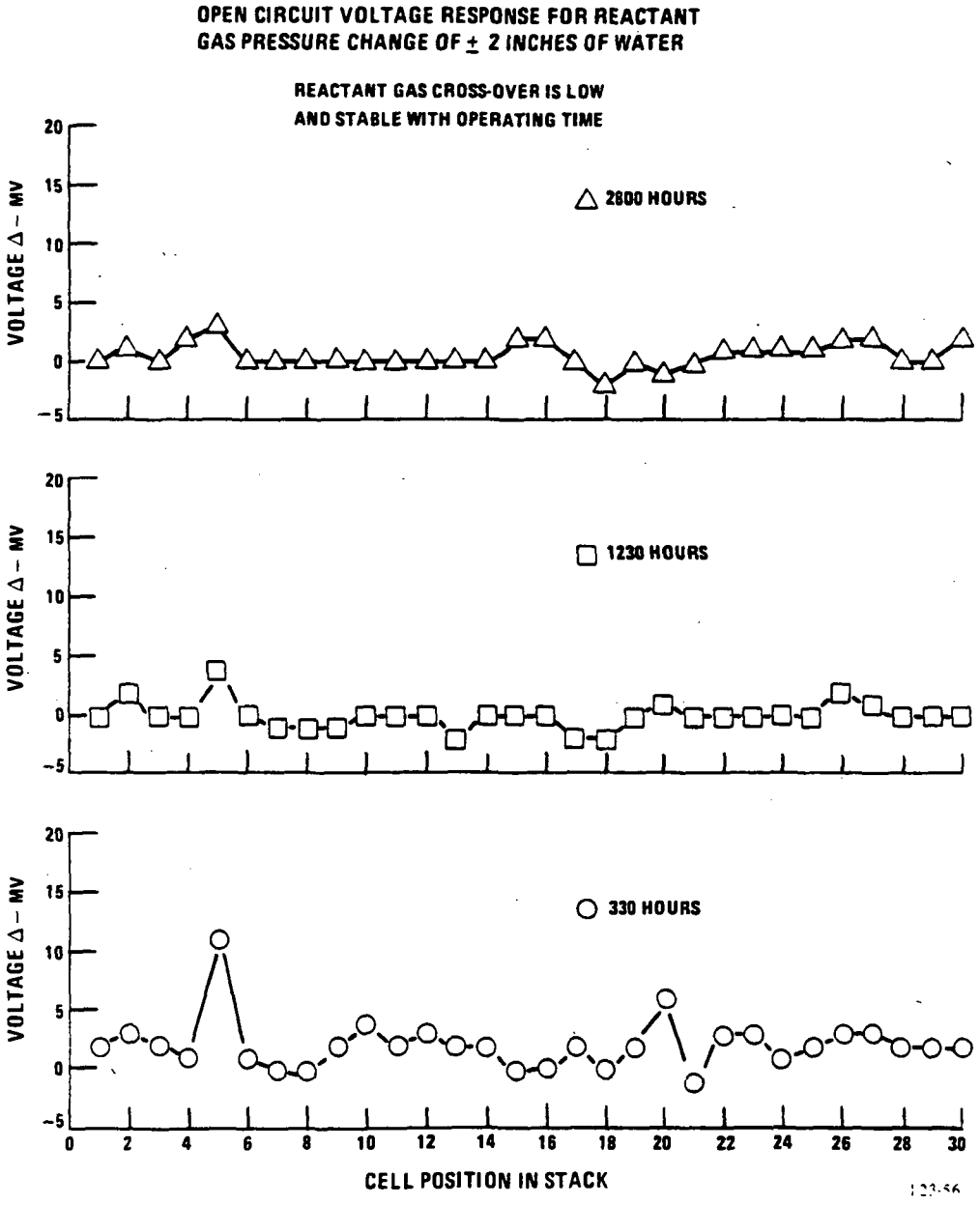

Figure 2.4-7 Reactant Gas Cross-Leakage Test

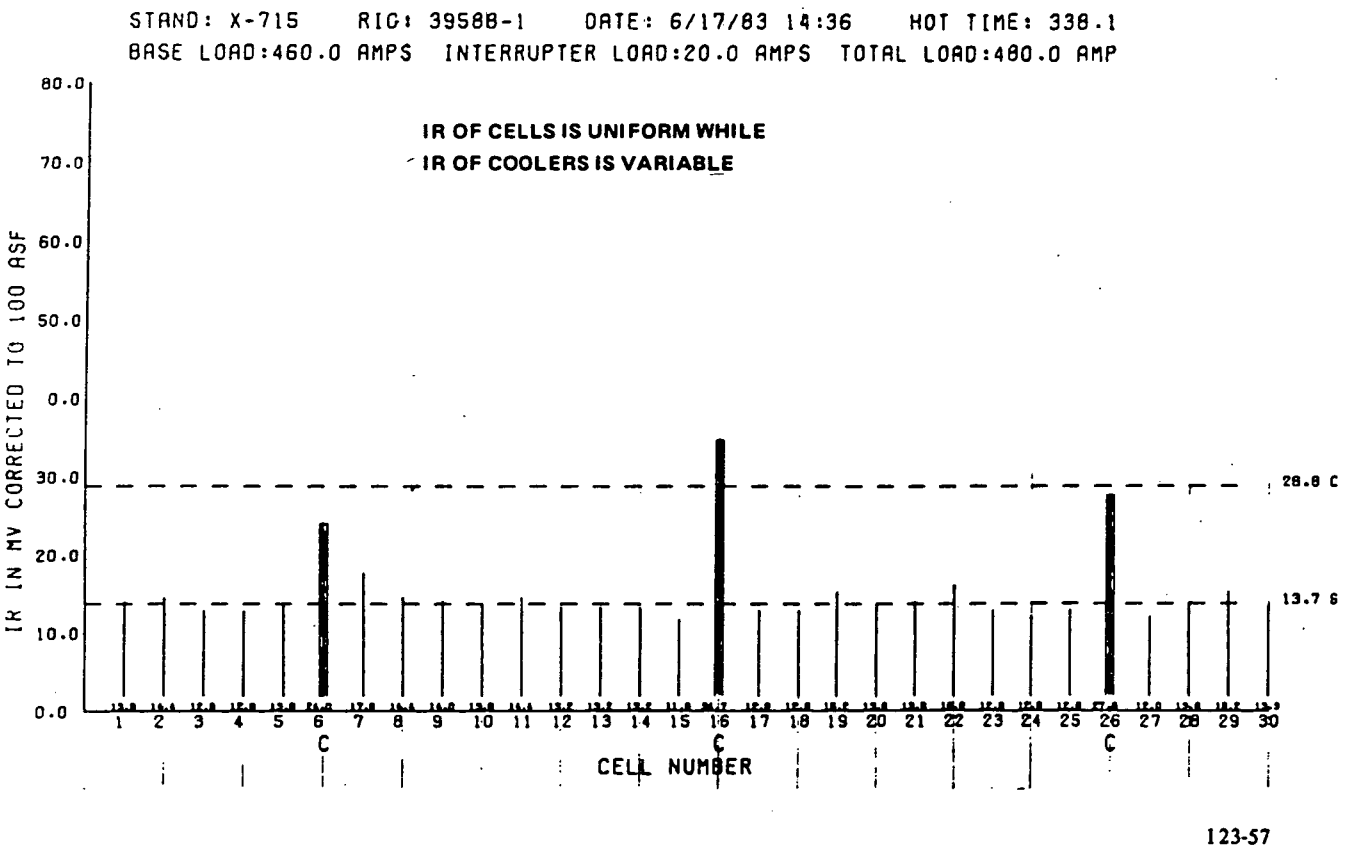

Figure 2.4-8 iR vs. Cell Position

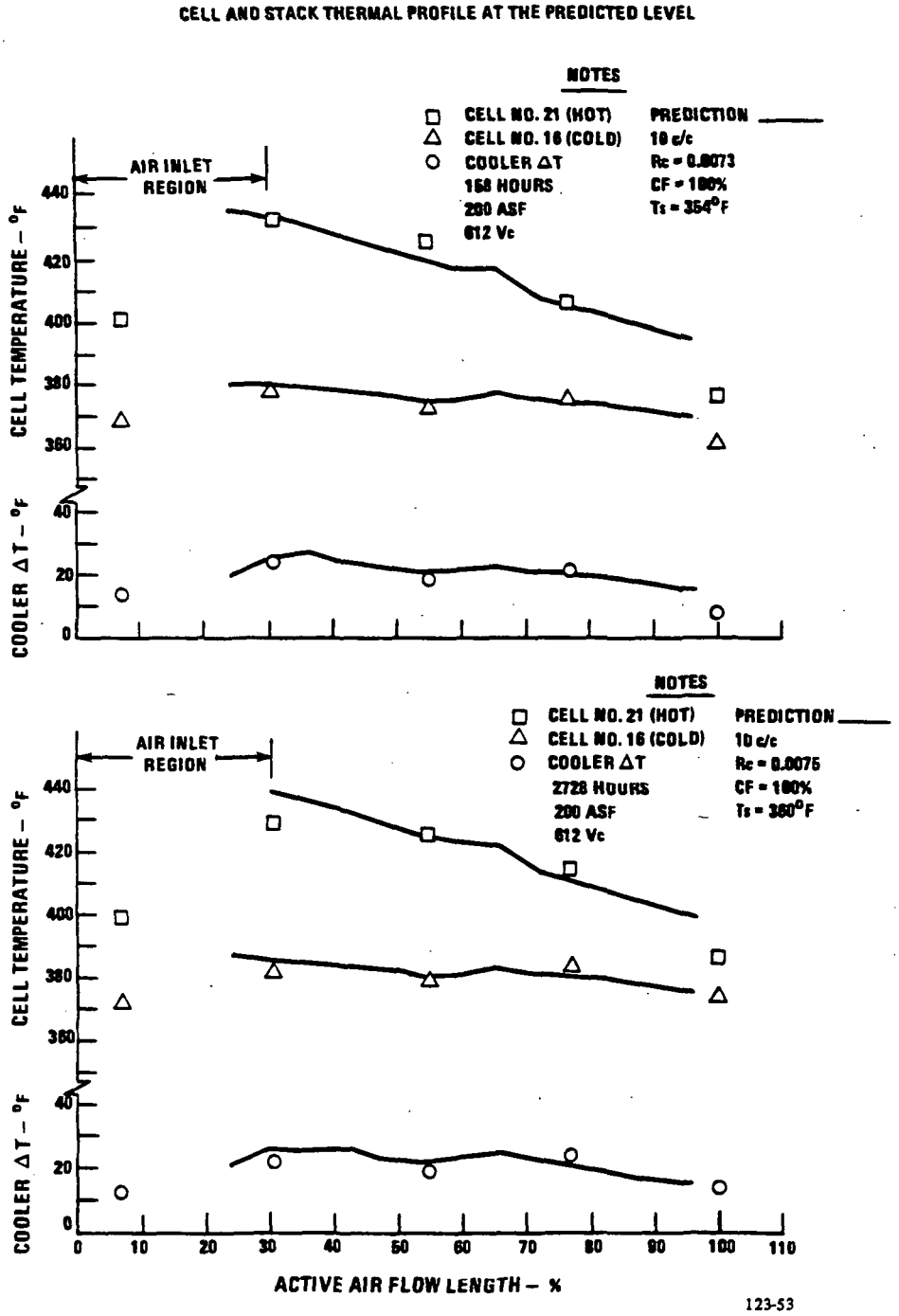

Figure 2.4-9 Cell Temperature Distribution

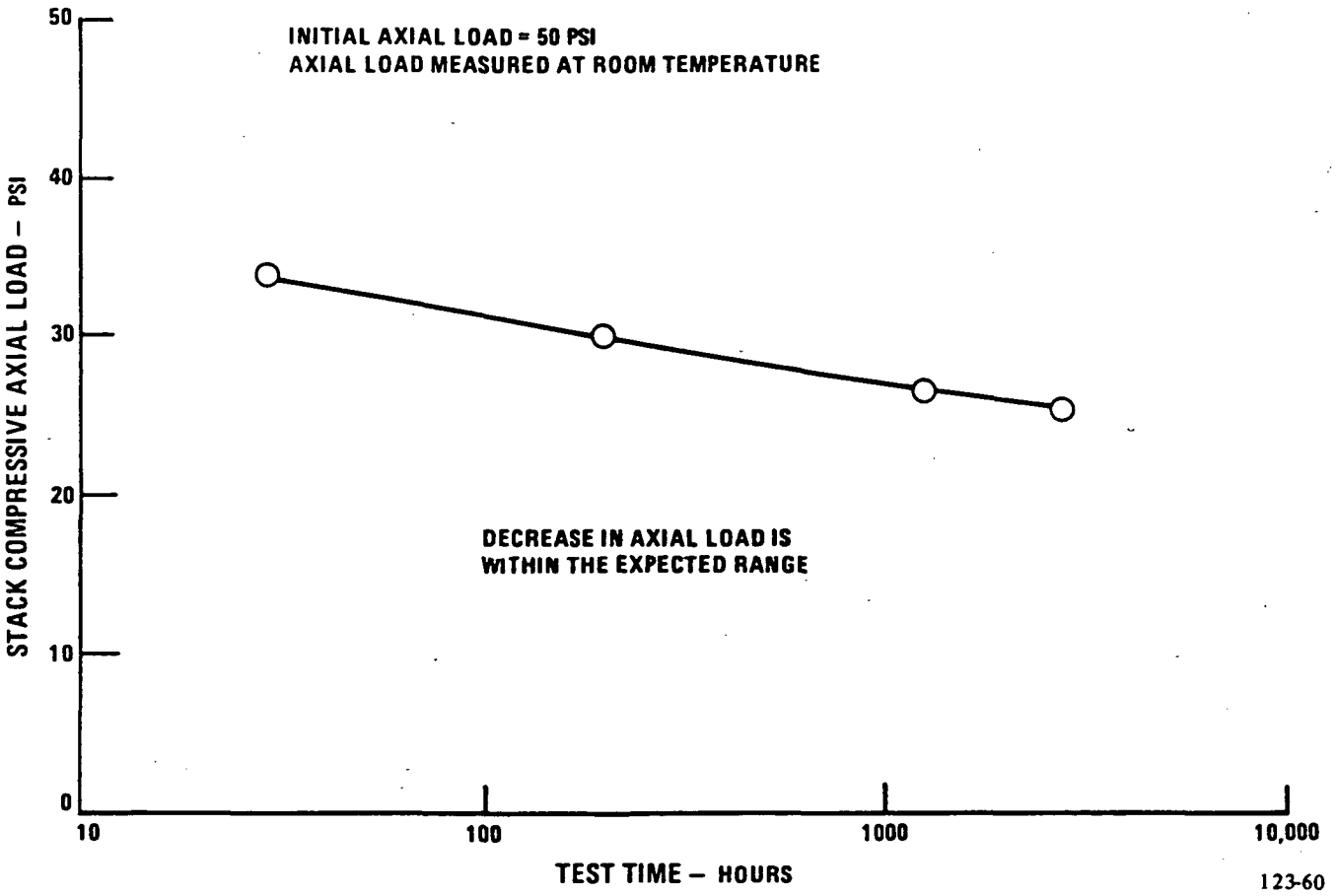

Figure 2.4-10 Axial Load vs. Test Time

acid-proofing concept for the cooler will be established. Also, at this time an acid refill test will be conducted to evaluate the acid refill procedure being developed under Subtask 2.3. The stack will then be reassembled for additional testing if judged useful and if the components are acceptable.

TASK 3 POWER PROCESSOR DEVELOPMENT

TASK 3 - POWER PROCESSOR DEVELOPMENT

Subtask 3.1 Define Inverter Technology

Objective

The objective of this subtask is to establish the design approach, control circuit options, and semiconductor technology for a high efficiency, low cost inverter.

Summary

The approach taken in this subtask was first to evaluate the impact of advanced semiconductor and power circuit technologies, control concepts, and improved magnetic components on inverter cost and efficiency. The basic inverter electrical power circuit design, as established in the 1982 GRI program, was modified and updated as a result of these optimization studies, system tradeoff studies, and identified beneficial technologies. A detailed electrical design was then established, along with a GRI-sponsored conceptual mechanical packaging design, for use in performance estimates and a subsequent cooling study.

The resulting design is a two-bridge, 200-kW inverter which, with auxiliary commutation for surge circuitry and a low loss output transformer, has a calculated full load efficiency of 94.8%. Use of more advanced asymmetrical silicon controlled rectifiers (ASCR's), expected to be available in the future, will result in a calculated 95.4% efficiency. The cooling study found conventional forced air cooling to be the best choice, based on acceptable performance, cost, and parasitic losses.

Highlights

- Established a bridge electrical design that results in a calculated full load inverter efficiency of 94.8%.
- Selected conventional forced air cooling for the bridges.

- Identified the efficiency benefits of auxiliary commutation for surge as 0.2% at full load and 1.0% at quarter load, and of a low loss output transformer as 1.0% at full load.

- Selected ASCR's for use in the brassboard inverter, identified expected efficiency improvements resulting from near term ASCR's, and selected GTO's for laboratory evaluation.

Discussion

Previous studies performed under a GRI-sponsored effort evaluated power circuit technology and identified designs that would improve cost and/or efficiency. The study determined that the individual commutation circuit provided both cost and efficiency advantages over the Split-C commutation circuit used in the 40-kW on-site inverter. The 40-kW inverter utilizes a dc-to-dc converter stage to provide regulated dc input to the inverter stage. This two-stage design was found to be unnecessary for the advanced on-site inverter, because the on-site fuel cell will operate over a much narrower dc voltage range (1.3:1 maximum to minimum dc voltage ratio compared to the 40-kW ratio of nearly 2:1). Elimination of the dc/dc converter stage decreases cost and improves reliability and performance.

The individual commutation circuit was tested in a one-quarter scale powerpole to confirm its feasibility for the on-site inverter. The 1983 NASA On-Site effort in this subtask then became one of providing a detailed on-site inverter system electrical design using identified technologies from tradeoff and optimization studies which, with mechanical design support from a parallel GRI program, would provide Subtask 3.2 with the necessary information for procuring brassboard inverter hardware.

System Definition - Other on-site program activity established a rating of 200 kW for the development inverter, defined the system as grid-connected only, provided an estimate of the fuel cell dc operating characteristics, and defined the ac utility line interface voltage. From this governing set of criteria an inverter system definition was established, as depicted in Figure 3.1-1. The primary elements are:

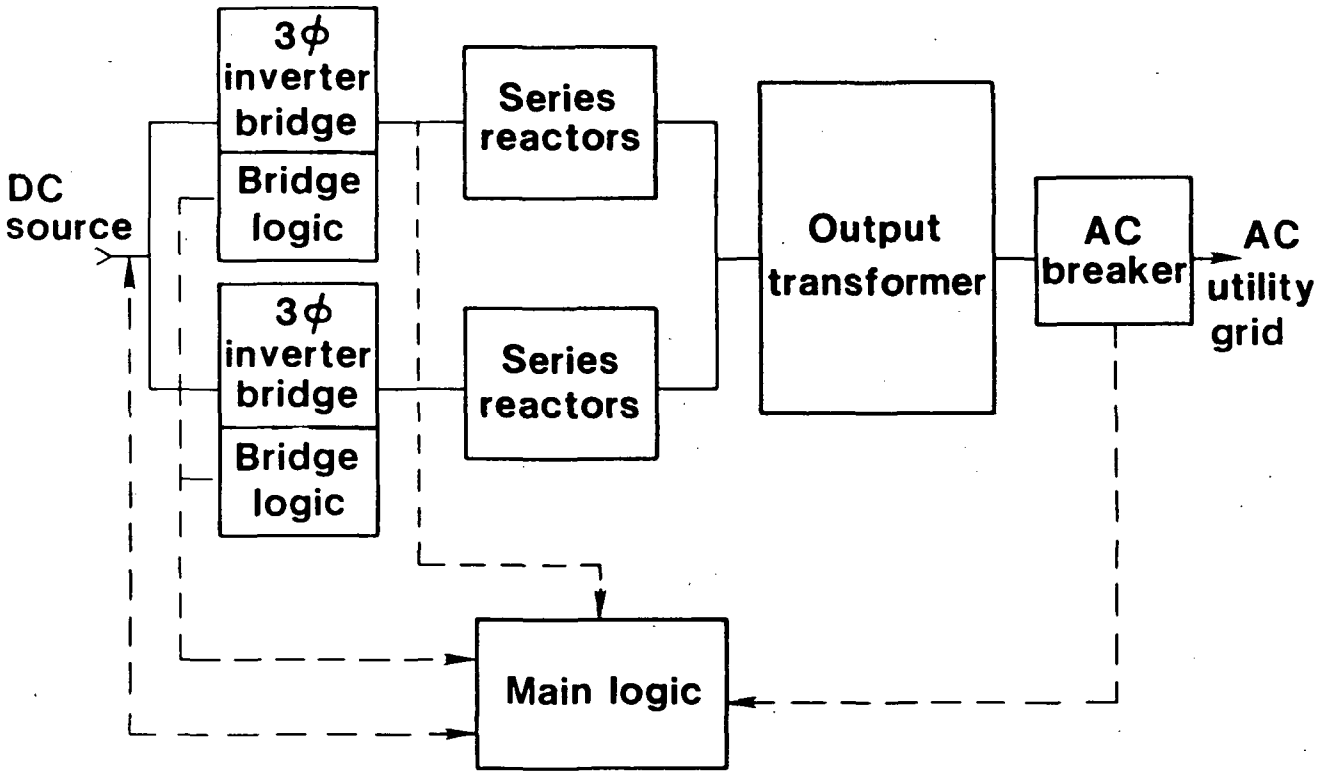

Figure 3.1-1. 200-kW Inverter System

- Two three-phase inverter bridges utilizing pulse width modulation for control of fundamental and harmonic voltages (the two bridges operate 30° displaced into a delta-wye transformer to magnetically eliminate the 5th/7th harmonics and their conjugate pairs).

- Series reactors which provide the bulk of the system's 22% impedance for the controls to work against and which provide a buffer between the bridges and the utility line.

- A full isolation two-winding power transformer that provides a voltage match between the bridge outputs and the utility line, as well as grounding isolation.

- The control and protection logic, which provides all necessary operating, regulating, and protective functions for automatic, unattended operation. The logic is comprised of two parts, bridge logic and main logic, of which the bridge logic was defined in detail in this year's program (see Subtask 3.2).

Initial efforts concentrated on three areas:

- Definition of electrical components.

- Selection of the most appropriate semiconductor for the electrical circuit operating requirements, and

- Identification of the least costly and/or most efficient circuits to meet the on-site inverter requirements.

Analyses and studies in these three closely interrelated areas were performed simultaneously, with proper visibility to insure compatible results.

Component Definition - An electrical circuit schematic for the bridges, series reactors, and output transformer was detailed by defining the specific component values necessary to meet the on-site performance requirements.

That configuration was then reviewed to insure functionality, with proper safety margins and optimization of components to achieve maximum performance. Minor component modifications were made in this step. The end result was an on-site inverter operating over a dc input voltage range of 190 to 260 V dc, delivering 200 kW at 1.0 + .05 power factor into a nominal 480 V ac, three-phase utility line with a calculated efficiency of 93.6% at full load. Table 3.1-1 shows the breakdown of losses and overall efficiency at full load, half load, and quarter load.

TABLE 3.1-1. CALCULATED INVERTER EFFICIENCY

	LOSS IN WATTS		
Subassembly	Full Load	Half Load	Quarter Load
Input Filter	200	230	260
Switching Modules	7,100	4,800	4,200
Magnetics*	4,700	2,100	1,450
Logic and Controls	300	300	300
Miscellaneous	1,400	1,070	890
	13,700	8,500	7,100
Efficiency	93.6%	92.1%	87.6%

* Assumes 2% losses in transformer and 700 watts in series reactors.

The lower part power efficiencies are due primarily to two items:

1. The magnetic losses are not linear with output power, due to the core loss portion.

2. The switching module losses are not linear with output, due to commutation and switching occurring at higher voltages at part power.

Optimization Studies - The purpose of these studies was to find a way to improve inverter performance in three areas (output transformer, commutation circuit, and semiconductors) while maintaining a cost penalty for the improvement that would not penalize the overall power plant. Improving inverter efficiency, in effect, will allow the dc module to contain fewer cells and still achieve the same system performance. To be of benefit, however, this improvement must cost less than the savings attributed to using fewer cells.

Of the three areas, the first area studied was the output transformer. Typical commercial magnetics in this power range have full load losses between 5% and 2% of rating. The baseline studies on efficiency had assumed 2%, which is commonly referred to as 85° C rise design. Several manufacturers were queried as to the cost and weight penalties in designing a transformer for 1% loss at full load. Initial feedback was not promising, with little detail provided. One manufacturer did show an interest in analyzing this question, however, and provided the information shown in Figure 3.1-2. The manufacturer performed a design analysis and estimated that an output transformer with a 1% full load loss would weigh 27% more and cost 20% more than a 2% loss design. Since the 20% cost increase was much less costly than equivalent dc module cells, the 1% transformer was included in the brassboard system, and the full load inverter efficiency estimate increased to 94.6%.

Another possibility for efficiency improvement was in the use of auxiliary commutation for surge circuitry (ACS). The baseline design incorporated one main commutation circuit sized to handle the energy required to commutate off the peak current necessary to handle surges at the minimum dc operating voltage. The ACS concept is to:

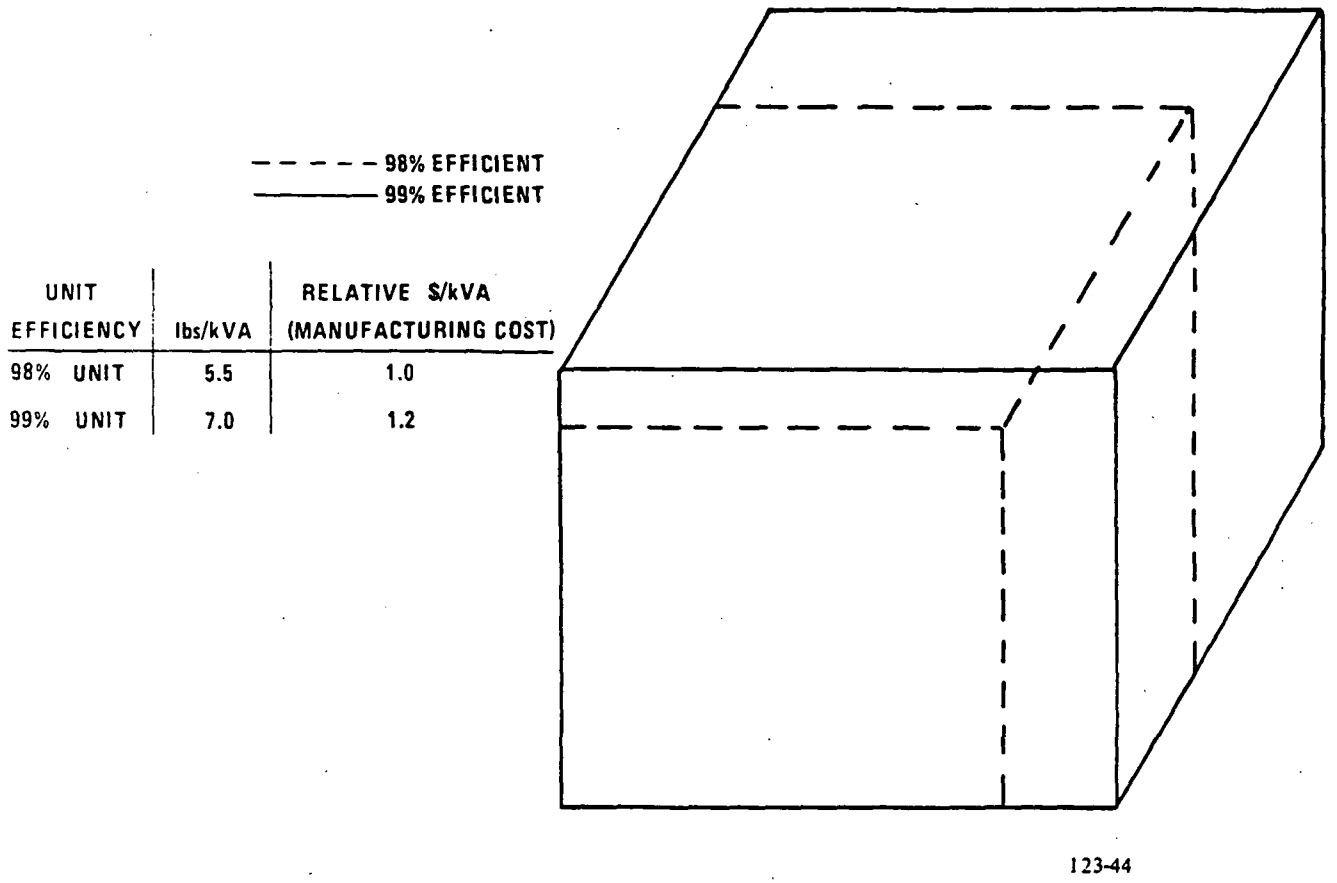

UNIT EFFICIENCY	lbs/kVA	RELATIVE $/kVA (MANUFACTURING COST)
98% UNIT	5.5	1.0
99% UNIT	7.0	1.2

Figure 3.1-2. Output Transformer Outline

1. Use a smaller main commutation circuit for normal full load current plus an approximate 30% margin to handle minor perturbations,

2. Use ACS whenever the current exceeds the 30% margin, to handle surges and faults.

This concept was investigated previously for MW-scale inverters. Evaluation of ACS designed for the 200-kW brassboard inverter showed the results in Table 3.1-2.

TABLE 3.1-2. AUXILIARY COMMUTATION FOR SURGE EFFECT ON EFFICIENCY

Load	Commutation Circuit Losses (Watts) Without ACS	With ACS	Delta	System Efficiency Increase (%)
Full Load	828	462	366	0.2
Half Load	1,116	702	414	0.4
Quarter Load	1,884	1,452	432	1.0

The 0.2% improvements at full load, when viewed as a function of the cost of the ACS on a system basis, resulted in a break-even situation. The ACS, however, was incorporated into the 200-kW brassboard design as a technology evaluation item and the inverter full load efficiency estimate increased to 94.8%. ACS was considered an important concept that may be applicable in grid-independent inverter designs, to handle overload requirements without impacting normal rated load operation.

The third area analyzed utilized the results of the semiconductor device investigation. As discussed below, that investigation selected the asymmetrical SCR (ASCR) for the 200-kW brassboard inverter design (the inverter will be capable of operating with and evaluating other candidate devices, but the initial design/construction will be with ASCR) and projected an improvement in the forward voltage drop from 1.7 V presently, to 1.3 V in the near future. Figure 3.1-3 shows the ef-

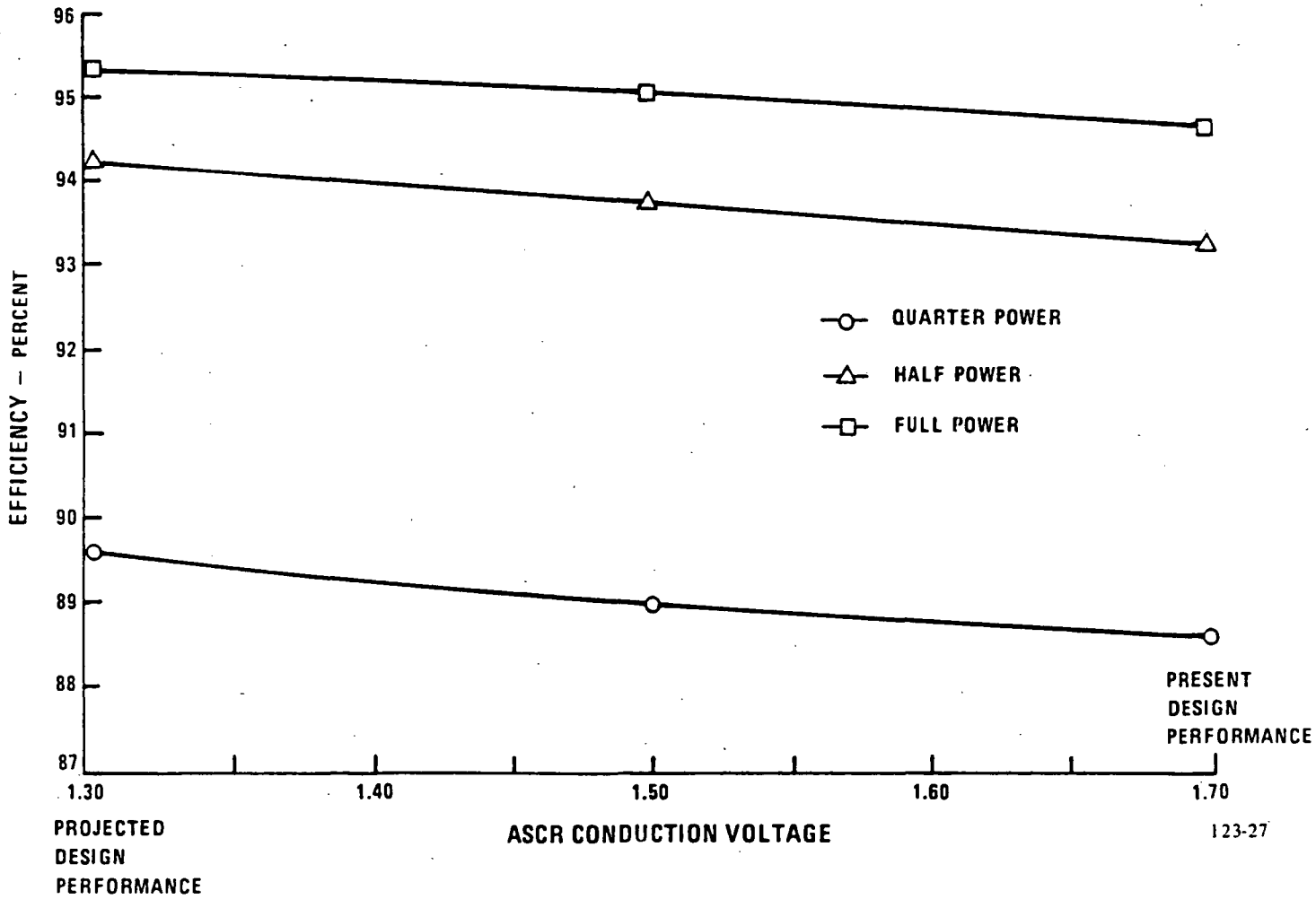

Figure 3.1-3. Inverter Efficiency vs. Projected ASCR Performance

ficiency benefit derived from that ASCR performance increase to be about 0.6% at full load, bringing the brassboard estimated efficiency up to 95.4%. In addition, the projection does not anticipate any cost increase associated with the better performing ASCR; it may even go down in cost.

Semiconductor Investigations - Semiconductor evaluation and forecasts were performed as on-going efforts in this On-Site task. The initial study effort looked at present (1983) SCR's, ASCR's, and GTO's versus near term projections (1985). The results are summarized in Table 3.1-3. Note that reverse conducting thyristors (RCT's) are not included, as they offer no advantage over the ASCR in performance and are more costly. From Table 3.1-3 it is not apparent that the brassboard current choice of a main thyristor would be the ASCR, as it is no better than the SCR. As discussed above, the ASCR does project much better future performance in forward voltage drop, pulse loss, and cost, and for those reasons was selected to provide early insight into that technology.

Continuation of discussions and information gathering with and from semiconductor manufacturers has resulted in the following recent conclusions:

1. RCT's may warrant another look; their pricing structure may become more favorable.

2. GTO's (gate turn-off thyristors) are presently not optimally designed for this application. (They may yet be considered, however, as their use deletes the need for commutation circuitry.) To properly evaluate and understand GTO's and their use, engineering samples are being purchased for laboratory evaluation and possible testing in the brassboard inverter in a derated configuration for one-half or one powerpole.

This subtask also evaluated different methods for cooling the brassboard inverter bridges. Once the electrical circuit was defined and the semiconductors identified, estimated losses were calculated. The parallel GRI effort provided a mechanical packaging concept from which the cooling study could evolve, using the estimated

TABLE 3.1-3. THYRISTOR PERFORMANCE PROJECTIONS

	Required Characteristics	Standard Thyristor		ASCR		Gate Turnoff Thyristor	
		Current	Projected	Current	Projected	Current	Projected
Forward Blocking Voltage - Volts	500	500	500	800	500	1200	800
Reverse Blocking Voltage - Volts	10	500	500	10	10	1200	800
Forward Voltage Drop at 700 Amperes	1.4	1.6-1.7	1.4-1.6	1.7	1.3	2.25[2]	2.5
Pulse Loss - For half sine wave of 700 amps and 8.3 milliseconds - watt - seconds	4.0	5.0-7.0	5.0-6.0	6.0	4.5	Not Avail.	-
Turn Off Time - Microseconds	20	15	15	15	15	NA	NA
Reapplied DV/dt	400[3]	400	400	400	600	300	500
Maximum Turn-off Current - Amperes (GTO's only)	1000					1000	1000
Cost - 600 - 1000 Quantity $ Per Device	-	45-100	40	60-130	50	700	100-350

for 20 quantity

[2] at 350 amperes

[3] 1000 volts/microsecond desired for GTO for high frequency circuit operation

losses for the semiconductors and other components. The study included three types of cooling:

- o Forced air
- o Liquid
- o Heat pipe

Table 3.1-4 shows results for the analysis of forced air cooling with extruded aluminum heat sinks. The maximum calculated semiconductor junction temperature is 109°C, with 120°F ambient inlet cooling air. The acceptable junction temperature limit is 125°C, with 115°C preferred for margin. A similar analysis for liquid cooling showed equivalent performance can be obtained, but at a much higher cost. Cost estimates based on parts requirements alone showed liquid cooling to be twice as costly. Also, previous studies and experience proved heat pipes to be cost effective at cooling loads significantly higher than those of the 200-kW inverter. The forced air/heat sink method was the logical choice to meet requirements at the minimum cost.

Preliminary results of the air cooling study are shown in Table 3.1-4. All selected heat sinks are either catalog items, or based on the 40-kW design. These results show that, at an ambient temperature of 43°C, all semiconductor junctions are maintained well below the 125°C maximum requirement, and that the cooling air temperature rise is about 7°C at a flow rate of 1560 cubic feet per minute. Blower and ducting design studies continue.

TABLE 3.1-4. BRIDGE COOLING SUMMARY

Item	*Watts Loss Each	Qty. Per Bridge	CFM Air Req'd Each	Calculated Junction Temp. °C
Main Thyristor	345	6	80	109°
Commutation Thyristor	170	6	80	108.7°
Main Diode	100	6	30	92°
Commutation Diode	75	6	30	91.5°
Clamp Diode	75	6	40	107°

Heat Load Due to Other Components	1410 Watts
Total Air Flow Per Bridge	1560 CFM
Max Inlet Air Temp	43.3°C
Max Exit Air Temp	50.7°C

*All semiconductor "worst case" losses do not occur simultaneously. Losses cannot be directly added to get total for pole.

The output of this effort was incorporated in the Subtask 3.2 activity, which procures the low cost, high efficiency brassboard inverter. The semiconductor investigation selected ASCR's for the brassboard inverter and has selected experimental GTO's to be purchased for laboratory evaluation and possible future operation in the brassboard inverter.

The 1984 effort in this subtask will:

1. Continue projections for advanced semiconductors to identify brassboard test candidates,

2. Provide a preliminary design definition for the brassboard main logic to allow line parallel operation.

Subtask 3.2 Verify Inverter Technology

Objective

The objective of this subtask was to construct a 200-kW brassboard inverter configured to facilitate evaluation of alternative semiconductors, incorporating the results of Subtask 3.1.

Summary

The beneficial technology, cost, and efficiency elements identified in Subtask 3.1 were incorporated into a detailed electrical bridge design for a 200-kW brassboard inverter. A subcontract was placed with a commercial electrical/electronics equipment manufacturer who provided a mechanical design (funded by GRI) and constructed two bridges and the series reactors for the 200-kW brassboard inverter. The brassboard inverter bridge logic, which was conceptually identified and based on distributed microprocessor technology under an earlier GRI study, was carried from the conceptual design to a detailed hardware and software design. A bridge logic vendor was selected to perform a six-phase subcontract effort, which culminates in delivery of two sets of brassboard bridge logic, one for each of two brassboard bridges. A vendor procurement for a low loss output transformer has also been established. The bridges and output transformer are scheduled for delivery to UTC in late December 1983, and the bridge logic is due in January of 1984.

Highlights

- Completed brassboard bridge logic hardware and software design and started laboratory refinement.
- Specified all brassboard inverter bridge electrical components, sensors, control/protection interfaces, series reactors, and output transformer for procurement.
- Placed a subcontract for the brassboard bridges and series reactors, with delivery scheduled for December 1983.

- Placed a subcontract for bridge control units, with delivery scheduled for January 1984.

- Delivery of an output transformer with 99% full load efficiency scheduled for December 1983.

Discussion

Beneficial results identified in Subtask 3.1 were incorporated into the brassboard inverter electrical design. Under this subtask, key subassembly and component procurement packages were defined and assembled to provide for hardware construction and delivery subcontracts.

A subcontract for the two bridges for the 200-kW brassboard inverter was established with NASA and GRI supporting different portions of it, as shown below:

Task 1 - Conceptual and Preliminary Designs - GRI
Task 2 - Final Design - GRI
Task 3 - Hardware Construction - NASA

The vendor is responsible for the design and assembly/delivery of the two bridges. He supplies all the materials and components except the thyristors and commutation capacitors, which have been supplied to him by UTC. The semiconductors (main) and commutation thyristors were purchased with specified performance test results, to allow proper evaluation of their performance in the brassboard inverter.

The vendor has completed Tasks 1 and 2 of the subcontract and is in the process of the Task 3 hardware assembly effort. Delivery is scheduled for late December 1983. A full-scale mockup of one-half of a powerpole for these bridges is shown in Figure 3.2-1. This mockup simplified his explanation of the design, and was used for full-scale cooling tests (results shown in Table 3.2-1) and to evaluate and measure the design's conformity to critical low inductance paths between specified components.

Table 3.2-1. Brassboard Inverter Half Pole Thermal Test Results

Test point	Heat loads (Watts)		T_{case}* (°C)	
	Measured	Spec	Measured	Spec
Q1	370	380	69.5	90
Q3	170	165	64.8	75
D3	135	125	78.6	90
D1	135	125	78.6	90
D5	70	75	81.9	90
D7	50	<50	63.1	90
Q5	30	30	60.6	90
Inlet air (plenum)	–	–	51.6**	–
Exhaust air	–	–	54.4	–

*Extrapolated to T_a = 49°C (120°F)

**Series reactor heat loss simulated

FC19589
R831512

Bridge Vendor – One Half Powerpole Mockup

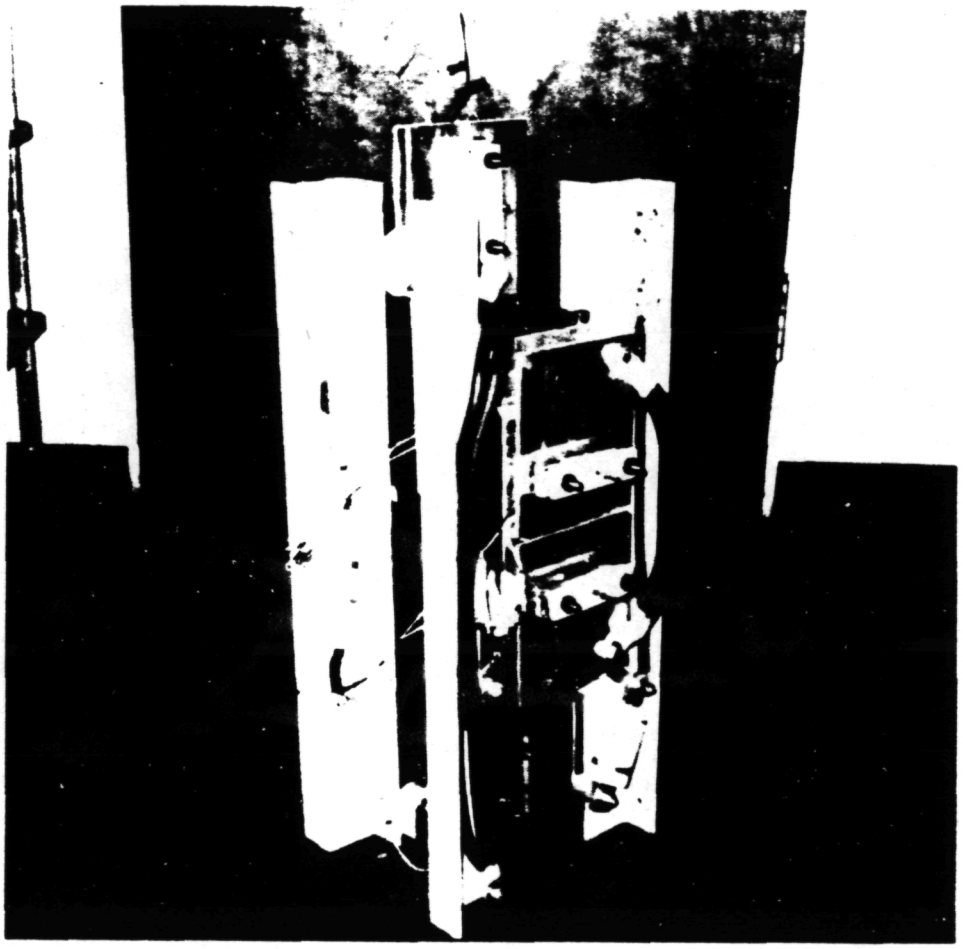

27"h x 10"w x 9"d

FC19288
830107

Figure 3.2-1. On-Site Brassboard Inverter One Half Power Pole Mockup

Performance specifications for the 200-kW brassboard inverter series reactors and output transformer were determined and assembled into component specifications for vendor design and fabrication. The series reactors are single-phase, iron core (six units required for the brassboard system), with open construction for natural convection cooling. They are specified as shown in Table 3.2-2.

TABLE 3.2-2. SERIES REACTORS SPECIFICATION

Operating Condition	Inductance microhenries	Inductance Tolerance (±%)	Max Rated ac Current (Amps)	Frequency (Hz)	dc Current Level (Amps dc)
Continuous	80	±5%	498 rms	60 Hz ±5%	5 Amps*
5 Second Overload	72**	--	1100 peak	60 Hz ±5%	5 Amps*

* Without Saturation
** Small signal ac inductance at peak current

- Conduction loss plus magnetizing loss of each inductor to be ≤167 watts at 498 amps rms.
- Duty Cycle: Continuous
- Special Requirements: Inductor to be iron core with laminations no greater than 14 mils thick. If air gap design, no magnetic materials can shunt air gap.
- Insulation level to be rated for electrical equipment used at 600 V ac at the following environmental conditions.

Max Temperature Rise	55°C
Max Ambient Temperature	50°C
Min Ambient Temperature	-34°C
Humidity:	80°F wet bulb or 90% relative humidity

For the brassboard inverter, the series reactors are included in the bridge vendor subcontract.

The output transformer is a three winding, delta-wye primary to wye secondary, full isolation power transformer. Requirements are as follows:

Rating - 211 kVA at 0.95 power factor leading or lagging

Losses - Maximum losses are rated kVA and nominal voltage are to be ≤2.0 kilowatts.

Primary Winding: (Low voltage side) two (2) windings (one delta and one wye) rated 141 volts rms line-to-line, 60 Hz, each winding. Low side windings and core shall be sized to carry:

1. 110% of full rated fundamental current,
2. Primary windings and core are to be able to handle 141 volts rms +10%, 60 Hz.

Secondary Winding: (High voltage side) one wye connected winding with ungrounded neutral connection and taps. High side winding shall be rated 480 V ac line-to-line (nominal) and 211 kVA at 0.95 power factor leading or lagging, and be sized to carry +4% (of rated fundamental current) harmonic current in addition to rated load current.

DC Unbalance: The primary side of the transformer shall be capable of withstanding up to 11 amperes dc net unbalance per wye leg.

Delivery of the output transformer is scheduled for December 1983.

The other major effort in this subtask is the design and procurement of bridge control and protection units.

Earlier efforts under the 1982 GRI Program established a conceptual design for the logic to control and protect the inverter bridges (shown in Figure 3.2-2). The conceptual designs presented this logic as a single custom card. However, a three circuit board configuration consisting of two special cards and one standard computer card was selected for the brassboard hardware. This configuration was identified previously in work done as part of the Program to Develop Advanced Converter Technology for Battery Applications (DOE Contract DE-AC01-79ET29079). The three-board configuration is necessary in that program to handle the more sophisticated operating and interface requirements of a multi-megawatt power conditioner.

Use of this three-board concept for the brassboard will segregate functions to allow design evaluation and provide necessary flexibility where design changes and circuit modifications are needed due to new logic control design. Test results will be used to define a single-board configuration, estimated to be the least costly design for on-site application. Therefore, the logic vendor will also be responsible for single-board design review to ensure that bridge logic requirements are satisfied.

The bridge logic conceptual design was modified to meet brassboard inverter requirements. Detailed hardware and software designs were established, along with designs for sensing interfaces, to allow the logic to communicate with the bridges.

Once the hardware designs were complete, wirewrap circuit boards were constructed to aid in the hardware and software development efforts. Figure 3.2-3 shows a photo of the wirewrap waveform processor board, and Table 3.2-3 shows the status of the overall bridge logic development activity at UTC.

A subcontract, jointly funded by GRI and NASA, has been established to translate UTC designs and requirements into a packaged hardware design and to construct two sets of bridge logic, one for each of the 200-kW brassboard bridges.

Task 1 Vendor Electrical Design Review - NASA
Task 2 Vendor Mechanical Design Review - NASA
Task 3 Vendor Testability/Maintainability Study - NASA

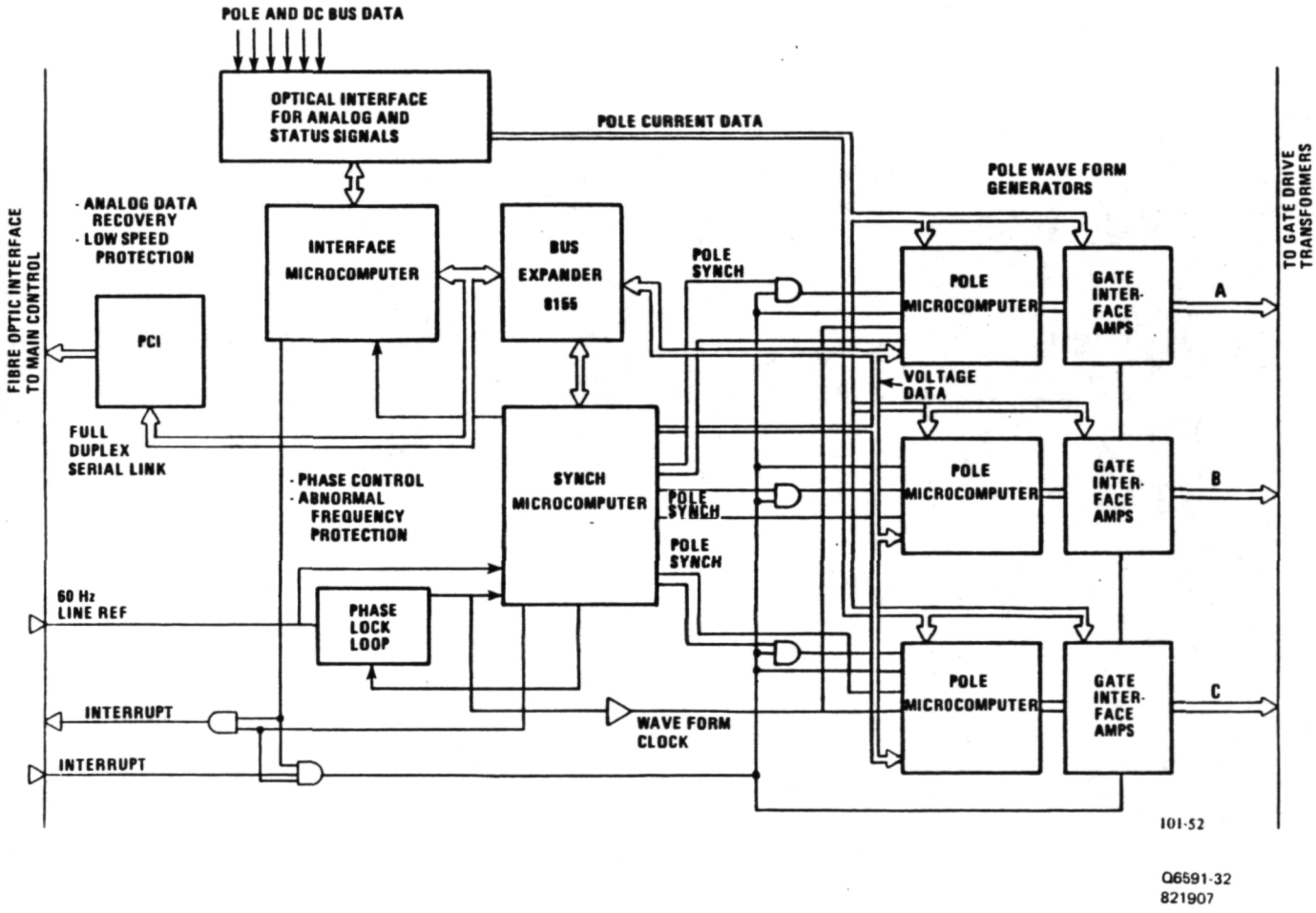

Figure 3.2-2. Schematic of Bridge Logic Control

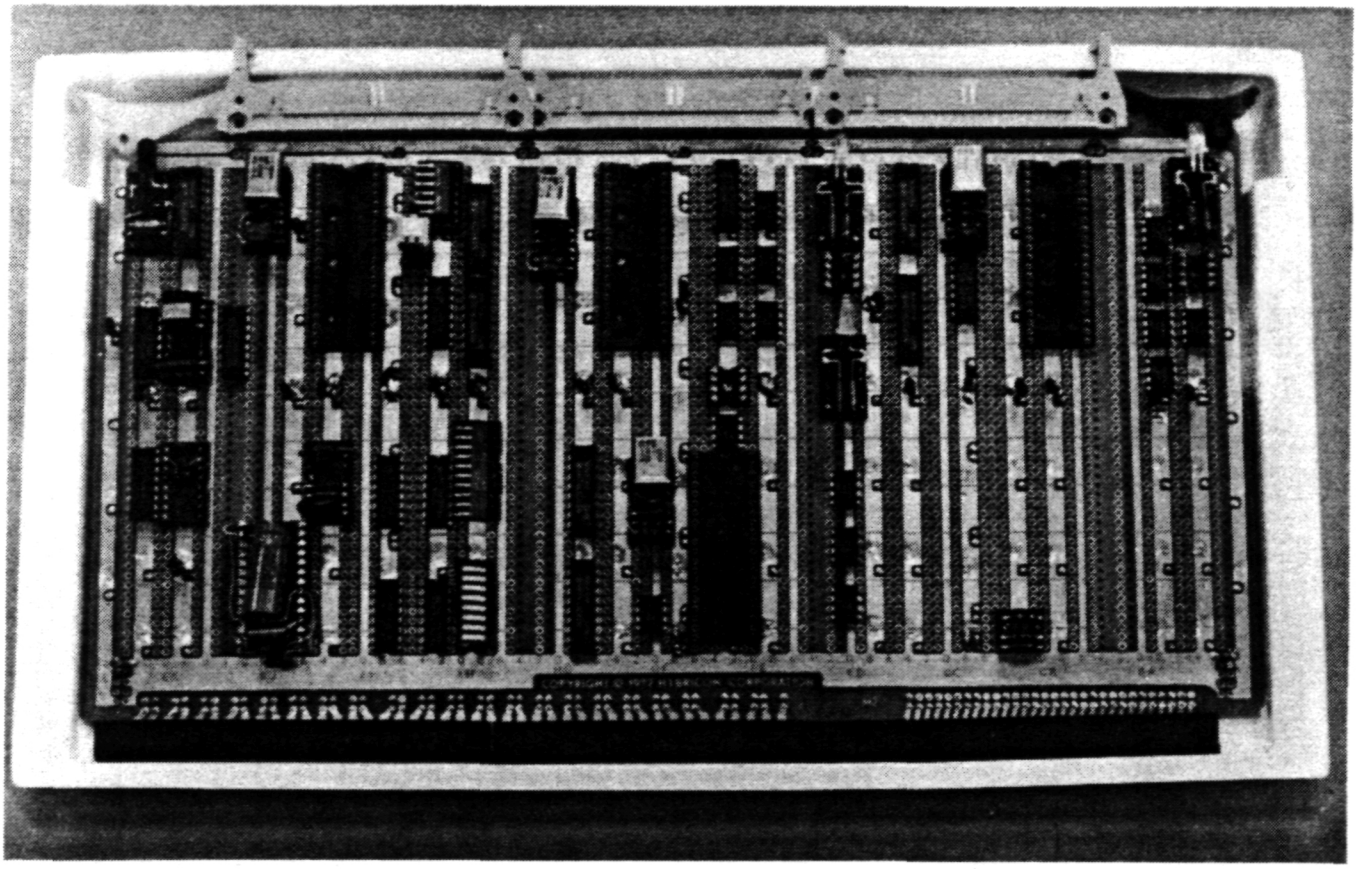

WCN-10614

Figure 3.2-3. Wirewrap Waveform Processor Board

C-2

Table 3.2-3. Bridge Logic Status Summary

C = COMPLETED
NA = NOT APPLICABLE
ND = NOT DONE

		WAVEFORM PROCESSOR	LINE SYNCH PROCESSOR	INTER-FACE PROCESSOR	SENSING
HARDWARE					
DETAILED REQUIREMENTS		C	C	C	C
CIRCUIT DESIGN		C	C	NA	C
BREADBOARD		C	C	NA	C
TEST		C	ND	NA	ND
SOFTWARE					
DESIGN		C	C	C	NA
WRITE CODE		C	C	C	NA
TEST CODE MODULES		C	C	C	NA
LINK MODULES		C	C	C	NA
SYSTEMS					
DEBUG SUBSYSTEMS		ND			
INTEGRATION		ND			

Q6212-106
R831612

Task 4 Vendor Mechanical Design - GRI
Task 5 Construction - NASA
Task 6 Vendor Low Cost Design - GRI

The bridge logic vendor effort began with a review of UTC's designs for compliance with commercial or user standard practices, making sure that the required processes could be performed at the specified speeds by a generic brand of hardware. This review is deemed important because subtleties in hardware specifications may result in a microprocessor overload.

The logic vendor has completed his Task 1 review described above and found no significant design problems or concerns. Some improvements were recommended. From there the vendor will perform a mechanical design and construct the hardware. In addition, the vendor will formulate an approach for rapid acceptance testing of this type of logic and perform a study to determine if the three card design can be reduced to a single card to reduce cost. The bridge logic for the brassboard inverter bridges is due to be delivered in January or February of 1984.

The 1984 effort in this subtask will:

- Test the brassboard system first as subassemblies and components and then as system operating in grid connect.
- Support the hardware test with analytical predictions from UTC computer programs.
- Complete final design and procure main logic, which functions with the bridge logic for system line parallel operation.

TASK 4 HEAT EXCHANGER DEVELOPMENT

TASK 4 - HEAT EXCHANGER DEVELOPMENT

Objective

The objective of this task is to define an acceptable low cost acid removal device for on-site power plant applications. Definition of the acid removal device shall be based upon system, technology, and cost assessments of the candidate configurations, and component testing to verify performance and function. Candidate configurations shall include heat exchangers constructed with corrosion resistant materials and direct contact water cooling.

Highlights

- Experimentally evaluated one heat exchanger and two direct contact water cooling approaches for acid removal on a 200-kW scale.
- Preferred acid condenser device for the on-site power plant is modified commercial heat exchanger with Teflon® covered metal surfaces; cost is 20% of the baseline 40-kW unit on a $/kW basis.
- Evaporative spray cooling and contact saturation meet performance requirements and project to lower cost, but add to system complexity.

Summary

Direct contact water cooling systems and heat exchangers constructed of corrosion resistant materials were evaluated on their ability to remove acid from the cathode exhaust stream. Three candidate direct contact water cooling methods for acid removal were identified: contact condenser, evaporative water spray, and contact saturator. Contact condensing was eliminated, due to the cost impact on the water treatment system. Evaporative water spray cooling and contact saturation were selected for experimental evaluation.

A 200-kW size evaporative spray cooler rig was sized and fabricated. Testing with various packed bed materials resulted in identification of a stainless steel wire mesh packing that gave acceptable performance; an acceptable water flow control system has not yet been defined.

A contact saturator, operating at a constant water flow rate, was sized for a 200-kW system. A test rig was assembled, and testing demonstrated feasibility of this concept for acid removal.

Two heat exchangers made of corrosion resistant Teflon and one design in graphite were analyzed for acid condenser application. The unit determined most suitable for on-site application is a modified vendor design that uses Teflon covered metal tubes and a Teflon lined enclosure. A prototype for a 200-kW system was procured and component testing showed design point performance to meet requirements. The projected cost is approximately 20% of the cost ($/kW) of the baseline 40-kW acid condenser.

Discussion

Development activity in this area includes evaluation of two methods of removing acid from the cathode exhaust stream. One approach is to use heat exchangers made of materials resistant to the corroding effects of phosphoric acid. The other approach is to use a form of direct contact water cooling, which would reduce the gas stream temperature and condense the acid.

Program History - Work was conducted under the GRI On-Site Technology Development Program to identify corrosion resistant heat exchangers able to meet requirements of the cathode exhaust acid condenser. In addition, limited work was conducted to evaluate evaporative spray cooling as a means of condensing the acid.

Three candidate heat exchangers fabricated from corrosion resistant materials and sized for a 300-kW power plant were identified in vendor surveys conducted during

the GRI Phase I and II programs. These are summarized below, along with planned follow-up activity.

- One of the candidates was a graphite-constructed unit. This unit met functional requirements but was expensive and large. No further activity is planned with this approach.

- The second candidate was a shell and tube configuration that incorporated Teflon tubes. In this unit the corrosive cathode stream flows through the tube side. However, due to the small diameter of the Teflon tubes, the pressure drop is above specifications. Since units of larger shell or tube diameters are not available, desired pressure drop cannot be achieved. The feasibility of placing the exhaust stream on the shell side was investigated in this program. Units with Teflon lined shells can be provided for this reverse stream situation.

- The third candidate was a configuration that featured Teflon covered metal tubes and a Teflon lined enclosure. This offering had a reasonable cost estimate, but did not meet all functional requirements. Discussions revealed that the changes necessary to meet on-site requirements would be within vendor capabilities, and activity to develop this configuration is considered worthwhile.

Heat Exchanger Development - The objective of the heat exchanger development effort is to define a more functional and less costly design than that presently used in the 40-kW power plant. Work conducted in this phase of the program included the assessment of corrosion resistant heat exchangers identified in the GRI program. A discussion of this effort follows.

Candidate A - Investigation continued on the shell and tube heat exchanger that uses Teflon tubes. The original configuration, which had the exhaust stream on the tube side, exceeded pressure drop allocation. Placing the exhaust stream on the shell side, to reduce pressure drop, results in an excessively costly unit. This prompted

investigation of alternatives, specifically, using one of the vendor's standard Teflon tube bundles and enclosing it in a Teflon lined, box-type enclosure. This approach provides flexibility in selection of a tube bundle to meet heat transfer requirements and allows the cathode stream to be conveniently placed on the enclosure (shell) side to achieve low pressure drop. A performance sizing study has shown that the smallest Teflon tube bundle that meets 200-kW performance requirements and the Teflon lined enclosure for this tube bundle are no less costly than other approaches. The Teflon tube bundle vendor is unable to provide the type of enclosure required and would have to subcontract this work. No further activity is planned with this less-developed approach, since there is no cost advantage (relative to the other candidate heat exchanger), and additional effort would be required to design and procure an enclosure.

Candidate B - The acid condenser heat exchanger with Teflon covered tubes and a Teflon lined shell was also evaluated. The vendor supplied a unit sized for a 300-kW system that did not fully meet requirements, since he took exception to power plant condensate water conditions and assumed 80°F customer water on the tube side. The tubes in this heat exchanger were made of copper, which would be affected by the carbonic acid in the condensate water. The vendor confirmed that stainless steel tubes, which provide the required corrosion resistance, could be substituted for the copper tubes. The heat exchanger was resized to meet 200-kW power plant requirements. It was determined that a core approximately 70% larger than initially offered would be required to meet 200-kW requirements. The larger core, in conjunction with stainless steel tubes, resulted in an unacceptably high cost.

The vendor then offered core designs with tighter tube spacing and smaller frontal areas in the direction of gas flow. This allowed for better utilization of the pressure drop allocation, which had been increased by 50% as a result of system optimization studies. A study was conducted to define a smaller, more effective core based on the new design alternatives, which resulted in a core approximately 10 inches wide by 24 inches high by 20 inches long. This is about one-third the size of the initial 200-kW heat exchanger.

Figure 4-1 shows the latest acid condenser heat exchanger design. The unit does not include gas side manifolds, which are required for power plant operation.

The vendor prepared a design for a 200-kW acid condenser heat exchanger. After review and approval, a prototype unit was procured for performance testing (Figure 4-2). A separator, required for removing residual acid mist from the exit stream in power plant operation, was designed and fabricated. The acid separator is similar to the 40-kW design that utilizes graphite substrate elements. Although testing was conducted with an acid-free stream, the separator was included to insure pressure drop values were representative of power plant operation.

The heat exchanger was instrumented and installed in a test stand to evaluate performance and operational characteristics. Testing was conducted without acid vapor in the hot gas inlet stream, due to the difficulty in producing an acid-laden stream without a cell stack. Verification of the heat exchanger's ability to condense acid was based on achieving an exit temperature of about 265°F or lower. Experience with 40-kW power plants shows this to be a valid standard.

A summary of the test results is shown in Table 4-1. Testing at the 200-kW design point showed that all performance requirements were met. The maximum local gas stream temperature at the exit of the core was about 260°F. Total pressure drop for the heat exchanger and acid separator was about 1" H_2O, which is well within the allocated level. No water side flow instability was observed. System heat and water balances were generally within 5%, which supported test data. A small amount of water leakage was observed at the tube joints during testing, which the vendor attributed to the type of stainless steel tubing used. The problem will be corrected by retrofitting the unit with higher quality tubing. The amount of leakage is minor and does not affect test results.

Testing at a low power operating point (30 kW) showed that the heat exchanger will overperform when the condensate water is in the 70-120°F range. This situation produced local gas stream exit temperatures that were below the dew point, causing water condensation. A solution to this problem would be to preheat the condensate

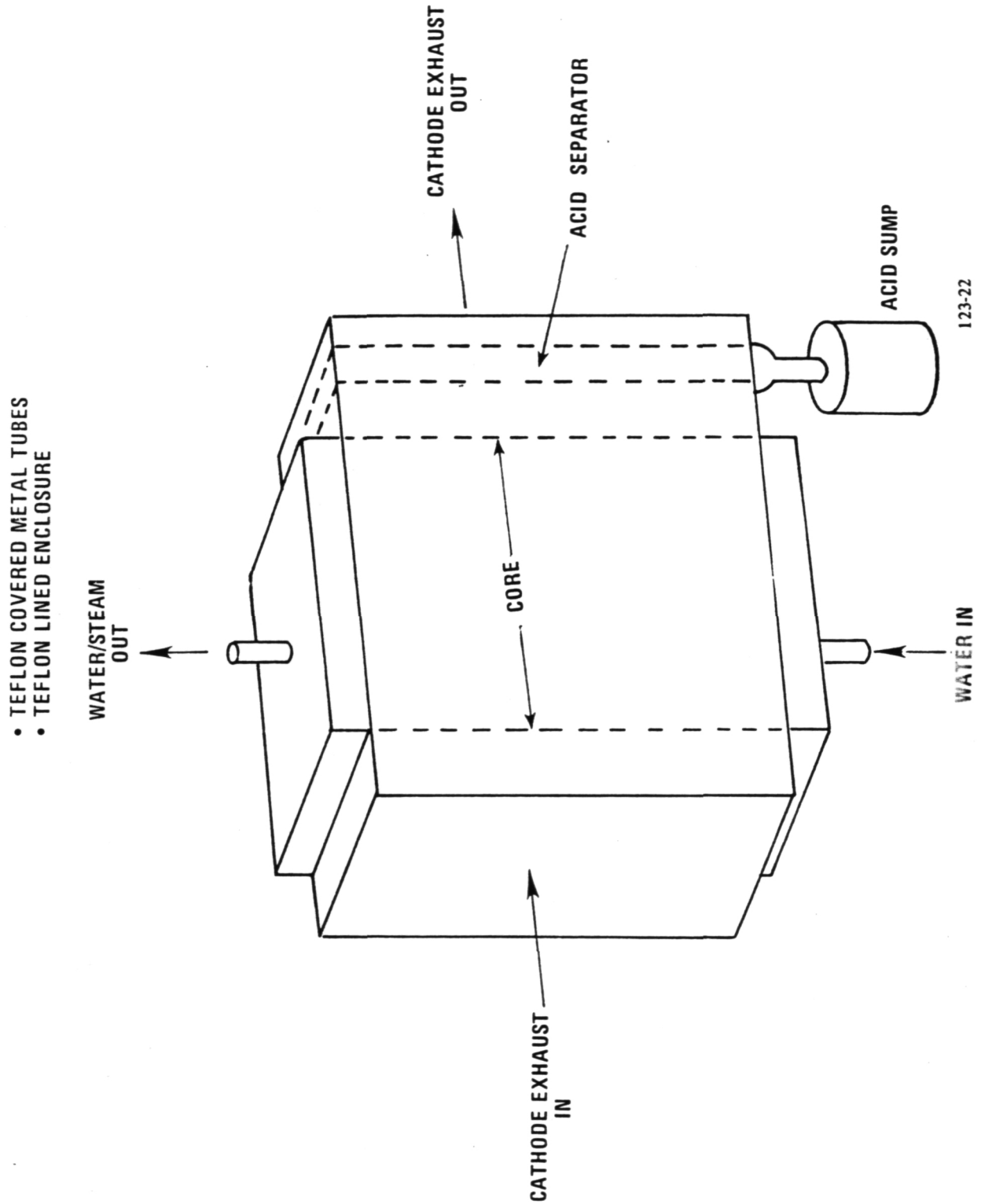

Figure 4-1. Modified Vendor Design for Acid Condenser Heat Exchanger

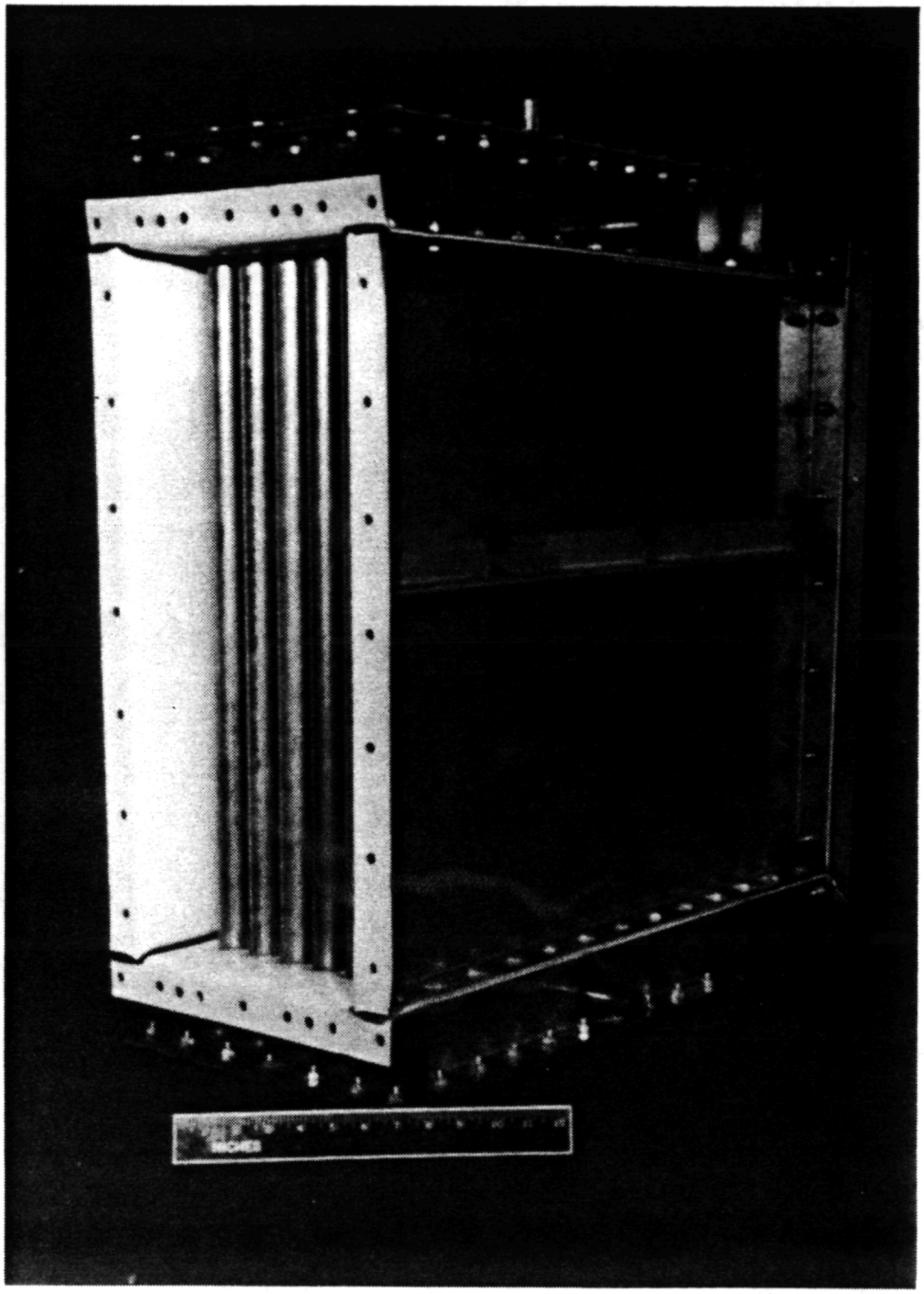

WCN-10710

Figure 4-2. Prototype 200-kW Acid Condenser Heat Exchanger

water to a temperature near the gas stream dew point, a convenient heat source being the 212°F exit water. There were no functional problems with the heat exchanger at the low power operating point.

With modifications to correct water leakage and low power overperformance, this heat exchanger is considered an acceptable acid removal device for the on-site power plant. The cost of this heat exchanger is slightly higher than direct contact water cooling approaches; however, its life, reliability, control free operation, and favorable system impact compensate for this.

Performance testing has shown that potential for further cost reduction does exist with this heat exchanger. A reduction in core size may be possible by incorporating multipass flow on the water side or the gas side, and these configuration changes could be incorporated by the vendor. The cost reduction potential of these changes will be investigated in a future program.

TABLE 4-1. ACID CONDENSER HEAT EXCHANGER TEST RESULTS

	Gas Stream Temperature (°F)		Water Temperature (°F)		Exhaust Gas ΔP
	Inlet	Exit	Inlet	Exit	(in. H_2O)
200-kW Design Point	400	190-260 range 242 average	128	212	0.9
Low Power Point (30-kW)	373	110-210 range 171 average	68	209	0.1

Direct Contact Water Cooling - Efforts were made to develop an alternative approach to the acid condenser heat exchanger. Various types of direct contact water cooling were considered, including evaporative spray cooling, contact saturation, and contact condensing.

The mechanism involved in these acid removal concepts is the evaporation of a water spray by direct contact with the cathode exhaust stream. In the case of the evaporative cooler, a controlled amount of water is injected into the cathode exhaust stream, cooling it to the desired acid condensing temperature of approximately 265°F. In the contact saturator and the contact condensor, acid is essentially washed out of the cathode exhaust stream by the injected water. In the latter concept both acid and water vapor in the cathode stream are condensed and removed.

A systems assessment was performed, and it was determined that all three candidate methods could be incorporated into an on-site power plant.

The impact of contact condensing on the water treatment system was determined. Based on the estimated acid loss rate, the load on the water treatment system would increase by a factor of about five, which increases the cost of the demineralizer by a like factor for equivalent bed life. Since this cost penalty is unacceptably high, no further activity is planned using this approach. Based on system and cost assessments, evaporative spray cooling and contact saturation were selected for experimental evaluation.

Evaporative Water Spray Cooling - Candidate nozzles were tested to determine spray pattern and turndown capability for evaporative spray cooling application. Steam assist water spray nozzles were selected for initial testing; these use steam energy to atomize the water. These nozzles have a larger orifice for a given flow rate than conventional nozzles and can be operated over a larger turndown. Bench testing was conducted and a selection was made for the full-scale evaporative spray cooler rig. The nozzle selected did not produce complete atomization at the 200-kW flow rate, but the downstream packed bed in the evaporative spray cooler should compen-

sate for this. Spray quality of the nozzle improved at lower flow rates, which means turndown should not be a problem.

The selected water source for evaporative spray cooling is power plant feedwater taken from the exit of the demineralizer. This is the cleanest water available and should minimize the possibility of nozzle plugging. For nozzle and rig testing, facility DI/DO water was used, since it closely resembles power plant feedwater.

A vessel and packed bed were fabricated to meet the requirements of the evaporative spray cooler. A schematic sketch of the test rig is shown in Figure 4-3. Figure 4-4 shows the test rig prior to installation in the test stand. The test results are discussed below and summarized in Table 4-2.

BUILD I - The first build of the rig utilized a ballast ring packing shown in Figure 4-5. The height of the packed bed was 10 inches. The spray cooler was tested initially with the water nozzle spraying in the direction of the hot gas flow, then reversed to spray counter to the gas stream. Spray cooler performance was acceptable in both configurations, at gas flows corresponding to about 100 kW. The gas exit temperature was reduced to 260°F, which meets requirements for complete acid removal. A system heat balance was obtained, indicating all the water was vaporized. At higher gas flows (representing that of a 150- to 200-kW operation) neither of the two configurations performed satisfactorily. The water was not fully vaporized in the distance between the spray nozzle and bottom of the packed bed, resulting in water collecting in the sump and a high gas exit temperature.

To improve water vaporization at full power flow rates, the height of the packed bed was increased from 10 inches to 16 inches. The increased bed height did not produce acceptable performance at the 200-kW operating point; water still collected in the sump, indicating incomplete vaporization. There was no significant reduction in water carryover into the sump for the increased bed height, indicating the packing material was not providing an effective surface for vaporization.

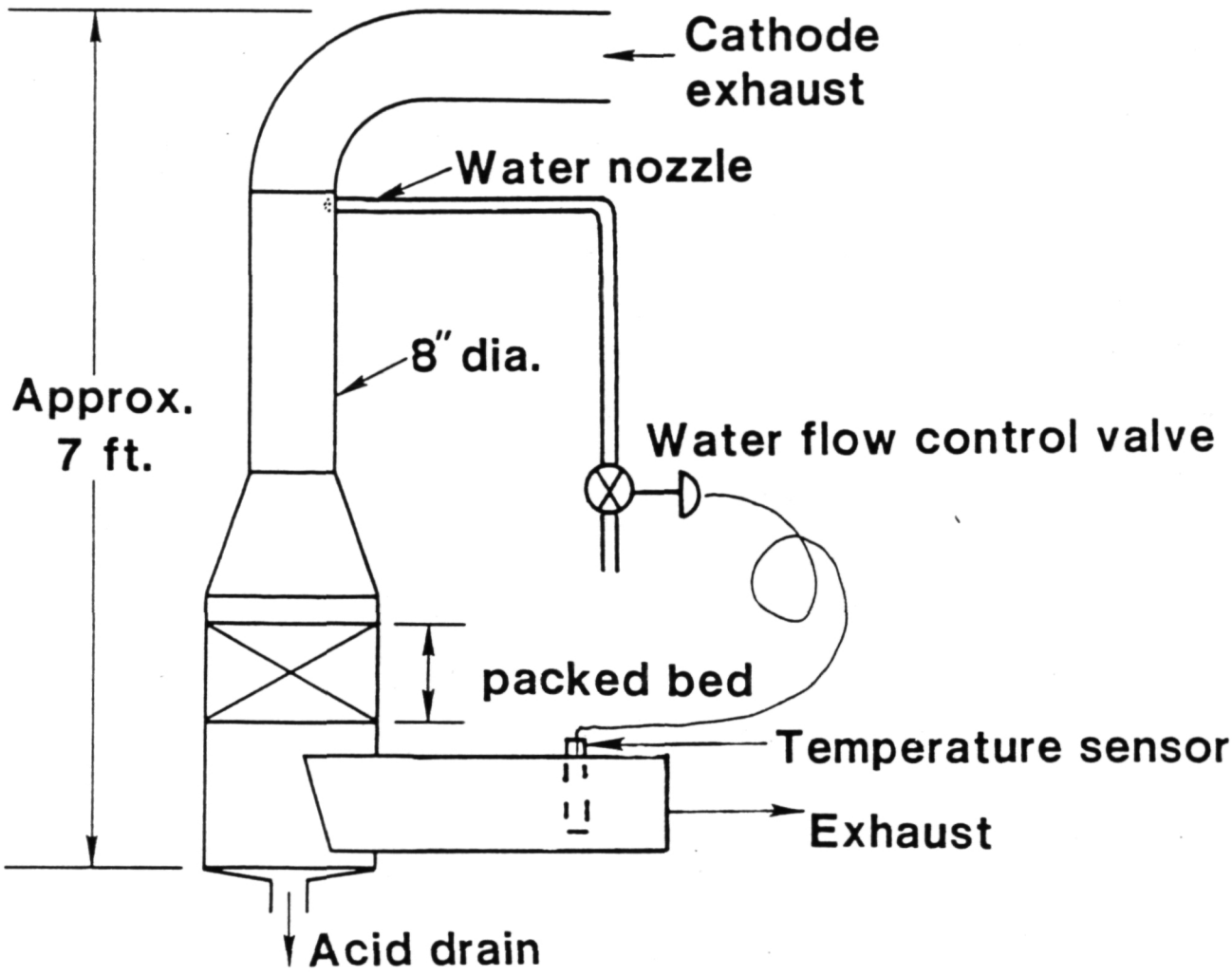

Figure 4-3. Evaporative Spray Cooler Rig for 200-kW System - Schematic

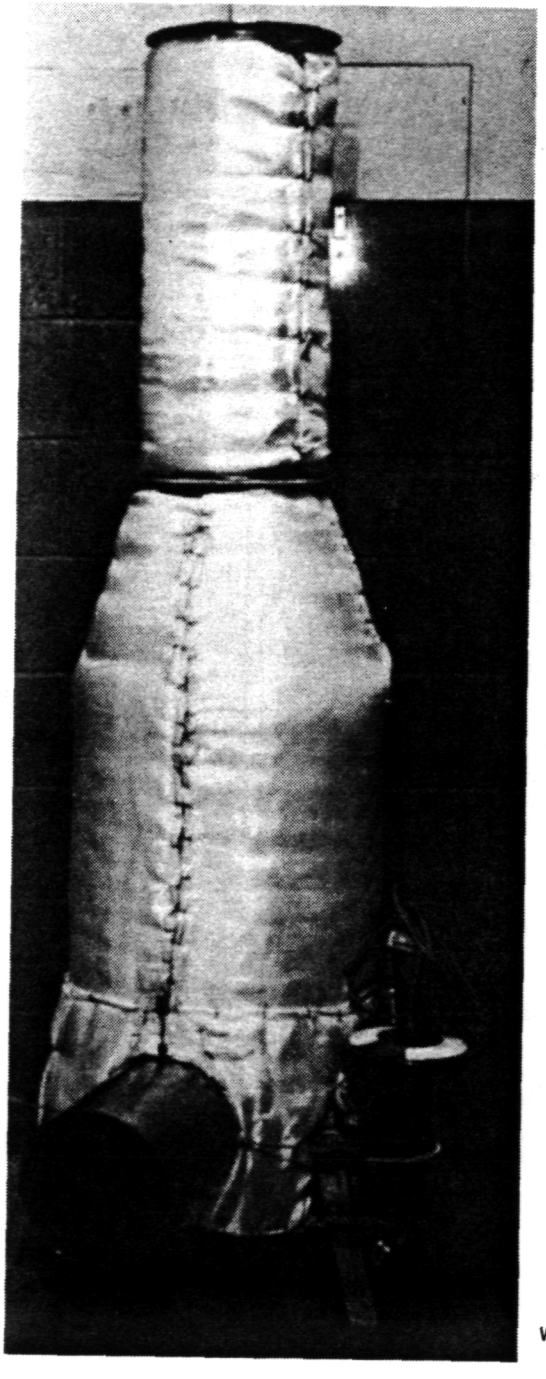

WCN-10011

Figure 4-4. Evaporative Spray Cooler Rig

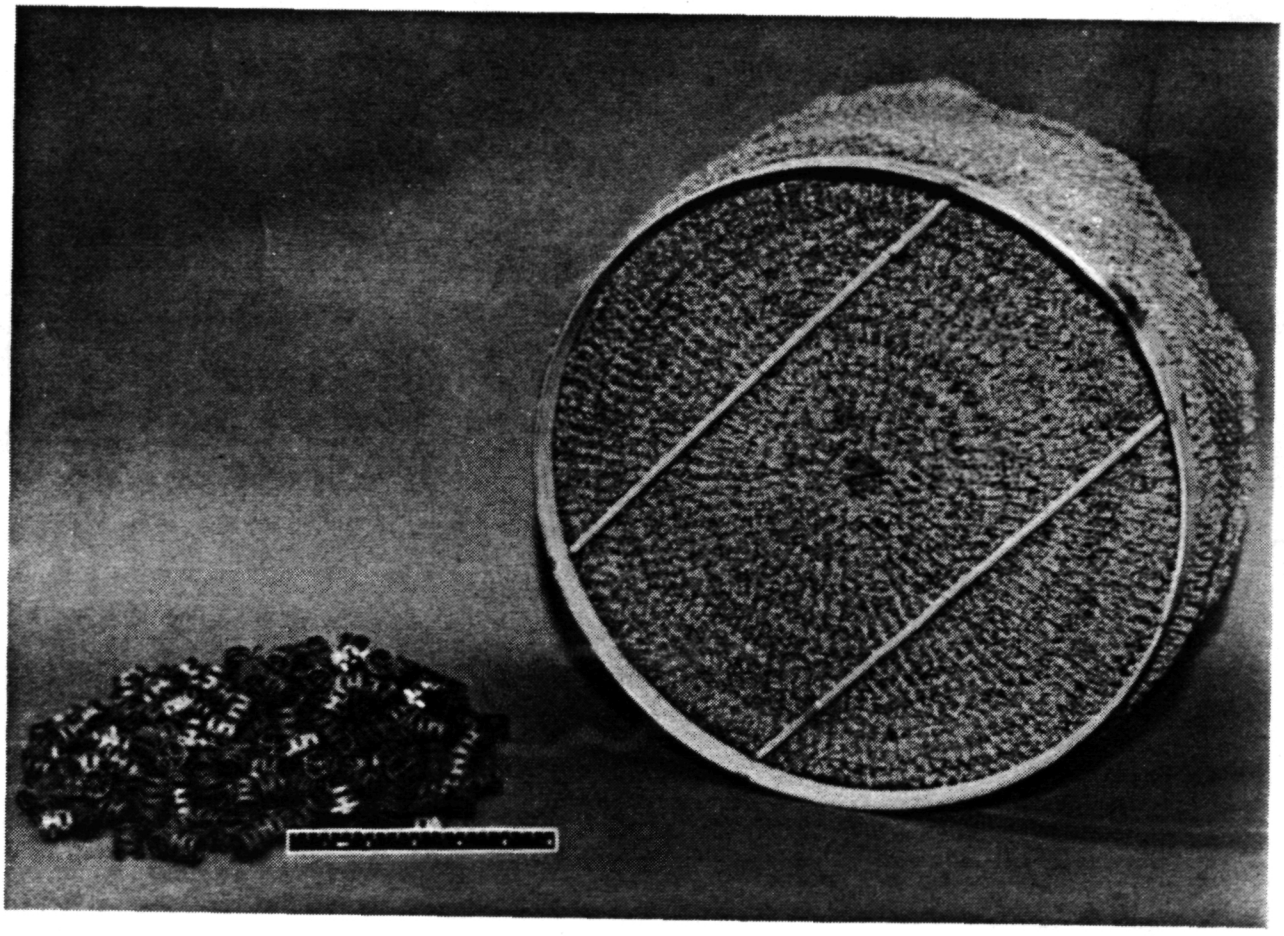

WCN-10704

Figure 4-5. Ballast Ring Packing (Left) and Wire Mesh Packing Evaluated in Evaporative Spray Cooler Rig

BUILD II - In the second build of the rig, a stainless steel wire mesh packing was tested. A significant performance improvement was obtained with this packing. At the 200-kW operating point, the amount of water carryover into the sump due to incomplete vaporization was about 50% less than with the ballast ring packing. The total pressure drop of the spray cooler rig was well within the allocation. The wire mesh packing is shown in Figure 4-5.

BUILD III - Build III of the rig used a higher density stainless steel wire mesh packing to improve water vaporization at high power points. Testing with the higher density packing produced acceptable results at the 200-kW operating point. There was no water carryover into the sump, and the gas stream exit temperature measured 20°F below the requirement for complete acid removal. The pressure drop was acceptable.

Testing of the evaporative water spray cooler up to this point had been conducted with a dry gas inlet stream. A test was then conducted with a humidified gas inlet stream, to determine whether there would be a significant performance difference. The gas inlet stream was humidified to 67% of the cathode exhaust moisture level, the maximum amount of humidification that could be obtained without significant changes to the test stand steam supply system. Performance at this level was acceptable. There was no water carryover into the sump, therefore the exit temperature was the same as obtained in the test with a dry gas inlet stream. Water breakthrough did not occur until the water spray flow was increased by 25% and the stream was cooled an additional 20°F.

On the basis of these results, it was analytically determined that the 6-inch bed height should be increased by about 30% to insure that no water breakthrough would occur at the 100% cathode exhaust stream moisture level. To provide an operating margin, a 50% increase in bed height will be specified. This does not present a problem, since the cost of increasing the bed height from 6 inches to 9 inches is minimal and pressure drop will still be within allocation.

An acceptable water flow control system has not been identified for the evaporative spray cooler. Testing with the standard commercial temperature sensing water flow control valve did not provide acceptable control. Definition of an alternative water flow control device was not pursued in this program.

TABLE 4-2. WATER SPRAY ACID CONDENSER TEST RESULTS

Build	Packing	Results
1	Ballast Ring	o Acceptable performance up to 150-kW flow rate
		o Water carryover at 200-kW flow rate
		o No improvement with increased bed height
		o ΔP 1.2 - 1.5 in H_2O
2	Stainless Steel Wire Mesh (low density)	o Improved performance
		o Water carryover reduced
		o ΔP 0.5 in H_2O
3	Stainless Steel Wire Mesh (higher density)	o Acceptable performance at 200-kW flow rate
		o 50% increase in bed height specified for power plant stream moisture level
		o ΔP 1.0 in H_2O for increased bed height

Contact Saturator - A contact saturator was evaluated to determine its ability to reduce the cathode exhaust stream temperature to the level required for acid condensation. Details of the contact saturator configuration cannot be disclosed at this time due to patent considerations. A contact saturator rig was assembled for a 200-kW system. Testing of the initial build of the contact saturator rig resulted in the gas stream being cooled to approximately the saturation temperature of the gas stream used in the test. This is significantly lower than the temperature required for complete acid condensation. The system performance impact of cooling

the cathode exhaust stream below the optimum 250-270°F temperature range is being assessed.

The water flow rate was decreased to demonstrate that the degree of cooling could be reduced if required. At this condition a higher gas stream exit temperature was obtained. This result indicates it is possible to define a configuration that cools to any desired temperature.

The contact saturator approach to acid removal is considered a viable method. This method utilizes basic components that do not require complex controls.

Conclusion

Table 4-3 summarizes characteristics of the three candidate acid condenser devices evaluated in this program. The preferred acid condenser device for the present on-site baseline system is the heat exchanger with Teflon covered metal tubes and Teflon lined enclosure. The higher cost of this heat exchanger, relative to the water cooling approaches, is offset by its advantages: system simplification, system performance, reliability, life, and maintenance. The alternative selection is the contact saturator, which has less control complexity and higher reliability than the evaporative water spray cooler.

Additional activity to investigate a potentially lower cost approach to the acid condenser heat exchanger is planned in the 1984 GRI and NASA On-Site Programs. This effort will address an uncoated metal heat exchanger, designed to operate with all surfaces (including the shell or enclosure) acting as heat exchanger surfaces. This maintains moderately low metal temperatures throughout, which reduces corrosion rates. Corrosion rates will be determined through laboratory tests and 40-kW field experience with uncoated stainless steel heat exchanger plates. If life and cost projections of this approach appear favorable, a prototype heat exchanger will be procured for experimental evaluation.

TABLE 4-3. COMPARISON OF ACID REMOVAL CANDIDATES

Feature	Heat Exchanger	Evaporative Spray Cooler	Contact Saturator
Manufactured Cost	Highest	Lowest	Lowest
Performance	o Meets requirements o Overperforms at low power	o Meets requirements o Turndown control not defined	o Feasibility of meeting requirements demonstrated
System Complexity	Lowest o No controls	Highest o Precision water flow control o Requires superheated steam addition	Intermediate o Make-up water control o Circulating pump
Reliability	Highest o Passive device	Lowest o Water flow control and nozzle plugging potential problems	Intermediate o Uses basic components with known reliability
Volume	Lowest	Intermediate	Highest o Large sump required for recirculating water inventory
System Performance Penalty	o No penalty	o 0.3 kW parasite power (WTS pump) o 1.5% loss in electric efficiency at half power due to steam consumption	o 0.3 kW parasite power (recirculating pump)
Impact on Condenser	Baseline	5% size increase for equivalent delta P	5% size increase for equivalent delta P
Estimated Life	Highest o Corrosion resistant materials used	Lowest o Bare metal surfaces subject to corrosion	Intermediate o Wetted metal surfaces have lower corrosion rate
Maintenance Items	o Acid sump	o Spray nozzle o Packed bed o Acid sump	o Pump o Level control o Packed bed o Acid/water sump

TASK 5 FUEL PROCESSOR DEVELOPMENT

TASK 5 - FUEL PROCESSOR DEVELOPMENT

Subtask 5.1 Develop Fuel Processor Catalyst Technology

Objective

The objective of this subtask is to define hydrodesulfurization and low temperature shift catalyst characteristics in order to minimize the bed sizes, and to define reforming catalyst performance and pressure drop in order to optimize the packaging configuration (length/diameter ratio) of the reformer.

Summary

Several reforming catalysts were identified which have significantly lower pressure drop than the 40-kW catalyst. Low pressure drop reforming catalyst is important to the design of the 200-kW development reformer, as it allows the required catalyst volume to be packaged into fewer longer tubes, for reduced cost. The catalysts were identified via visits and telephone contacts with catalyst vendors. Of eight candidate catalysts tested, four were found to have performance equivalent to that of the 40-kW catalyst. One of these has been selected for evaluation in the endurance test, since its small size permits design of a reformer with a thinner bed than would be possible with the other catalysts.

An alternative shift converter catalyst has been identified to have higher performance than the 40-kW catalyst. Since the long-term life characteristics of the 40-kW catalyst are known, this new catalyst has been selected for endurance test evaluation. This test could then be used as a basis for qualifying this catalyst for use in on-site power plants.

A hydrodesulfurizer catalyst has been prepared by PSD. This catalyst does not require the costly, time-consuming presulfiding operation required for the 40-kW catalyst. Problems were encountered during performance testing of this alternate catalyst, however, which called for analysis of the extremely low sulfur concentrations in the gas streams. This resulted in a delay in test completion and selection of catalyst for the endurance test.

Highlights

- Selected a reforming catalyst for the endurance test having significantly lower pressure drop and equivalent performance to the 40-kW catalyst.

- Selected an alternate shift converter catalyst for stability testing in the endurance test.

Discussion

Reformer catalyst testing was conducted in an electrically heated subscale reactor capable of testing catalysts under controlled temperature conditions. The pressure drop and heat transfer effects in this reactor are analogous to those found in full-scale reformers. A schematic diagram of the reactor is shown in Figure 5.1-1. The reactor is 46.5 inches in length and has an I.D. of 1.38 inches. Sample taps are located at intermediate positions along the length of the reactor so that the degree of fuel conversion can be determined along the length of the reactor as well as at the reactor exit. The temperature in each of the reactor sections is controlled by separate heaters that can be adjusted to maintain constant wall temperatures for a variety of conditions. A photograph of the reactor installed in the furnace is shown in Figure 5.1-2.

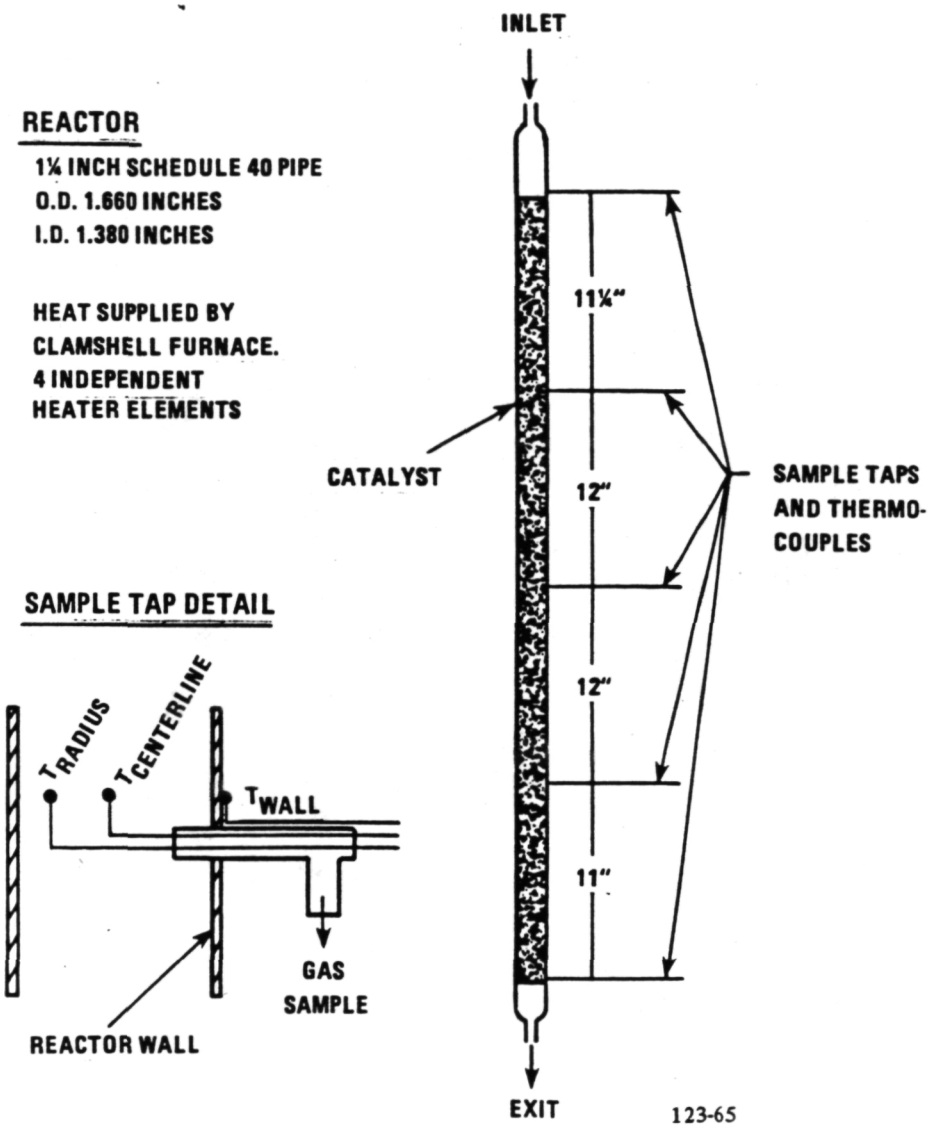

Figure 5.1-1. Subscale Reactor Schematic

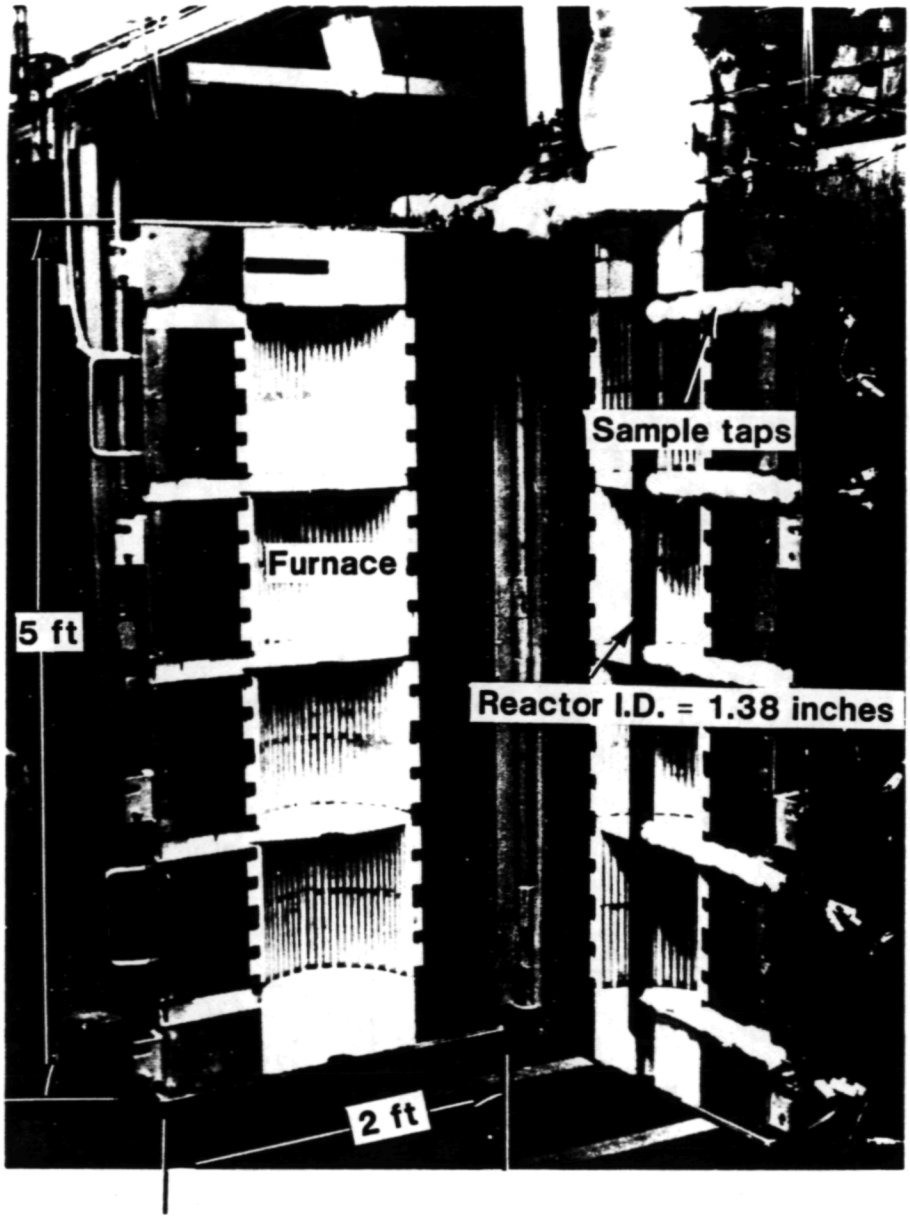

FC18708
R840503

Figure 5.1-2. Subscale Reactor and Furnace

A total of eight candidate catalysts plus the 40-kW reformer catalyst were tested. Figure 5.1-3 shows a comparison of the data for the 40-kW catalyst and three of the candidate catalysts. As shown by the data in the figure, varying degrees of pressure drop reduction can be attained while maintaining good reform conversion at the reactor exit. Reforming conversion for these catalysts was also measured at the intermediate taps along the length of the reactor. The results indicate that there is very little difference in reform conversion between the 40-kW catalysts and the low pressure catalysts (Figure 5.1-4). The data presented in the two figures above were taken at a mass flux (lbs. of fuel/hr. per unit reactor cross section) equal to the mass flux used in the 200-kW reformer design. Reactants were fed to the reformer at 650°F and the same reactor wall temperature profile was maintained for all the catalysts with a 1400°F wall temperature at exit (see Table 5.1-1). The 1x tests were run at a space velocity of 17.1 lbs. fuel/ft^2-hr. Tests were also run at more severe conditions where the mass flux was twice that of the present 200-kW design mass flux, and a 1500°F wall temperature was maintained at the reactor exit. The 2x tests were run at space velocity of 34.2 lbs. fuel/ft^2-hr. Results of these more severe conditions are shown in Figure 5.1-5. The reform conversions in this figure show only a small difference between the lowest pressure drop catalyst and the 40-kW catalyst. Data for all the catalysts tested are listed in Tables 5.1-2 and 5.1-3. The data for catalysts not shown in the foregoing figures but listed in the table are slightly lower than for the three catalysts used in the illustration.

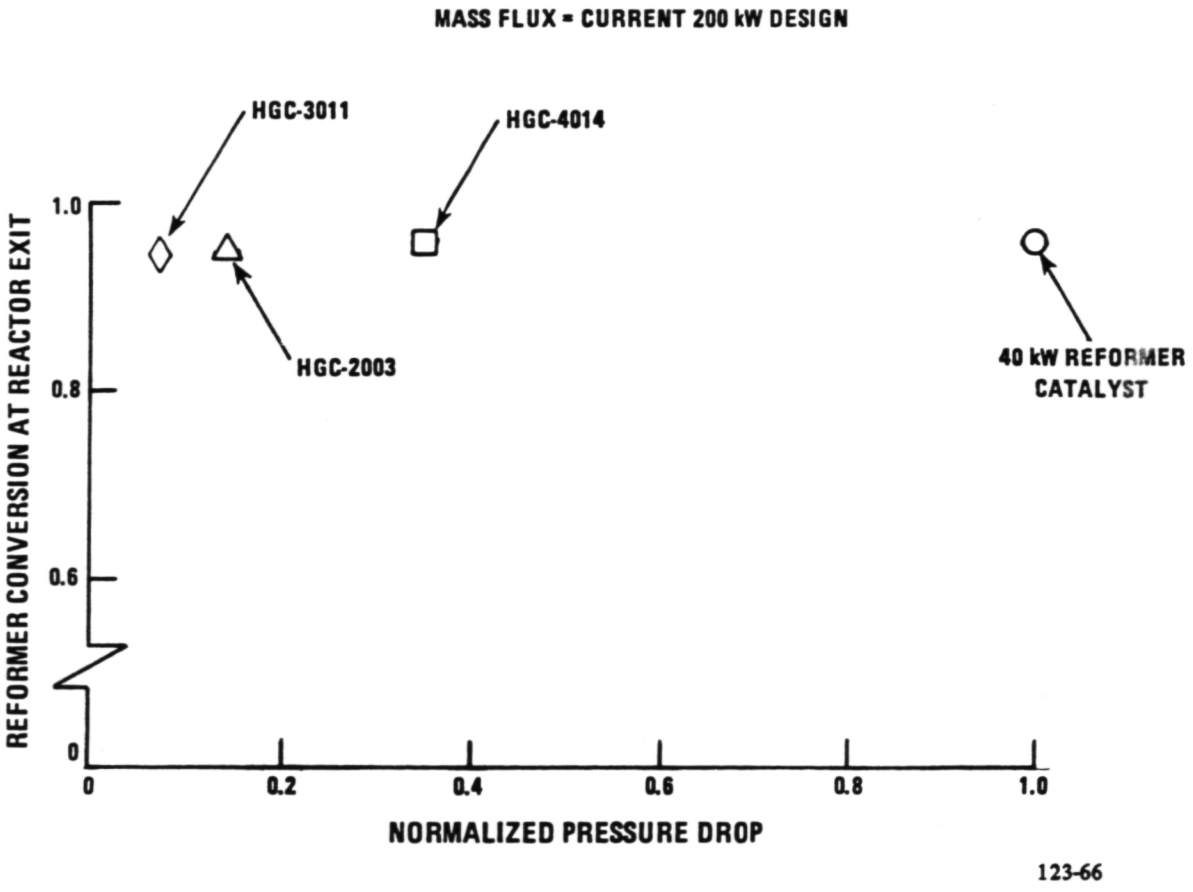

Figure 5.1-3. Low ΔP Catalysts Reform Conversion

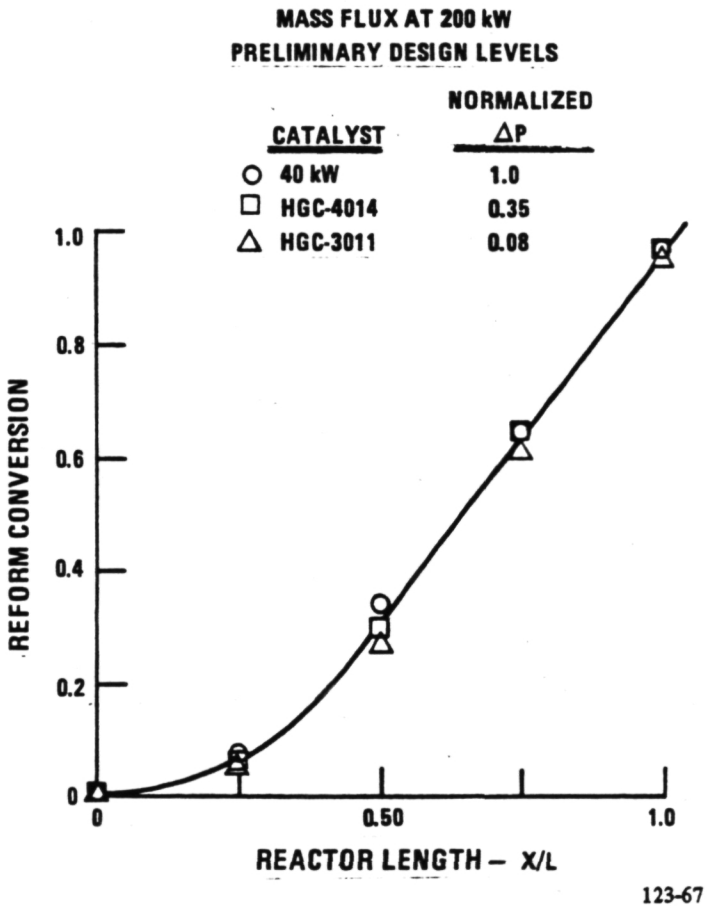

Figure 5.1-4. Reform Conversion with Reduced ΔP Catalysts

TABLE 5.1-1. WALL TEMPERATURE PROFILES
(Temperatures in °F)

Relative Mass Flux (lb/ft^2-hr)	Normalized Reactor Length (X/L)				
	0	1/4	1/2	3/4	1
1x	650	800	1000	1200	1400
2x	700	900	1100	1300	1500

HCG-4014 has been selected as the reforming catalyst for the endurance test, since its small size permits design of a reformer with a thinner bed than would be possible with some of the other catalysts. The thinner bed minimizes the catalyst volume required.

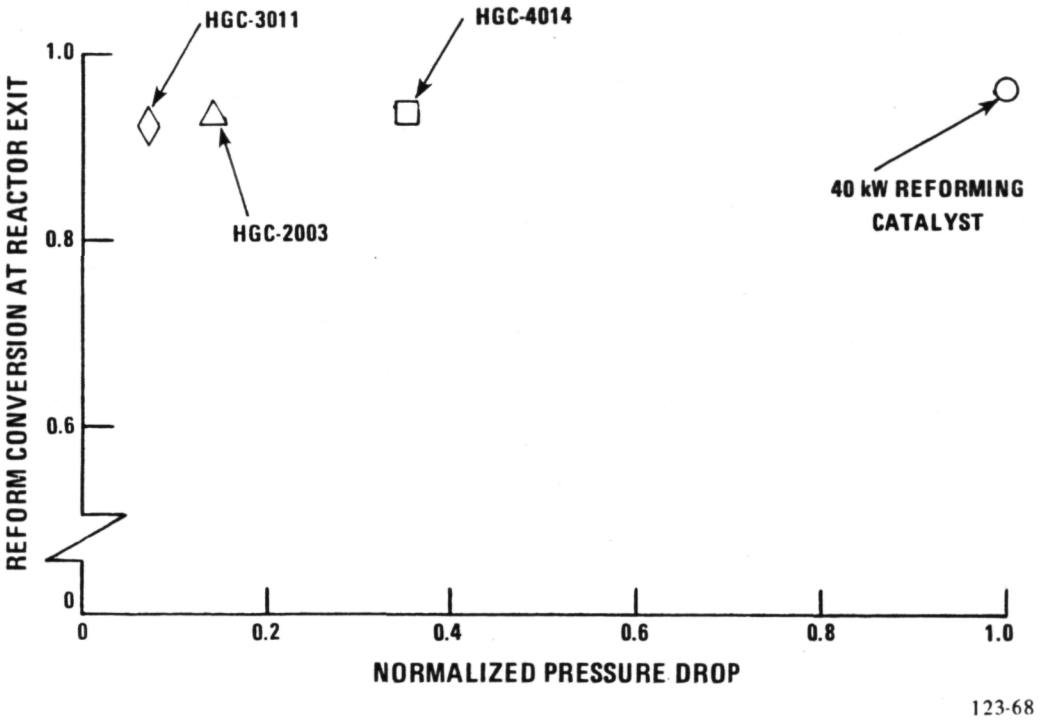

Figure 5.1-5. Performance of Catalysts at 2x Design Mass Flux

Table 5.1-2. Performance of Low ΔP Catalysts

Reform Catalyst Comparison Data											
				Fuel Conversion(θ)(2)							
Catalyst	Shape	Size	Normalized P (1)	Design Flux	2X Design Flux	Commercial Experience	Normalized Geometric Surface Area	Normalized Solid Volume	Catalyst Condition Post Test	Catalyst Void Fraction (Subscale)	Relative Cost (Ft^3)
40 KW	Pellets	3/16x1/8	1.0	.96	.97	Yes	1.00	1.00	Acceptable	.36	1.0
HGC-2000	Pellets	5/32x3/16	.92	.94	.94	Yes	1.02	.95	Acceptable	.39	N/A
HGC-1009	Pellets	1/4x1/4	.45	.91	.84	Yes	.64	.94	Acceptable	.40	N/A
HGC-4014	Rings	5/16x5/16	.35	.96	.94	Yes	.79	.88	Acceptable	.44	1.0-1.3
HGC-8001	LPDS	1/4"	.25	.91	-	No-Lab	2.78	.59	Acceptable	.62	N/A
HGC-2003	Rings	7/16x7/32	.14	.95	.94	Yes	.62	.75	Acceptable	.52	1.0-1.3
HGC-3011	LPDS Cross-Partioned	3/8"	.07	.94	.92	No-Pilot	-	.45	Acceptable	.71	N/A
HGC-4012	Rings	5/8x5/16	.07	(3)	(3)	Yes	.80	.59	Acceptable	.62	N/A
HGC-2004	Rings	7/16x7/16	.04	.90	.88	Yes	.55	.59	Acceptable	.62	N/A

Notes: (1) Average of hot reform test data at 1, 2x design flux.

(2) Fuel conversion, $= \frac{CO + CO_2}{CO + CO_2 + CH_4}$

(3) Early tests not run at these exact conditions. Conversion falls between the HGC-3011 and HGC-2004 catalyst.

Table 5.1-3. Experimental Data on Activity Screening of Low ΔP Catalysts

CAT ID/Gas Flow	Axial Temp, Location X/L = 0					Axial Temp, Location X/L = .25					Axial Temp, Location X/L = .50					Axial Temp, Location X/L = .75					Axial Temp, Location X/L = 1.0					Methane Conversion at Various X/L				
	Wall	Δ	Radius	Δ	Center	Wall	Δ	Radius	Δ	Center	Wall	Δ	Radius	Δ	Center	Wall	Δ	Radius	Δ	Center	Wall	Δ	Radius	Δ	Center	0.0	0.25	0.50	0.75	1.00
40 kW/Normal	747	98	649	12	637	797	60	737	4	733	996	51	945	44	901	1196	46	1150	83	1067	1404	73	1331	21	1310	0.005	0.085	0.327	0.653	0.965
2X Normal	832	120	712	16	696	894	110	784	5	779	1093	89	1004	63	941	1298	91	1207	117	1090	1500	129	1371	49	1322	0.005	0.114	0.395	0.683	0.968
Normal	751	95	656	0	656	800		--		722	999	69	930	15	915	1200	105	1095	5	1090	1400	92	1308	40	1268	0.006	0.073	0.340	0.643	0.964
2X Normal	882	171	711	8	703	892		--		764	1098	117	981	16	965	1301	170	1131	6	1125	1499	160	1339	24	1315	0.008	0.098	0.410	0.698	0.973
HGC-4014/Normal	703	127	576	9	567	803	53	750	2	748	1001	68	933	33	900	1200	48	1152	81	1071	1401	72	1329	13	1316	0.006	0.061	0.296	0.641	0.961
2X Normal	834	144	690	8	682	900	94	806	2	804	1099	120	979	40	939	1299	99	1200	109	1091	1500	135	1365	41	1324	0.006	0.085	0.342	0.651	0.940
HGC-2003/Normal	814	162	652	14	638	804	-69	873	92	781	1003		--		918	1198	89	1109	28	1081	1400	131	1269	-65	1334	0.006	0.127	0.324	0.635	0.952
2X Normal	1028	310	718	14	704	899	-150	1049	88	861	1099		--		983	1299	128	1171	46	1125	1500	181	1319	-64	1383	0.006	0.188	0.420	0.694	0.956
HGC-3011/Normal	745	94	651	-5	656	788	45	743	15	728	985		--		888	1197	59	1138	77	1061	1409	104	1305	-6	1311	0.005	0.049	0.263	0.608	0.945
2X Normal	844	147	697	1	696	901	80	821	27	794	1099		--		945	1301	111	1190	108	1082	1502	200	1302	9	1293	0.005	0.091	0.300	0.596	0.924
HGC-2000/Normal	739	71	668	18	650	796	52	744	20	724	997	52	945	53	892	1199	67	1132	58	1074	1400	91	1309	22	1287	0.006	0.068	0.309	0.600	0.935
2X Normal	848	134	714	16	698	892	89	803	29	774	1092	93	999	66	933	1296	131	1165	68	1097	1497	152	1345	45	1300	0.006	0.096	0.359	0.632	0.942
HGC-1009/Normal	709		--		643	802	57	745	6	739	1005	79	926	47	879	1203	44	1159	130	1029	1403	112	1291	14	1277	0.005	0.065	0.253	0.547	0.912
2X Normal	783		--		698	898	97	801	7	794	1097	103	994	64	930	1302	80	1222	143	1079	1497	134	1363	70	1293	0.005	0.007	0.254	0.513	0.840
HCG-8001/Normal	721	66	655	3	652	800	29	771	9	762	999	75	924	3	921	1201	72	1129	93	1036	1400	143	1257	3	1254	0.009	0.016	0.147	0.505	0.906
2X Normal							0																							
HGC-2004/Normal	737	86	651	8	643	791	54	737	2	735	990	50	940	38	902	1193	21	1172	141	1031	1400	69	1331	27	1304	0.005	0.051	0.211	0.537	0.898
2X Normal	839	175	664	13	651	895	106	789	1	788	1086	99	987	36	951	1288	55	1233	188	1045	1492	146	1346	21	1325	0.005	0.061	0.266	0.545	0.885

A shift converter catalyst having activity comparable to that of the 40-kW catalyst has only been available from one source. An effort was made, therefore, to identify an alternative source for such a catalyst. This has been done and vendor performance data from this alternate catalyst shows that its activity is higher than that of the 40-kW shift catalyst. For this reason it has been selected for the upcoming endurance test. If the claimed performance improvement is verified at the low pressure conditions used in the 200-kW power plant, then the volume of the power plant shift converter could be reduced.

An alternative hydrodesulfurization catalyst that does not require any presulfiding to become active, as does the 40-kW catalyst, was prepared at PSD. The catalyst's activity was evaluated by placing a segmented bed in an electrically heated reactor (see Figure 5.1-6) and determining its ability to decompose thiophane, a sulfur compound frequently used as a natural gas odorant. Measurements of the thiophane concentration were made at the various sample taps using a DOHRMANN microcoulometric sulfur analyzer. Data obtained using this technique was not repeatable, and for this reason the thiophane approach was replaced by measuring the level of hydrogen sulfide, the product of thiophane decomposition. This measurement was taken using KITAGAWA hydrogen sulfide detection tubes. The data is now repeatable and shows that this catalyst has higher activity than the 40-kW catalyst. The testing, however, is not expected to be completed until early January 1984. An HDS catalyst selection for the endurance test will be made at that time.

Subtask 5.2 Fuel Processor Catalyst Endurance Testing

Objective

The objective of this subtask is to carry out a 2000 hour endurance test featuring one of each of the catalyst types selected in Subtask 5.1.

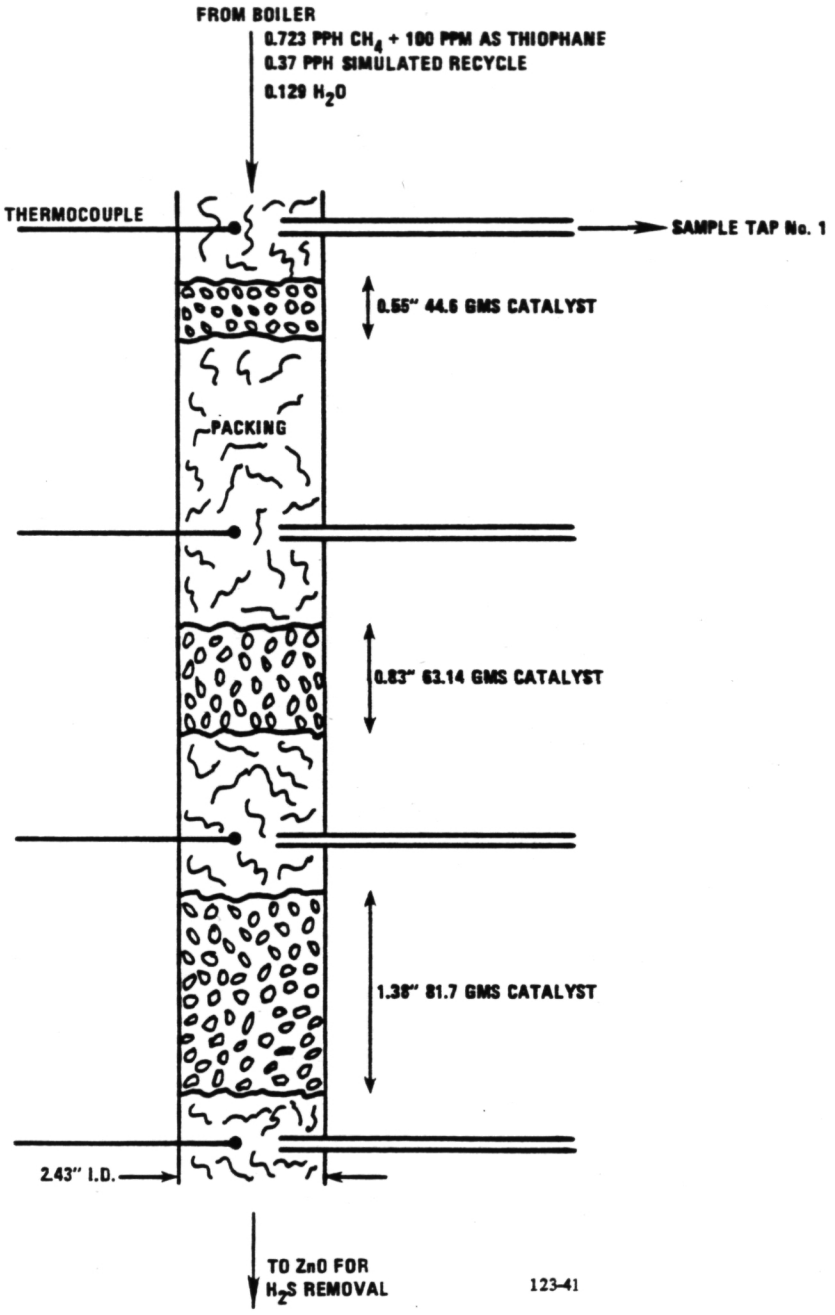

Figure 5.1-6. Subscale HDS Test Reactor Schematic

Summary

A 2000 hour endurance test of a fuel processing catalyst train is planned in order to demonstrate long-term stability of the selected catalysts. The catalyst train is comprised of a hydrodesulfurizer, steam reformer, and shift converter connected in series, as they would be in a power plant. A test stand has been modified to accept the subscale reactors, which have been fabricated. The reforming and shift converter catalysts have been selected, and a supply of them is on hand. Problems measuring gas stream sulfur concentrations in the Task 5.1 hydrodesulfurizer testing have delayed the selection of this catalyst for the endurance test. This has postponed the start of the endurance test until January 1984.

Highlights

- A test stand has been prepared for the endurance test.
- The reactors have been fabricated and loaded with catalyst, with the exception of the hydrodesulfurizer.

Discussion

A 2000 hour endurance test of a fuel processing catalyst train is being planned. This test will provide experience with certain catalysts that offer potential benefits relative to the 40-kW catalysts. The endurance train will be comprised of a fuel clean-up section (hydrodesulfurizer/ZnO sulfur scrubber), a steam reformer, and a low temperature shift converter. These will be arranged as shown in Figure 5.2-1. The individual vessels have been fabricated and loaded with catalysts selected in subtask 5.1, with the exception of the hydrodesulfurizer, since final selection of this catalyst has been delayed. This catalyst train is planned to operate on a representative pipeline quality natural gas. The throughput will be varied over the anticipated range of the power plant, and gas compositions will be monitored at periodic intervals in order to establish catalyst stability characteristics.

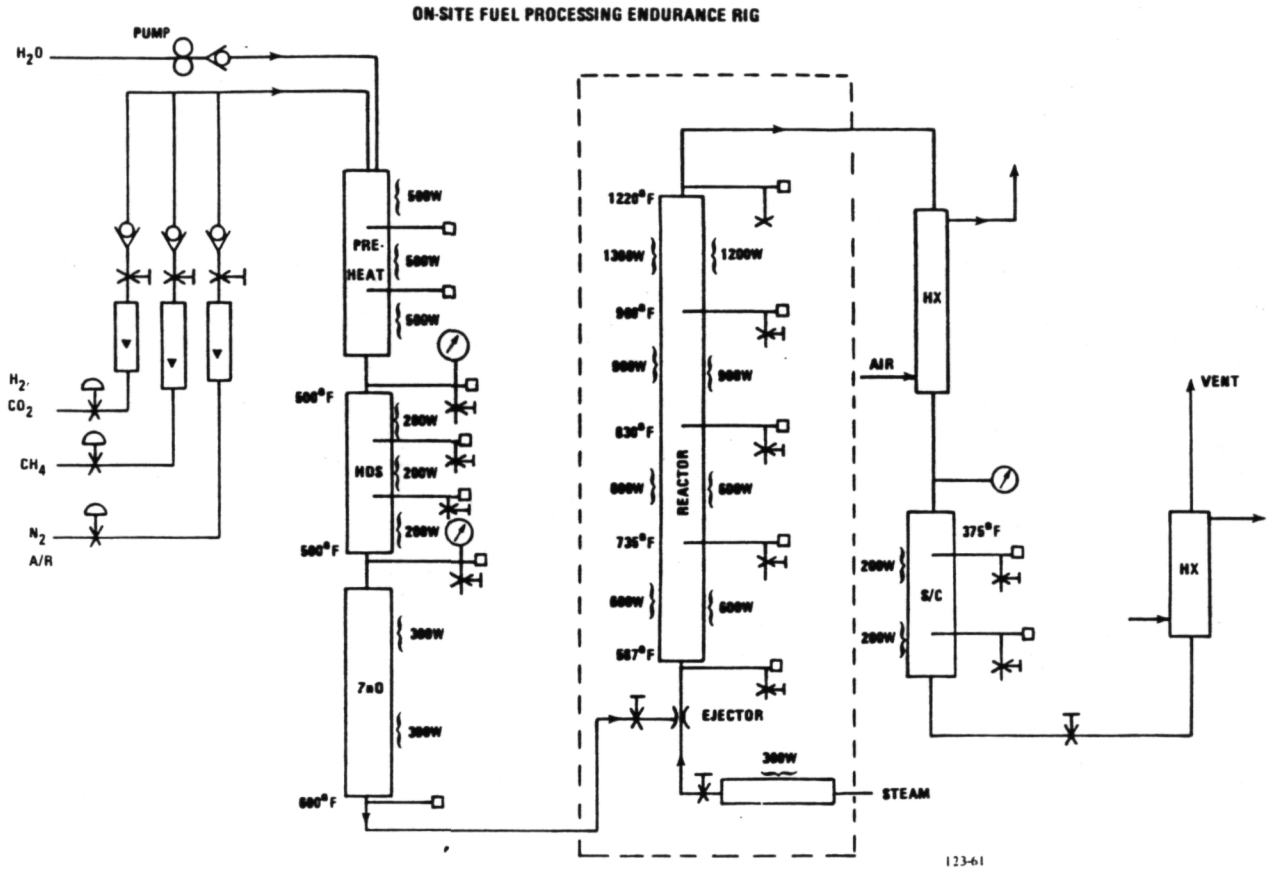

Figure 5.2-1. Catalyst Endurance Train for On-Site Fuel Processor

The catalyst vessels are designed so that each catalyst type will be subjected to operating conditions similar to those found in the power plant. The reformer was fabricated from a four foot section of 1.25 inch schedule 40 pipe, and contained 1362 grams of HGC-4014 steam reforming catalyst. The shift converter was fabricated out of a 41 inch section of three inch tubing and contained 6808 grams of HGC-4015 shift catalyst. The test stand was designed to operate at fuel flows up to 1.4 pounds per hour.

Subtask 5.3 Verify Reformer Technology

Objective

The objective of this subtask is to prepare a development reformer for testing.

Summary

A tubular configuration for the 200-kW development reformer was selected and analyzed under GRI Contract No. 5080-344-0405. A burner test rig was fabricated, and a commercial burner was purchased and is being evaluated. In addition, a two dimensional flow model of the first of three potential burner arrangements was fabricated, and water flow table testing has begun. An infra-red pyrometer has been purchased and will be evaluated as an alternate means of reformer temperature control. This technique has the potential for higher reliability and stability. Design of the reformer is being addressed in the parallel GRI effort.

Highlights

- Selected a seven tube reformer from among five candidate configurations for the 200-kW development reformer design. Performance estimates confirmed that this selection satisfies system performance requirements.

- Prepared a facility for testing a commercial burner and began tests to map burner performance.

- Prepared facility for conducting water table model tests of the burner arrangement.

- Purchased equipment for infra-red pyrometric tube temperature sensing and control.

- Development reformer design is underway under the parallel GRI effort.

Discussion

A development reformer is being designed under the parallel GRI design task. Work done to support this effort has included screening and selection of a reforming catalyst, performance analysis estimates, modification of an existing UTC test facility for testing candidate reformer burners, flow model testing of various burner arrangements, and procurement of an infra-red pyrometer for evaluation as a possible means of reformer temperature control.

Analysis of the proposed seven tube, 200-kW development reformer confirmed that it would meet the required rated power performance level of 92.5% fuel conversion at 88% efficiency over the full expected power range. Performance characteristics are shown in Figure 5.3-1. The tube geometry will be based on the use of standard pipe and tube sizes wherever possible, in order to reduce cost and improve availability.

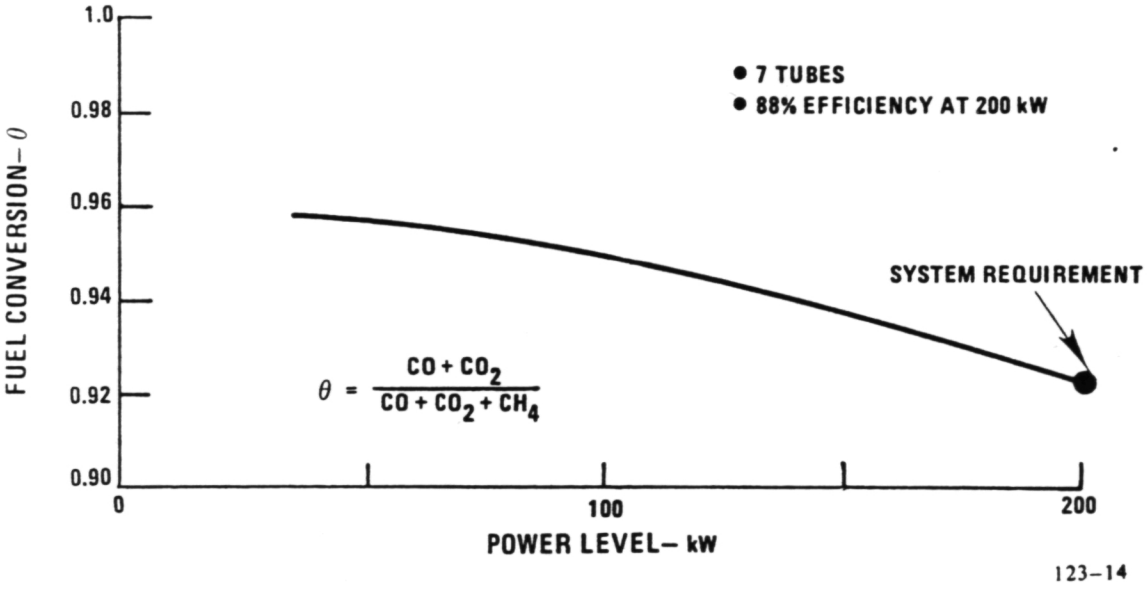

Figure 5.3-1. 200-kW Development Reformer Performance Estimate

An industrial burner was selected for evaluation in the development reformer, and an existing UTC facility has been modified for testing the burner at 200-kW operating conditions. Figure 5.3-2 shows the test arrangement, and Figure 5.3-3 shows the burner that has been purchased for evaluation. The purpose of this test is to establish the following:

- maximum heat release capability
- air and fuel pressure drop
- capability for start-up on natural gas and steady operation on low BTU anode exhaust gas
- ignition characteristics
- turndown ratio
- operating margin with changing air/fuel ratio, etc.

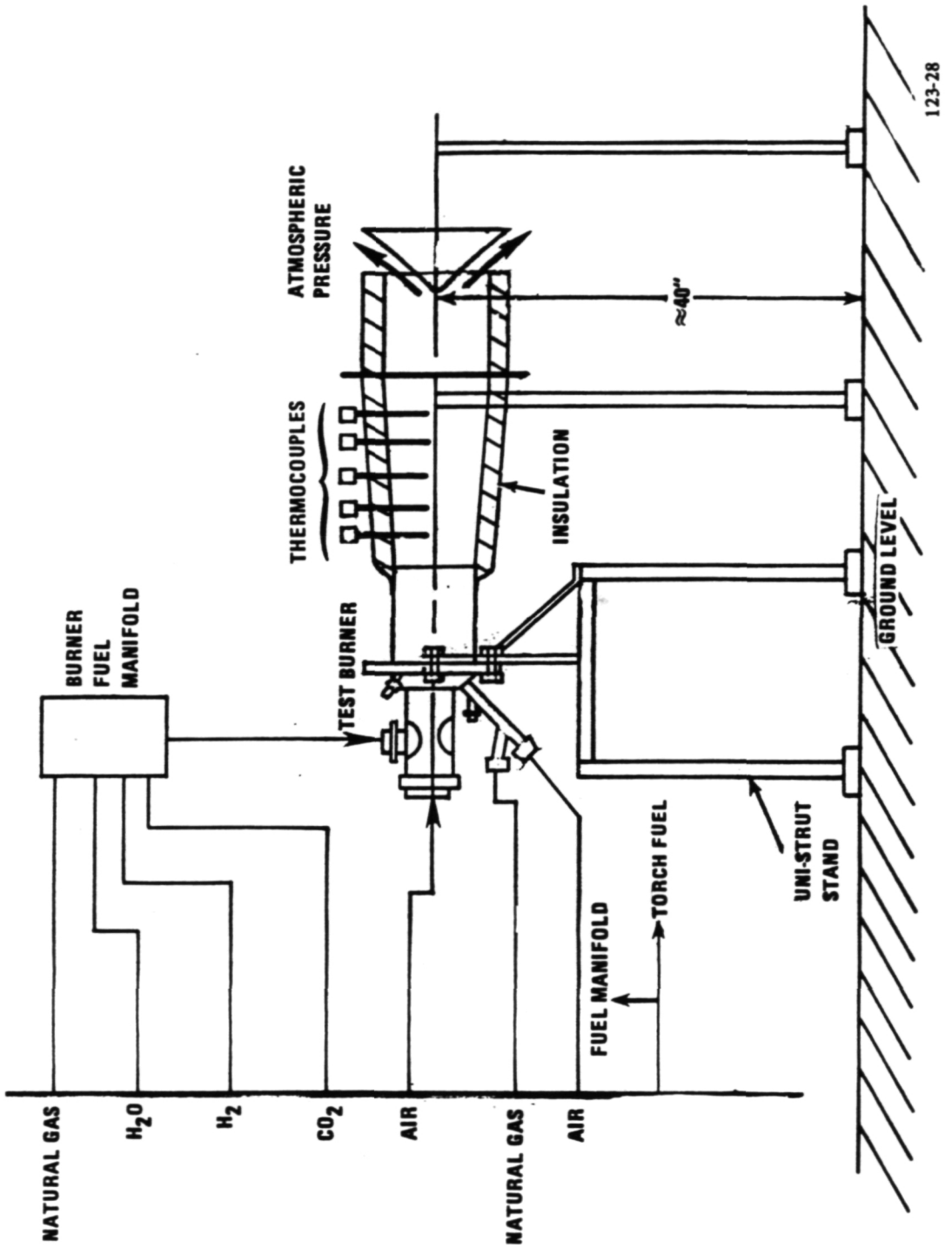

Figure 5.3-2. Test Set-Up Used for Evaluating Commercial Burner

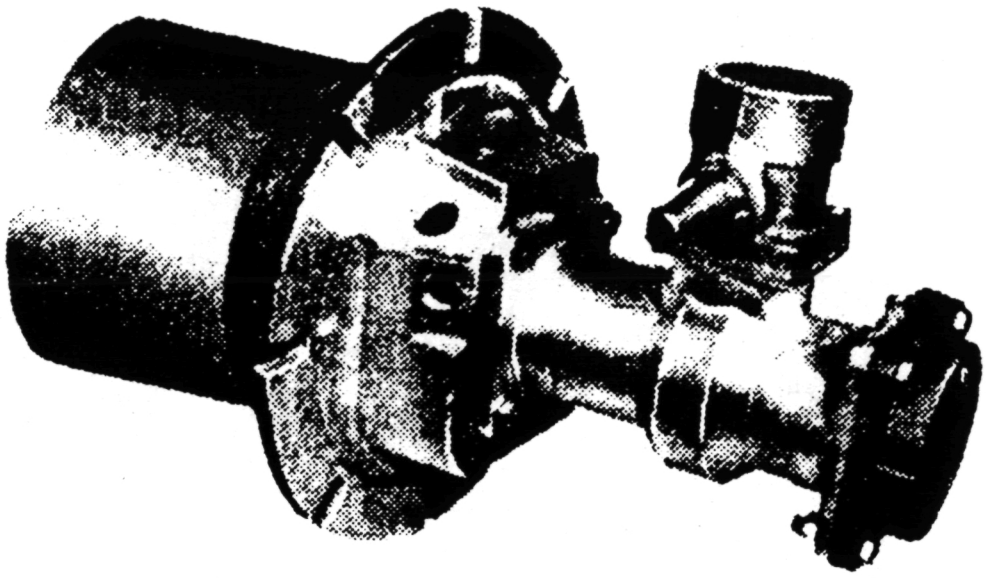

Q6212-8
R841901

Figure 5.3-3. Commercial Reformer Burner Candidate

Three potential arrangements for using this burner have been defined:

- down fired
- side fired
- upfired

Water table flow tests of various burner/reactor arrangements are planned to aid in the selection of the optimal configuration. Figure 5.3-4 shows the water table set up with a model of one burner arrangement in place. The objective of these tests is to use a proven water analogy to study the flow distribution provided by each arrangement and to make burner/flow path geometry changes as required. Testing will be conducted using talcum powder as a tracer and pulse photography of individual particles to determine streamline velocities. This will be used to define areas in the burner cavity where flow distribution improvement is required.

An infra-red pyrometer has been purchased for evaluation as a means of controlling reformer temperature. The objective is to develop an alternate, more reliable means of temperature measurement than thermocouples, which are subject to drift with aging. This evaluation will take place during testing of the development reformer.

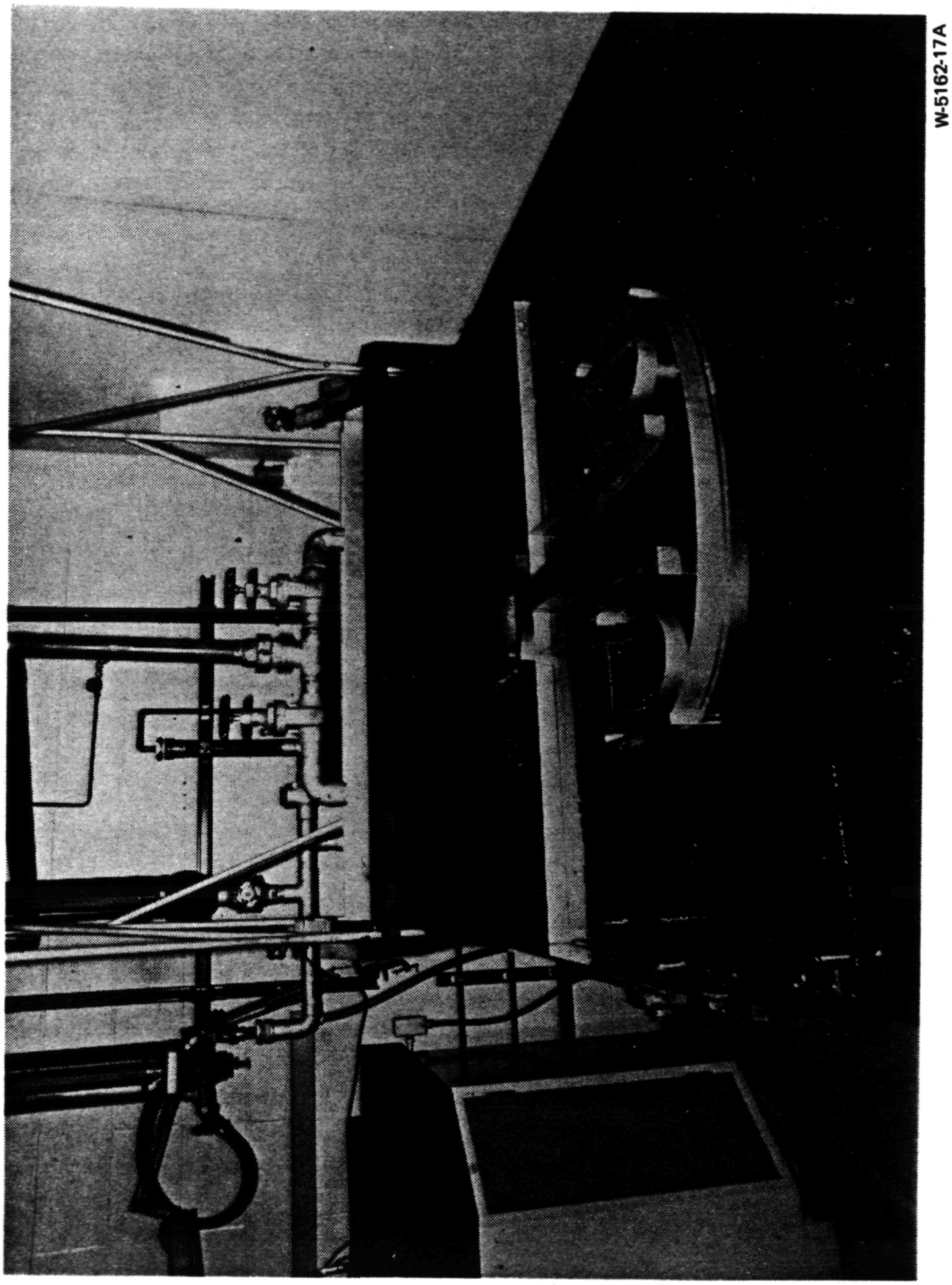

Figure 5.3-4. Water Flow Table with Burner Model Set Up for Test

TASK 6 ASSESS PREPROTOTYPE AND VERIFICATION TEST RESULTS

TASK 6 - ASSESS PREPROTOTYPE AND VERIFICATION TEST RESULTS

Objective

The objective of this task is to review operating experience with the verification test unit at United Technologies' South Windsor, Connecticut plant and experience with preprototype units located at UTC in South Windsor; in Portland, Oregon; Rockville, Connecticut; and two privately purchased units. The results of this review were assessed to determine whether additional technology development activities or changes in emphasis are required to overcome these power plant reliability deficiencies in future power plants.

Summary

The activities in Task 6 included review of power plant shutdown experience for six early 40-kW power plants. Each unscheduled shutdown was examined to determine the classification of failure. All failures have been addressed by design or procedure changes for the 47 Power Plant Field Test Program. A number of changes were made to the Technology Development Program activity to develop a basis for design of future power plants that will not be susceptible to these failure causes.

Highlights

- The operating experience with early power plants was reviewed and the unscheduled shutdowns classified by type of cause.

- The failures were reviewed and two changes made to the Technology Development Program to provide an improved reliability base for future power plants. These changes involved institution of activities to investigate coolant loop issues and initiation of an activity to establish guidelines for improved logic card reliability.

- Several other technology program activities are already underway that will provide improved components addressing other failures experienced in the early power plant testing.

Discussion

The shutdown experiences of the verification power plant, three DOE/NASA preprototype field test power plants, and three private preprototype field test power plants were analyzed to provide additional reliability information for use in the prototype technology design and development program.

The power plants whose operating histories were included in the data base included:

The verification test power plant. This unit was constructed and tested under DOE Contract No. DE-AC-03-77ET11302 and GRI Contract No. 5010-344-0060 to evaluate improvements on earlier 40-kW power plants that had been built and operated under private funding.

Three preprototype power plants constructed under DOE contract No. DE-AC01-80ET17109. One of these units containing design modifications to approximate field test units remained at UTC's South Windsor, Connecticut facility for further development testing. One was installed in Portland, Oregon by Northwest Natural Gas, supplying power and cogenerated heat to a laundry. The third unit was installed by Northeast Utilities in Rockville, Connecticut. This unit supplied power and cogenerated heat for a telephone company switching center.

Two privately purchased units, of the same design as the three units constructed under DOE contract.

These early power plants were operated as field development units to identify improvements to: power plant components, manuals, and training, which would result in improved operating experience for the power plants in the 47 unit field test program. Deliveries under this program began in the Fall of 1983. The 47 Power Plant Program is sponsored by GRI and DOE and managed by NASA under Contract No. DEN3-255.

The scope of field test experience employed in the assessment is summarized.

S/N	Start-up Date	Hours of Operation	Operating Status
8218	4/16/83	3217	Operating
8219	9/13/83	2593	Deactivated
8220	6/19/83	1375	Operating
8221	3/25/82	1219	Operating
8222	3/25/82	972	Operating

The shutdown histories of these power plants were reviewed to determine whether changes in emphasis of existing tasks or addition of new tasks would be appropriate in the Technology Development Program. These changes would be made to ensure development of technology that would improve reliability for future power plants.

Power plant shutdowns were reviewed to determine if they were scheduled or unscheduled. Unscheduled shutdowns were defined as power plant failures and were reviewed further to define primary cause. Failures were then classified into the following categories:

Non-Relevant Failures - Failures arising from circumstances not normally found in the intended application.

Relevant Failures - Failures caused by circumstances or conditions relevant to power plant technology and development.

Process Failure - A failure attributed to a power plant function performed unsatisfactorily by one or more components.

Inadequate Component Failure - A failure caused by a component that satisfies specified design requirements but predictably limits power plant operation.

Human Error Failure - A failure caused by a direct human action.

Component Failure - A failure caused by a component that meets specified design requirements. Failures of this type are often referred to as random failures.

Non-relevant failures, which represented only about 2% of the shutdowns reviewed, were excluded from further consideration.

All relevant failures were categorized a second time as either failures during start or failures during operation. For the purpose of this analysis, failure to achieve load or failure within 24 hours of achieving load was defined as a start failure.

Table 6-1 shows the percent of relevant power plant failures by cause. A further review of the failures of these power plants shows that all the failures have been addressed with design changes (85 percent) or procedural changes (15 percent) for the 47 power plants to be delivered beginning in the Fall of 1983. The operation of these improved power plants will demonstrate whether the changes were effective in resolving the problem.

Tables 6-2, 6-3, 6-4, and 6-5 break down process failures, inadequate component failures, human error failures, and component failures. These tables are then discussed with respect to Technology Development Program effects.

Table 6-2 shows that the process failures are all associated with water system issues. Corrosion products have deposited in flow restrictions which control coolant distribution in the cell stack. This problem has resulted in the largest change in the Technology Development Program. In the GRI Technology Development Program, alternative designs for the flow restrictions and alternative water loop configurations, materials, and approaches are being evaluated in subscale rigs, and the mechanisms of corrosion product deposition are being evaluated. Results of these activities have been used to design cooling system modifications, which are currently being evaluated in the 40-kW power plant design. In addition, work on an alternative cooler is already underway in the Technology Development Program. This cooler does not require flow restrictions.

Table 6-3 shows power plant shutdowns that were due to inadequate components. These problems are associated with components not meeting the requirements for fuel cell operation. As a result of the deficiencies identified in failures of the early units, revised requirements and modified components have been defined for the 40-kW Field Test Program. The adequacy of these revisions will be verified in the field test and the design information can then be used to select components for future power plants. There are several technology development activities associated with these problem areas.

First, an activity was added to the GRI Technology Development Program to develop guidelines for avoiding logic card problems. Second, inverter control logic and power plant control logic using few parts was already under investigation. This improved logic is based on more highly integrated logic elements that permit use of mass produced hardware for the fuel cell application. Alternative control actuation approach studies to reduce the number of control devices, and evaluations of integrated fuel controls and feedwater pumps with improved design margin are also being evaluated. These activities are expected to reduce failures associated with pumps and valves. Heat exchangers that eliminate concerns with trapped protective coatings are also being pursued in the Technology Development Program.

Tables 6-4 and 6-5 show shutdowns associated with component failures and human errors. These failures have been addressed in the 40-kW field program. Because they involve power plant specific issues, no action is appropriate in the Technology Development Program.

The review of power plant operating experience to identify appropriate changes to the technology program will continue under the GRI Technology Development Contract in the future.

TABLE 6-1. PERCENT FAILURES BY CAUSE

	Percent of all Failures
Component Failures	7
Inadequate Components	78
Process Failures	7
Human Errors	8
All Causes	100%

TABLE 6-2. POWER PLANT SHUTDOWNS DUE TO PROCESS FAILURES

1.	Water Cleanliness Problems	-	5
2.	Water Tank Flow Path	-	3
	Total		8

TABLE 6-3. POWER PLANT SHUTDOWNS DUE TO INADEQUATE COMPONENTS

1.	Logic Card Problems	-	41	9.	Fitting Leakage	-	4
2.	FCV 101 Leakage	-	6	10.	FCV 102 Sticking	-	2
3.	Insulation Degradation and Related Harness Shorts	-	5	11.	Coating Restriction in Heat Exchangers	-	2
4.	Pump Leakage	-	5	12.	Wrong Valve Size	-	1
5.	Level Controls	-	5	13.	Power Section Coolant Leak	-	1
6.	Actuators	-	5	14.	Ignitor Corrosion	-	1
7.	Feedback Potentiometers	-	4	15.	Shorted Heater (Air bubble)	-	1
8.	Solenoid Valves	-	4	16.	Feedwater Pump	-	1
					Total		88

TABLE 6-4. POWER PLANT SHUTDOWNS DUE TO COMPONENT FAILURES

1.	Relay Switch	-	1
2.	Door Switch	-	1
3.	GCU Switch	-	1
4.	Fan Motor	-	1
5.	Fuse	-	1
6.	Thermal Switch	-	2
7.	Flow Switch	-	1
	Total		8

TABLE 6-5. POWER PLANT SHUTDOWNS DUE TO HUMAN ERRORS

1.	Loose Wires (Assembly)	-	2
2.	Wire Failures (Related to Previous Maintenance Action	-	3
3.	Operator Error (GCU Switch in Wrong Position)	-	4
	Total		9

CONCLUSION

CONCLUSION

Subscale endurance cells were run containing GSB-18 cathodes and HYCAN anodes, which perform within seven millivolts of the program goal (E+20mV) after 2000 hours of testing.

Dual porosity substrate electrodes which are predicted to have a wider electrolyte fill tolerance were evaluated and found to perform equivalently to those using conventional substrates. Control of substrate pore size was found to be improved by blending fibers of various diameters. Although low cost substrate materials have been identified, resulting substrate characteristics are not at the desired levels; therefore, further processing development is required.

An acid condensation zone cell design was developed which has the potential of doubling the time between acid refills. The concept is being evaluated in the short stack currently being evaluated in this program. An encapsulated serpentine cooler design was developed which improves cooling performance, improves the reliability of the cooler assembly by eliminating flow control orifices, and reduces the cost of the cooler. This cooler design is also being evaluated in the program's short stack test.

Three acid addition techniques were evaluated in a laboratory rig, and the spray approach was selected for full-scale verification testing. The spray acid addition approach was tested on a 270-cell 40-kW stack. This technique will be further evaluated on the short stack when it reaches 5000 hours of testing.

An advanced 30-cell short stack was tested for 2,900 hours at 400°F atmospheric pressure and 200 ASF. The major features of this stack are dry mix and wet mix GSB-18 cathodes, encapsulated serpentine coolers, acid condensation zone, and acid refill capability. The performance of this stack is 5-10 mV below E-line and is decaying at E-line rate.

An inverter bridge design was established with full power efficiency of 94.8%, as compared to a baseline of 93%. The proposed design is a two-bridge 200-kW inverter with auxiliary commutations for surge circuitry and a low loss output transformer. A bridge coolant study resulted in a decision to select forced air/heat sink cooling for the design. A 200-kW brassboard inverter was designed in the complementary GRI program, and vendor fabrication was completed in this program by December 31, 1983. The bridge vendor fabrication completion is scheduled for January 1984.

A commercial Teflon® coated heat exchanger was successfully evaluated as the acid condenser for the 200-kW on-site power plant. The specific cost of this unit ($/kW) is estimated to be 1/5 that of the 40-kW acid condenser. In addition to water cooling, acid condensation approaches were successfully evaluated as a backup for the condensate heat exchanger.

Several reforming catalysts were identified as having less than 35% of the pressure drop of the baseline catalysts, with near equivalent conversion. These catalysts allow for a simpler development reformer design. Reformer, shift converter, and hydrodesulfurizer catalysts will be selected in 1984 for a 2000 hour endurance test, to verify the catalyst selections. The design for the development reformer has begun under the parallel GRI On-Site Technology Developmental Program. A commercial burner and infrared pyrometer for temperature sensing and control have been obtained for use in the development reformer tests.

Shutdown experiences from the verification power plant, three DOE preprototype power plants, and two private preprototype power plants were reviewed. A number of changes to the Technology Development Program were made as a result of this review.

1. Report No.	2. Government Accession No.	3. Recipient's Catalog No.
NASA CR-174709		

4. Title and Subtitle	5. Report Date
Advanced On-Site Power Plant Development Technology Program 1983 Annual Report	June 1984
	6. Performing Organization Code

7. Author(s)	8. Performing Organization Report No.
Fred S. Kemp	FCR-5715
	10. Work Unit No.

9. Performing Organization Name and Address	11. Contract or Grant No.
United Technologies Corporation Power Systems Division P. O. Box 109 South Windsor, CT 06074	DEN3-289
	13. Type of Report and Period Covered
12. Sponsoring Agency Name and Address	Contractor Report
U. S. Department of Energy Morgantown Energy Technology Center Morgantown, WV 26505	14. Sponsoring Agency ~~Code~~ Report No. DOE/NASA/0289-1

15. Supplementary Notes

Annual Report. Prepared under Interagency Agreement DE-AI21-80ET17088.
Project Manager, S. Simons, Energy Technology Division, NASA Lewis Research Center, Cleveland, Ohio.

16 Abstract

A 30-cell, full area short stack containing advanced cell features was placed on test and accumulated 2900 hours by the end of the report period. A stack acid addition approach was selected and will be evaluated on the stack at 5000 hours test time. A brassboard inverter was designed and fabrication was initiated. Evaluation of this brassboard inverter will take place in 1984. A Teflon® coated commercial heat exchanger was selected as the preferred approach for the acid condenser. A reformer catalyst with significantly less pressure drop and equivalent performance relative to the 40-kW baseline catalyst was selected for the development reformer. A reformer configuration that takes advantage of the low pressure drop reformer catalyst was selected for the development reformer. The early 40-kW field power plant history was reviewed and adjustments were made to the On-Site Technology Development Program to address critical component issues.

17. Key Words (Suggested by Author(s))	18. Distribution Statement
On-Site Fuel Cells Acid Technology Development	Unclassified – Unlimited STAR Category – 44 DOE Category – UC-97d

19 Security Classif. (of this report)	20. Security Classif. (of this page)	21. No. of Pages	22. Price*
Unclassified	Unclassified	145	

* For sale by the National Technical Information Service, Springfield, Virginia 22161